Institut für Verkehr und Stadtbauwesen
Univ. Prof. Dr. Bernhard Friedrich

Technische Universität Braunschweig

Schriftenreihe
Heft 62

Qinrui Tang

Minimization of road network travel time by prohibiting left turns at signalized intersections

Braunschweig 2019

Minimization of road network travel time by prohibiting left turns at signalized intersections

Von der
Fakultät Architektur, Bauingenieurwesen und Umweltwissenschaften
der Technischen Universität Carolo-Wilhelmina
zu Braunschweig

zur Erlangung des Grades einer
Doktor-Ingenieurin (Dr.-Ing.)
genehmigte

Dissertation

von
Qinrui Tang
geboren am 18.05.1988
aus Guangxi, China

Eingereicht am: 17.01.2018
Disputation am: 27.04.2018
Berichterstatter: Prof. Dr.-Ing Bernhard Friedrich
Prof. Dr. Dirk C. Mattfeld

.

(2019)

Acknowledgments

This thesis presents the result of my doctoral project at the Institute of Transportation and Urban Engineering, Technische Universität Braunschweig. I have conducted a challenging project for which I have learned a lot in the last three years. I would like to thank several people who supported me during the project.

First of all, grateful acknowledgment is made to my first supervisor Prof. Bernhard Friedrich who gave me considerable help by means of suggestion, comments, and criticism. With his profound knowledge of traffic signal control and queueing theory, I could quickly correct the errors in my method and deeply understand the mechanism of critical approaches. Thus, I could conduct my doctoral project efficiently. Moreover, I would like to thank my second supervisor Prof. Dirk C. Mattfeld from the Decision Support Group, Technische Universität Braunschweig, for providing me advice, especially on building up the conceptual structure.

Second, I would like to thank my colleagues from "SocialCars" and the Institute of Transportation and Urban Engineering. Mr. Aleksandar Trifunovic and Dr. Inbal Haas gave me valuable comments on my papers and patiently discussed my research topics. Ms. Andrea Thiele helped me a lot with various administrative affairs. I also had a good time with other colleagues in all activities like Christmas parties, Harz hiking, and drinking in beer gardens. In these events, I experienced typical German life and enjoyed the communication atmosphere.

I would like to thank my family and friends. My parents always support my decisions and encourage me to insist in what I like, so that I can concentrate on my research in a place far away from China. I also thank my husband, Di Wang, from the Braunschweig Pavement Engineering Centre (ISBS), Technische Universität Braunschweig for his meaningful advice on result display. I especially thank these friends: Qiao Huang from College of Computer Science and Technology, Zhejiang University for his suggestions on algorithms and graph theory; Junchen Jin from the Department of Transport Science, KTH Royal Institute of Technology for excellent discussions on optimization.

Finally, this research is supported by the German Research Foundation (DFG) through the Research Training Group SocialCars (GRK 1931). With this funding, I have had opportunities to attend international conferences and other training activities. This support is gratefully acknowledged.

Abstract

Left turns have potential efficiency problems. Permitted left turns are interrupted by opposing vehicles because conflicts exist between permitted left turn vehicles and opposing through vehicles. Protected left turns shorten effective green times, which may lead to greater intersection delays. In this thesis, the prohibition of left turns is explored as means of shortening total travel time and improving overall efficiency performance.

The objective of this thesis is to explore whether prohibiting left turns can improve the efficiency of urban road networks using existing infrastructure. Improving the efficiency refers to reducing the travel time of all vehicles in the network. A model is proposed to determine the effects of left turn prohibition with the objective to minimize the total travel time. The principle upon which a decision being made is whether the total travel time with left turn prohibition is less than that without this prohibition.

The first task is to forecast the distribution of demands as vehicles are redistributed in the network after left turns are prohibited. Prohibiting left turns not only affects the route choices of the affected vehicles, but also influences the vehicles' other movements because the prohibited turns may increase traffic flows on some links and cause delays. Therefore, all vehicles in the network would repeatedly modify their routes until travel costs were minimal for all vehicles. In this thesis, a stochastic user equilibrium model is applied to forecast the distribution of demands.

Optimizing signal settings is another important task in the absence of left turns. The whole signal timing plan of the affected intersection has to be changed because the prohibited left turn is removed from the signal group. The corresponding signal timing is adjusted according to the redistributed traffic flow. Further, the lanes for prohibited left turn should be reassigned to make use of their capacities at intersections. This thesis presents two methods of signal setting optimization: the stage-based method and the lane-based method. The principle of signal generation in the stage-based method is to avoid conflicts between movements at intersections while all movements are included. The optimal cycle length and green times are then calculated using Webster's formulas. The stage-based method in this thesis can deal with a situation in which several stages share the same movements. In the lane-based method, both lane assignment and signal timing optimization are determined in the integrated model, using mixed integer linear programming. The lane-based method is enhanced to fix the problem of possible movement conflicts in the original method. Both methods consider the influences of left turn phasing types and left turn prohibition.

Using the proposed method, it is determined that prohibiting left turns may reduce the total travel time in the network, though this reduction has not been observed for every

origin-destination path. The proposed method can handle various traffic demands. Protected left turns with small flows, left turns with large opposing flows, and permitted left turns at intersections with high saturations have a higher probability of being prohibited.

This research provides insight into network design and congestion management in urban road networks. Using the proposed model, the left turn prohibition problem can be solved analytically. Signal setting optimization methods are improved, and can handle the absence of left turns. The findings from the numerical solution could contribute to the usage of left turn prohibitions in practice.

Contents

1. Introduction

1.1. Background

Traffic managers make efforts to improve urban road mobility and efficiency. Left turns may generate efficiency problems. Permitted left turns, referring to the left turn phasing type that is in the same green time as the opposing through movements, cause extra delays because they are interrupted by the opposing through movements. Protected left turns, referring to the left turn phasing type that is not in the same green duration as the opposing through vehicles, are applied to avoid interruption. However, these protected left turns may reduce effective green times and consequently lead to more delays. Moreover, to avoid merging conflicts, both types of left turn phasing cause more intergreen times in signal cycles, resulting in lower traffic capacities.

To deal with the left turn problem, traffic managers and scholars design unconventional intersections. U-turns, mid-block, continuous flow intersections, and jughandle intersections are all possible solutions to this problem as they could improve the safety and efficiency of left turns. However, when improving the performance of urban road networks by adding new modes/infrastructures, traffic managers may not always achieve their goals. Unconventional intersections cost 49% more to build than conventional intersections (Gyawali, 2014), and cannot always reduce accidents and delays. For example, U-turns may conflict with opposing through movements when two movements merge, and the opposing road may not deal with the U-turn traffic flows. In developed cities, the space for constructing unconventional intersections is limited. Moreover, previous studies have focused on isolated unconventional intersections so that the influence of these intersections on the entire network is not clear. For these reasons, unconventional intersections can only partially work well in urban road networks.

Directly prohibiting left turns, which is an alternative solution for improving performance, is explored in this thesis. Although some scholars doubt the efficiency of left turn prohibition, with the exception of unconventional intersections, in this work it is shown that directly prohibiting left turns can be a feasible solution. In the case of Braess' paradox, which shows that building a highway does not always contribute to shorter travel times, restricting movements may shorten total travel times, or result in other benefits for road networks.

1.2. Objectives

The objective of this thesis is to explore whether prohibiting left turns can improve the performance of urban road networks by taking advantage of existing infrastructures in a long-run fixed time period. The performance refers to travel time reduction of all vehicles

in the network. Prohibiting left turns improves safety, but this thesis does not evaluate the safety performance. A model is proposed to determine the effectiveness of left turn prohibition in minimizing total travel times. The factor by which the effectiveness will be evaluated is whether the total travel time with left turn prohibition is smaller than that without this prohibition.

When directly prohibiting left turns, it is key to also make sure that the prohibited traffic flows are accommodated. That is, it is key to estimate whether the roads in the network have enough capacity for the prohibited traffic flows. In an urban road network, the road capacity is a function of traffic flows, saturation flows, and signal timing. It is necessary to forecast traffic flow changes after left turns are prohibited in a reasonable manner. Saturation flows, if the intersection geometries do not change, are affected by lane assignments, which are relevant to signal settings. Signal timing is also a part of signal setting optimization. Thus, there are two critical research issues to consider: demand forecasting and signal setting optimization.

Demand forecasting is necessary because vehicles are redistributed in the network after left turns are prohibited. The vehicles intending to turn left turn cannot choose the same paths and have to find other routes. Prohibiting left turns also influences the vehicles turning right and going straight through. The vehicles in the prohibited direction may choose through movements and right turns as alternatives, and increase the traffic flows of relevant links, which could cause delays. All vehicles in the network would attempt to find the shortest routes according to their limited knowledge of the route travel time. They repeatedly modify their routes until the perceived travel times are minimal for all vehicles, that is, an equilibrium state has been reached. A stochastic user equilibrium model, being suitable to describe the traffic demand redistribution with left turn prohibition, is used in this thesis.

Optimizing signal settings is another important issue to consider. A straightforward influence of left turn prohibition on signal setting optimization is that the prohibited left turn is removed from the signal group, so the lanes of the prohibited left turn and relevant signal timing should be reassigned. The intersections in the network without left turn prohibitions are influenced as well due to the redistributed traffic flows. Therefore, signal setting optimization must be applied for all of the intersections in the network. Lane reassignment is necessary to better reflect estimated the lane saturation flows, and signal timing must be recalculated to reflect the new estimated capacity. Along with lane assignment and signal timing, link delays, which influence link travel time, can be calculated. Thus, the signal setting optimization method must deal with both lane assignment and signal timing optimization.

This thesis presents two methods of signal setting optimization: the lane-based method (Wong and Wong, 2003; Wong et al., 2006; Wong and Heydecker, 2011; Zhao et al., 2016b) and the stage-based method (Webster, 1958; HBS, 2001; Memoli et al., 2017). In the lane-based method, both lane assignment and signal timing are determined using a mixed integer linear programming model. The lane-based method can deal well with the lane assignment of the prohibited left turns, but the method is only theoretically developed because this method may generate uncommon signal timing. In the stage-based method, which is widely used in practice, the lane assignment is a given input, but

the stages need to be regenerated when the leading principle is to avoid conflicts between movements. The stage sequence is then optimized by minimizing the total intergreen time, followed by a signal timing adjustment using Webster's formulas. To adjust the signal setting optimization methods to the left turn prohibition problem, one has to answer an additional question: what should be the left turn phasing type? The left turn phasing type is defined according to whether left turns are protected from conflict from oncoming traffic. If a left turn is protected from conflict from opposing vehicles, it is a protected left turn; if not, it is a permitted left turn. The left turn phasing type influences the conflict matrix, which is used to determine the signal timing plan and influences the saturation flow of left turns. Further, the methods themselves are also

The computing complexity of left turn prohibition problems is challenging. The binary variables of the left turn prohibition result in exponential complexity. For example, a network with four standard intersections is a small network, but will have 16 left turns. With 2^{16} possible left turn prohibition permutations, it is difficult to apply left turn prohibitions in large networks by enumerating all left turn prohibition combinations. The additional task is to apply suitable algorithms and to reduce the search space of the proposed model. The factors influencing left turn prohibition are analysed because they might contribute to narrowing the search space.

In summary, this thesis completes the following tasks:

- prohibiting left turns to minimize total travel times in urban networks,
- forecasting demands in networks using the stochastic user equilibrium model, and
- optimizing signal settings by improving the lane-based method and the stage-based method when considering left turn phasing types.

1.3. Outline

Chapter 2 explains relevant concepts surrounding the theme and presents previous research on left turn prohibition, signal setting optimization, and traffic assignment models.

Chapter 3 presents the overall proposed model, which consists of left turn prohibition, stochastic user equilibrium, and two methods of signal setting optimization. The objective of the overall problem and the objectives of each sub-question are explained. The connections between each sub-question are also clarified.

Referring to Chapter 3, left turn prohibition (Chapter 4), stochastic user equilibrium (Chapter5) and signal setting optimization (Chapter 6) are explained in detail. The construction of the objective functions and relevant constraints and their algorithms can be found in these chapters. The measurements of the proposed model and the signal setting optimization methods are mentioned as well.

The proposed model is tested on two networks in Chapter 7. The effect of demand variance and the factors influencing left turn prohibition are analysed. Finally, conclusions are drawn in Chapter 8.

2. Literature review

2.1. Overall

This chapter introduces the theory and previous research relevant to this dissertation. In the section "Left turns", the types of left turn phasing, concepts of left turn treatment, and previous studies about left turn prohibition are introduced. In the section "Signal setting optimization", basic definitions of signal control and classical signal control systems are summarized. Finally, traffic assignment models are reviewed, which include the methods of travel time estimation and discrete choice models.

2.2. Left turns

2.2.1. Left turn phasing type

There are two main types of left turn phases: the permitted left turn phase and the protected left turn phase. Permitted left turns are in the same green time as the opposing through movements, whereas protected left turns are not in the same green time as the opposing through movements. If these types are shown in stages, Figure 2.1 shows permitted left turns in (a) and protected left turns in (b).

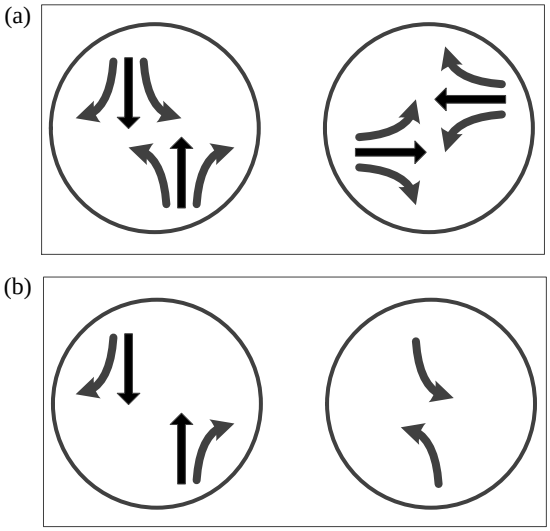

Figure 2.1.: (a) Permitted left turns in stages and (b) protected left turns in stages.

Permitted left turns, due to less clearance time in the signal cycle, may reduce the total delay at intersections. However, as the left turns are interrupted, the delay of the per-

mitted left turn increases. There are also safety problems because permitted left turn vehicles may conflict with opposing through vehicles. Protected left turns can avoid these interruptions, but may increase the total delay at intersections as the clearance time increases. Due to the mixed application of permitted and protected left turns, the options for left turn phasing include permitted only, protected only, permitted-protected, and split phasing (Koonce et al., 2008).

Left turn prohibition could be one option for left turn phases. Usually, left turns are only prohibited for a specified time interval during a day. The purpose of left turn prohibition in practice is safety. Using left turn prohibition to optimize total travel time is rarely studied.

2.2.2. Guidelines for left turn treatment

There are several guidelines providing recommendations for left turn treatment at signalized intersections. The following factors are mentioned in the guidelines:

Accidents

Accident experience is the criterion mentioned most often. Besides historical accident data, Agent (1985) took speed limits, the number of opposing through lanes, intersection geometries, and sight distance to forecast the accident potential at intersections. Agent (1985) described the following safety hazards for protected left turns:

- poor sight distance,
- speed limit of opposing through vehicles is more than 45 miles per hour,
- left turn vehicles must cross three or more lanes,
- more than six accidents per year, and
- unusual intersections.

These criteria were later adopted by Kell and Fullerton (1991); Roess et al. (2004); RiLSA (1992); Pline (1996). However, HCM (2000) described an additional volume condition in which the number of through lanes is three or more, which is not consistent with Agent's criteria (1985).

Volume

The volume consists of two criteria: left turn flows and the product of left turn volume and opposing through volume. The latter is developed based on the gap acceptance theory (Drew et al., 1967). The basic form of this criterion is listed below:

- left turn flow $\geq$ a constant.
- left turn flow $\times$ opposing through flow / number of opposing through lanes $\geq$ a constant.

In different guidelines, the values of constants are different. For example, Roess et al. (2004) valued the first constant at 200 veh/h, but HCM (2000) valued the first constant as 240 veh/h. The reason behind these differences is that different factors influence the values. Stamatiadis et al. (1997) thought that accidents should be considered when determining the volume criteria.

As the capacity of left turns is the key to determine left turn phasing, some researchers question their conditions. Al-Kaisy and Stewart (2001); Stamatiadis et al. (2015) think the product is a poor indicator, and developed new conditions for the capacity of left turns by using simulations. However, their findings have not been widely accepted.

Delays

Agent and Deen (1978) collected field data from three two-phase semi-actuated signalized intersections. They estimated the minimum protected left turn volume by summing up the number of left turn vehicles leaving in the amber period and took the minimum necessary left turn delay as the indicator as well. Agent and Deen (1978) compared the delay before-and-after protected left turn installation with stable left turn volume, and concluded that protected left turn increases the total delay of the intersection then may not always hold. Although these criteria were tested on other six intersections, the criteria were not estimated by optimization and might not be fit for other signal timing plans. Al-Kaisy and Stewart (2001) solved this question in a more analytical way. They optimized the signal timing using the stage-based method by minimizing the total delay. As they focused on isolated intersections, the influence of left turn phase types on networks is not clear.

2.2.3. Benefits of left turn prohibition

Prohibition is applied when gaps in traffic are unavailable and the operation of permitted left turns may be unsafe. If the straight lanes have a large volume, left turn drivers cannot find an available gap in which to turn left, and thus the permitted left turn should be prohibited. Prohibiting permitted left turns could be beneficial because on the one hand, the safety of the intersection would be improved, and on the other hand, the left turn vehicles would not be interrupted, so the mobility of the intersection would also increase. For the protected left turns, it is believed that the clearance time could be saved for the effective green time. In summary, after prohibiting left turns, three aspects of performance should be improved: safety, delays, and capacity.

Safety

Permitted left turn vehicles conflict with opposing through vehicles, so more accidents take place. Prohibiting left turns results in a lower number of conflicts, so safety is improved.

Delays

Drivers from the left turn lane may hesitate to cross the intersection because they may be interrupted by opposite through flow. This increases the delay in the left turn direction, especially when volumes are large. Moreover, left turn vehicles and through vehicles

may block each other, which increases the delays at an intersection (See Figure 2.2). Signal timing also generates delays, but for protected left turns, the effective green time is reduced.

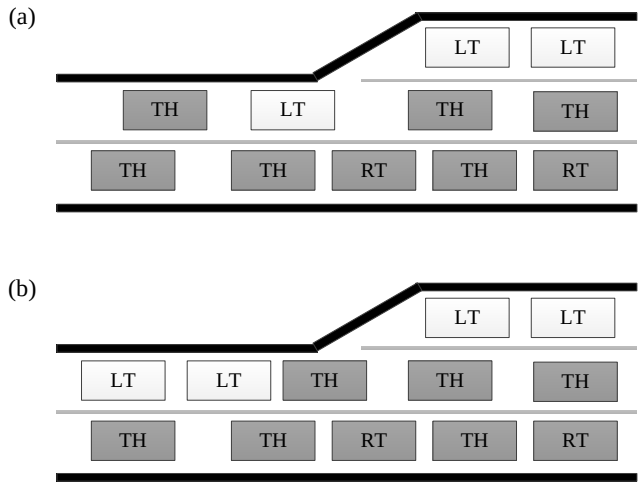

Figure 2.2.: (a) Left turn vehicles block through vehicles; (b) Through vehicles block left turn vehicles.

Capacity

After prohibiting left turns, greater capacity could be saved for through and right turn lanes, so capacity might increase.

2.2.4. Left turn prohibition at isolated intersections

Left turn prohibition at isolated intersections is solved as an infrastructure design problem by using unconventional intersections. The main principle of the design of these unconventional intersections is to avoid or to reduce the conflicts between left turns and other movements. U-turns at the median of a road or at the next intersection is are frequently mentioned (Bared and Kaisar, 2002; Lu et al., 2001b,a, 2005; Chowdhury et al., 2003, 2004, 2005). Avoiding left turns is usually evaluated by simulations. For example, a study by Leng et al. (2009) used the VISSIM simulation tool. Constructing U-turns may reduce the travel time in networks (Bared and Kaisar, 2002), and improve the safety due to fewer conflict points compared with direct left turns (Lu et al., 2005). Other unconventional intersections, such as continuous flow intersections and jughandles, also aim to reduce conflicts, but are more expensive than U-turns and conventional intersections (Gyawali, 2014). Zhao et al. (2015b) analysed the feasibility of displaced left-turns, in which vehicles turn left before entering the an intersection. For more information, sSee the unconventional intersections in Figure 2.3.

However, unconventional intersections may not improve performance. Chowdhury et al. (2005) found little operational difference between no restrictions on direct left turns and

a U-turn at a median block. Although the number of conflicts at U-turns is less than the number of conflicts of direct left turns, there are more U-turn conflicts than the number of conflicts created by prohibiting left turns. Vehicles taking U-turns may conflict with opposing vehicles when they merge, which reduces the safety level. The exit lanes may not have a great enough capacity for the vehicles taking U-turns, which may cause efficiency problems. That is why in different papers, the conclusions of applying U-turns are different, for example , Bared and Kaisar (2002) and Chowdhury et al. (2005). For other examples, like mid-block left turns, the safety was also questioned by Roudsari et al. (2007), as the authors found that crashes at mid-block left turns are more severe than crashes at intersection-related left turns for front seat passages. Therefore, the decision to apply an unconventional intersection must be carefully analysed.

2.2.5. Left turn prohibition in networks

Left turn prohibition in networks is usually formulated as a network design problem. In such a problem, whether turning movements should be prohibited is the decision variable. Long et al. (2010, 2014); Guang and Wu (2013); Foulds et al. (2014) treated road networks as networks without road geometrics and seldom involving signal settings. Hajbabaie et al. (2010); Zhao et al. (2015a); Tang and Friedrich (2016) then considered the signal timing optimization in the left turn prohibition problem.

2.2.6. Factors influencing left turn prohibition

According to previous research, left turns with certain features have high probabilities of being prohibited. However, these features, or the factors influencing left turn prohibition, are qualitatively described, rather than analysed. The influencing factors of prohibited left turns consist of following categories:

Left turn flow

Left turns with minor flows should be prohibited (Pline, 1996; Lu et al., 2001b; Hajbabaie et al., 2010; Tang and Friedrich, 2016), as left turn vehicles have less of an effect on the network when they are redistributed.

Opposing through flow

When the opposing through flow is large, left turns should be prohibited (Hajbabaie et al., 2010; Lu et al., 2001b). The high-demand opposing through vehicles create a higher potential for accidents with permitted left turn vehicles and reduce the capacity of the whole intersection. Because the left turn vehicles have difficulty accessing the intersection safely and quickly, it may be necessary to prohibit left turns.

Turning capacity

Li et al. (2009) concluded that left turns should be prohibited when the left turn flow is larger than its capacity, according to their unsignalized T-intersection study. Hence, the capacity is an important condition for determining left turn prohibition, but is also similar to the concept of the degree of saturation.

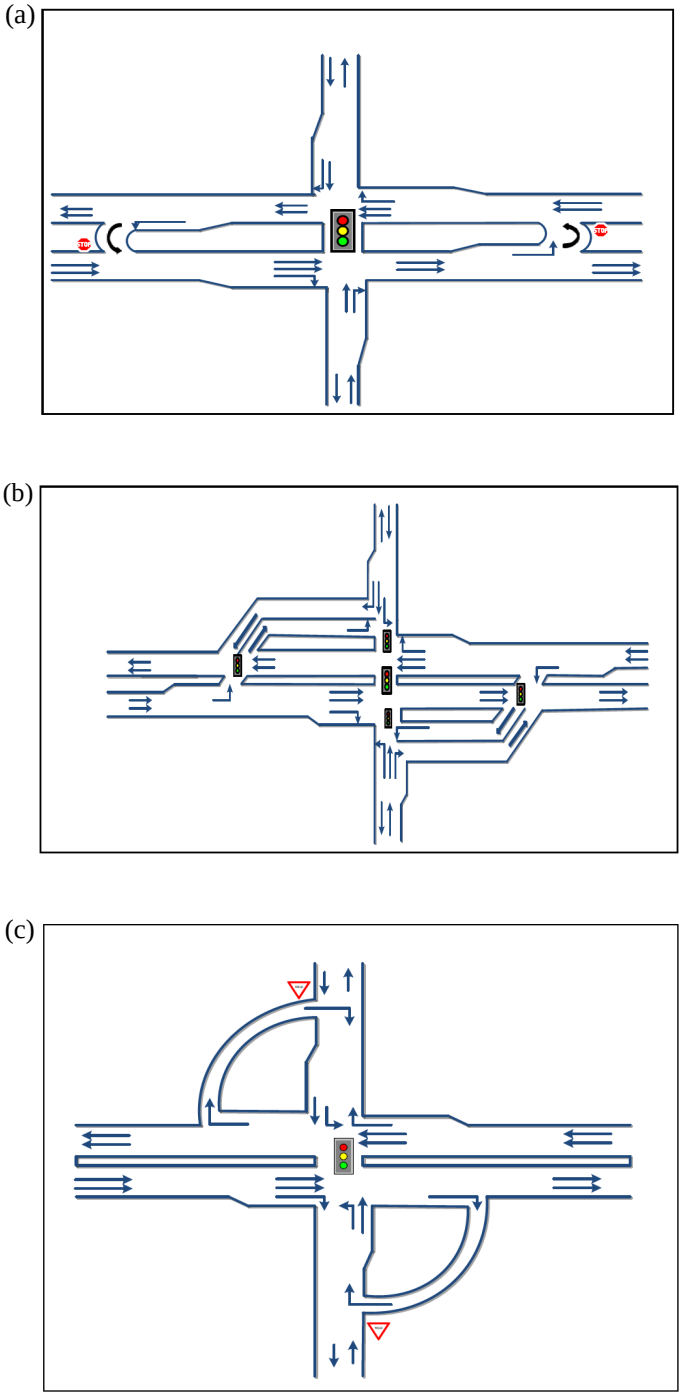

Figure 2.3.: (a) U-turns at mid-block. (b) Continuous flow intersection. (c) Jughandle (Gyawali, 2014).

The average degree of saturation at intersections

Long et al. (2010) suggested that turning restrictions should be implemented at congested intersections because prohibition at congested intersections forces vehicles to move to less congested intersections, resulting in better network usage. As the degree of saturation is an indicator used to measure the congestion level, the average degree of saturation at intersections is also considered.

2.3. Signal setting optimization

2.3.1. Terminology

To better understand signal setting optimization, some basic concepts need to be defined.

A **cycle** is a complete sequence of the green times of all signal operations at an intersection.

Cycle length/cycle time is the time duration of a cycle in seconds.

Green time/green duration is the time duration in seconds of vehicles having the right of way to turn in a given direction.

A **split** refers to the ratio of green duration to cycle length. In some studies, splits are decision variables rather than cycle length and green duration.

The **start of green** is the time point in seconds when a signal light turns green. It is highly relevant to the signal sequence.

A **conflict matrix** records the conflict states between movements. If the value in the conflict matrix is 1, two movements conflict with each other. A value of 0 indicates that the movements do not conflict. The conflict matrix ensures that two conflicting movements cannot be in the same green duration, so that safety is guaranteed.

A **stage** is a group of non-conflicting movements in the same green duration. A stage requires compatibility between movements. All movements must be included in the stages of a signal cycle.

A **phase/signal group** is a group of signal heads that display exactly the same signal at all times.

Intergreen time is the time duration between the end of green of one signal group and the start of green of the next signal group if the two signal groups are conflicting.

Transition time is the minimum duration between two sequential stages; it is the maximum intergreen time between the signal groups related to the stages.

Clearance time refers to the time loss at a transit stop in seconds, not including passenger dwell times (Koonce et al., 2008).

The **offset** is the time difference between the start of green of corresponding signal groups at a sequential intersection in arterial roads or networks.

The **signal sequence** is the sequence of signal groups of movements turning green.

The **saturation flow** is the maximum flow obtained at a stop line from a discharging queue during green. The unit can be vehicles per hour or vehicles per second.

The **flow ratio** is the ratio of flows divided by the saturation flows.

The **capacity** is the maximum number of vehicles departing the intersection in an hour. It is equal to the product of the saturation flow and the split.

The **degree of saturation** is the ratio of the actual flow to the capacity. It is used to measure whether a link or a lane is over-saturated. If the value of the degree of saturation is more than 1, the link or lane is over-saturated. If the value is less than 1, then it is not over-saturated. The degree of saturation influences the delay.

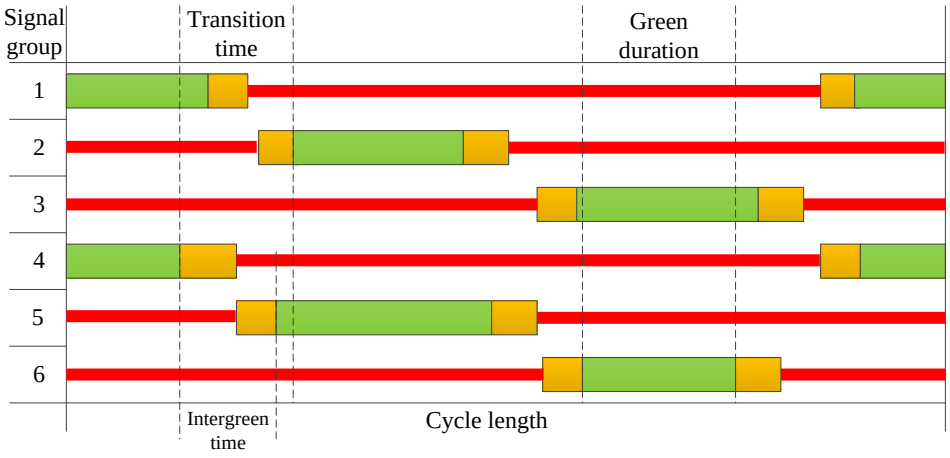

Figure 2.4.: A signal plan and the relevant terms of signal control.

2.3.2. Objectives

The goal of signal setting optimization is usually to either improveing the safety level at intersections or to gaining efficiency. Efficiency refers can refer to many different measurements. At isolated intersections, gaining efficiency could be refer to the minimization of delays (e.g. Gartner (1990, 2001)) or the maximization of reserved capacity or capacity (Wong and Wong, 2003; Chiou, 2014). In the arterial traffic optimization, gaining efficiency usually refers to the maxi- mization of green bands (Rathi, 1988). In networks,

minimization of delays or travel times could be the goal. As environmental problems are concentrated are increasingly considered nowadays, minimization of emissions or noises becomes could become the objective (e.g., Ma et al. (2014)). When multiple in- tersections are saturated, the maximization of capacity is better than the minimization of delays, because the former provides extra green time for the saturated links (Smith, 1988).

2.3.3. Methods

To optimize signal settings, one can formulate the models in different ways. According to the formulation of decision variables, Tthe different methods are classified sorted into three classesaccording to the formulation of decision variables. These methods are described as: stage-based, phase-based, and lane-based. In the stage-based method, the signal settings of stages are optimized. Similarly, the signal settings of phases and those of lanes are optimized in the phase-based method and the lane-based method, respectively.

The stage-based method assigns cycle lengths for different stages. The most classical stage-based method is was developed by Webster (1958). Webster (1958) optimized the green durations of stages by minimizing delays and also deduced the formulas of for de- termining optimal green duration and cycle length. In the stage-based method, stages and their sequences are usually given in the form of a stage matrix, but some of the re- searchers also include stage generation and sequence optimization in their models (Memoli et al., 2017). All of traffic control systems being used in real-world networks are inuse the stage-based method.

The phase-based method is also called as group-based method. The phase-based method decides the maximum cycle length, the green duration, and the start of green for each approaching lane and its sequence in binary mixed integer linear programming (Improta and Cantarella, 1984; Gallivan and Heydecker, 1988; Wong, 1996; Silcock, 1997; Ma et al., 2014; Lee and Wong, 2017). The objective can be the minimization of delays or cycle length or the maximization of reserved capacity.

The lane-based method has been extended from the phase-based method by Wong and Wong (2003); Wong et al. (2006); Wong and Heydecker (2011); Wong and Lee (2012). The main difference is that the lane-based method includes lane allocations as decision variables, whereas the lane allocation is given in the phase-based method. The lane-based method was applied by Zhao et al. (2015a) in their turning movement restriction problem. Both the phase-based method and the lane-based method focus on isolated intersections.

2.3.4. Fixed-time signal control systems

Fixed-time signal control systems assume that the current traffic conditions are stable . In practice, the fixed-time signal control is used for isolated intersections (HBS, 2001). TRANSYT, the most famous off-line control system, can be applied in real networks (Robertson, 1969, 1986). TRANSYT can optimize cycle length, green split, and offsets by minimizing the weighted combination of delays and stops. Although it is thought that adaptive control systems are superior to fixed-time control systems, the fixed-time control system is still studied by many scholars, including Wong (1996); Ceylan and Bell (2004a,b), due to its simplicity and integration with traffic assignment models.

2.3.5. Adaptive traffic control systems

Adaptive systems optimize signal settings considering the stochastic fluctuations of vehicle arrivals. Detectors collect traffic demand data , and the demand in a short-term state is forecasted. The adaptive systems being applied in practice are summarized in Table 2.1. The green duration of stages, cycle length, and offset are optimized, for example, SCOOT (Split Cycle Offset Optimisation Technique). Some systems optimize green splits rather than green duration and cycle length, for example, SCAT (Sydney Coordinated Adaptive Traffic System), UTOPIA (Urban Traffic Optimisation by Integrated Automation), and PRODYN. The systems in Germany - MOTION (Method for the Optimization of Traffic Signals In Online controlled Networks), BALANCE - also optimize the stage sequence. OPAC (Optimization Policies for Adaptive Control), the adaptive system from the USA, determines a sequence of switching time instead.

In addition to these practical adaptive systems, some systems are developed for theoretical innovation. Heydecker et al. (2007) adjusted the stage durations based on traffic flows. The cell transmission model (CTM), in which roads consist of sequential cells, has attracted attention, as the CTM covers both saturated and unsaturated conditions and it is validated by field data (Lo, 1999). Lo (1999, 2001) and Lin and Wang (2004) formulated the signal control problem in mixed integer linear programming by using the CTM. With these models, as proposed in the papers, the signal timing is optimized. Although the focus of these models is dynamical scenarios, they can also be used in the fixed-time case. Pohlmann and Friedrich (2010) optimized the offsets with the CTM, as offsets are the core of coordination (Koshi, 1989).

2.4. Traffic assignment models

2.4.1. Overall

Traffic assignment models are the models of estimation of the traffic flows in networks. Traffic assignment models are based on the assumption that drivers in the network will try to minimize their travel time from origin to destination. The travel time of each link is dependent on link flows, and thus, the link travel time changes as the link flow changes. Once drivers cannot improve their travel time by changing routes, the condition is called a user equilibrium (UE) state. It is proven that a UE exists, and that it is unique and stable (Smith, 1979a). The UE condition assumes that drivers have sufficient knowledge of the travel time of every route and can always make correct route choices. Another assumption is that the route choice behaviour of each driver is independent, which is the primary assumption of equilibrium in economics. These assumptions are difficult to meet in reality. Hence, the first assumption can be relaxed. Drivers can choose their routes based on perceived travel time, which is formulated as a random variable distributed in drivers. The stochastic user equilibrium (SUE) meets the condition that "no drivers believe that their path travel time can be reduced by changing routes" (Sheffi, 1985). As traffic dynamics have attracted attention in recent research, dynamic traffic assignment models have been studied. In traffic assignment models, the drivers' behaviour is more complicated, as the travel cost of the previous period influences the present choices based

Table 2.1.: Summary of adaptive signal control systems

System	Country	Objective	Communication	Detector location	Citation
MOTION	Germany	Minimization of delays and stops.	Centralized	At all entries and exits of the network, and approaches of intersections. Additional detectors at 40 meters in front of the stop lines.	Bielefeldt and Busch (1994)
BALANCE	Germany	Minimization of total costs.	Bi-level	Upstream of each approach.	Friedrich (2000)
SCOOT	UK	Minimization of queue length, delay and the number of stops.	Centralized	Vehicle detectors.	Hunt et al. (1981) Bowen and Bretherton (1996)
OPAC	USA	Minimization of total delays.	Bi-level	Upstream of each approach	Gartner (1990, 2001)
SCATS	Australia	Minimization of delays, stops or maximization of throughput.	Bi-level	At stop-line.	Sims (1979) Lowrie (1982) Sims and Finlay (1984)
UTOPIA	Italy	Minimization of delay of private cars while public cars have priority.	Bi-level	upstream for private cars and buses, additional at bus stops.	Donati et al. (1984) Mauro and di Taranto (1990)
PRODYN	France	Minimization of total delays.	Decentralized	At upstream junction and 50m upstream of stop line.	Henry et al. (1983) Farges et al. (1990)

on drivers' experience and information. Dynamic traffic assignment models cannot reach equilibrium.

A system optimum is always accompanied with UE when researchers decide the objective function in different problems. The objective of a system optimum is the minimization of the total travel time in networks, whereas the objective of UE is the minimization of the path travel time. The difference between the system optimum and UE is an interesting phenomenon called Braess's paradox. Only when travel times are not dependent on flows are the results of system optimum and UE are the same. In the SUE model, as drivers select routes based on perceived travel time, the travel time of all paths may not the same as the equilibrium state.

When explaining the traffic assignment models, Cascetta (2009) divided the traffic assignment models into two categories: demand models and supply models. The demand model estimates the link flow distribution. As the route choice influences the link flows, route choice behaviour is the most important part of the demand model. The supply model estimates the link travel time. Thus, it is critical to apply suitable measures to estimate link travel time.

2.4.2. Route choice

In a UE model, drivers select routes with the rule of all-or-nothing. Namely, all drivers choose the shortest route between one origin-destination pair, and none of the drivers choose other routes. In a SUE model, drivers choose routes with the random utility of different routes. The utility function of each path is expressed as an addition to systematic utility and random residual. Drivers are considered perfectly rational; hence, they try to maximize their benefit (represented as utility in the function). The systematic utility is the expected value of utility, which may include travel time, transportation mode, or user preference. Horni et al. (2016) explained the utility function compositions in MATSim, but these compositions can be considered in the systematic utility. According to the different distribution of random residuals, random utility models are divided into two types: logit models and probit models. The random residuals of logit models follow a Gumbel distribution, while the random residuals of probit models follow a normal distribution.

Logit model

The multinomial logit model is the simplest logit model. It was developed byWilliams (1977) and summarized by Ben-Akiva and Lerman (1985). The Gumbel distribution in the random residual has a zero mean value and scale parameters. The random residuals are independent, and then the covariance between any pair of residuals is zero. The probabilities of different routes being selected are then calculated with the multinomial logit model. The path size logit model is a multinomial logit model, and the path size is included in the systematic utility (Ben-Akiva et al., 2009).

However, the assumption that the random residuals are independent does not always hold. Different routes may have overlapping links. Different transportation plans may

have the same transportation mode. Therefore, some logit models are developed based on the multinomial logit model to relax this assumption. The multilevel hierarchical logit model, which is generalized from the single-level hierarchical logit model, can deal with the case that different choices overlap using a "tree" covariance structure (Daganzo and Kusnic, 2004). As the covariance structure could not be a tree, the logit model is further generalized as a cross-nested logit model (Wen and Koppelman, 2001).

Probit model

As mentioned, the random residuals in probit model follow a normal distribution. The covariance matrix in the probit model is more flexible, as the elements in the matrix can be assigned any values. However, this flexibility can be a problem in practice (Cascetta, 2009).

The estimated probabilities of the logit model and the probit model are similar if the covariance matrices are the same. Sheffi (1985) compared the multinomial logit model and the probit model when overlapping exists. Compared with the logit model, the results of the probit model are more reasonable, but the probit model has higher computational costs. Thus, in practice, the logit model is more efficient to use.

Route search

Both the logit model and the probit model are relevant to the choice set of routes. To calculate the probabilities of each route, all routes from one OD (Origin-Destination) pair can be found by using a depth-first-search algorithm. However, it this is not efficient. Some algorithms are have been developed to avoid searching all routes. The STOCH algorithm in the logit model and the Monte Carlo simulation processes in the probit model are recommended (Sheffi, 1985; Cascetta, 2009). In a STOCH algorithm, only the shortest route is found, rather than all the routes, which increases the efficiency of the algorithm.

2.4.3. Travel cost estimation

Travel cost estimation directly influences the route choice, as travel cost is a concept similar to the utility in the discrete choice model. Although the utility function can include many factors, in traffic assignment models, travel time is the most commonly applied. In some cases, emissions can also be a factor in the utility function.

Bureau of Public Roads function

The Bureau of Public Roads function is usually called the BPR function. It was developed by the Bureau of Public Roads in the USA. For each link, the link travel time is a function of the link flow. The free flow travel time and the link capacity are the inputs. The parameters in the BPR function can be obtained from field data.

This function is widely used in the highway networks or the urban networks without considering signals. The BPR function is limited at signalized intersections, as the function was developed by fitting data from uncongested freeways (Skabardonis and Dowling, 1997;

Davis and Xiong, 2007). Spiess (1990) found that the BPR function is over sensitive in congested conditions.

Link travel time with signal timing

The travel time function must be fit for the application in signalized networks. The link travel time at signalized intersections is the sum of the free flow travel time and the link delay (Ceylan and Bell, 2004b). Thus, it is critical to estimate link delays.

Webster's delay formula is a classical formula to estimate delays at signalized intersections (Webster, 1958). Smith (1979b) shows an example of an application of Webster's delay formula in a UE model. The formula is developed based on queuing theory and is corrected based on simulation data. The assumption of queuing theory, which postulates that the traffic demand must be less than the traffic capacity, limits the usage scenario of this formula. That is, the formula can be only applied in uncongested networks.

In the first few iterations of the traffic assignment models, some of the links are more likely to be congested. Hence, a delay model applicable in congested networks is necessary. Queuing theory is the base of most of the delay models, but two issues have to be solved.

The first issue is developing a delay model to be used in both uncongested and congested networks. When a link is not congested, the delay is accumulated as steady-state delays. When the link is congested, which means that the link does not have enough capacity for the arriving vehicles, the delay is accumulated as a deterministic delay. Between the steady state delay and the deterministic delay, there is a gap that needs to be filled (see the degree of saturation with Value 1 in Figure 2.6). To fill this gap, Kimber and Hollis (1979) developed a coordinate technique so that the curve of the delay model can be smoothly transferred to a congested condition. Later, this technique is applied in many manuals (Akcelik, 1980; HCM, 2000) and by other researchers (Han, 1996).

The second issue is developing a delay model with non-Poisson arrivals and departures. In queuing theory, the inter-arrival and inter-departure times follow a Poisson distribution Webster (1958). However, due to periodic red lights, the arrivals may follow other

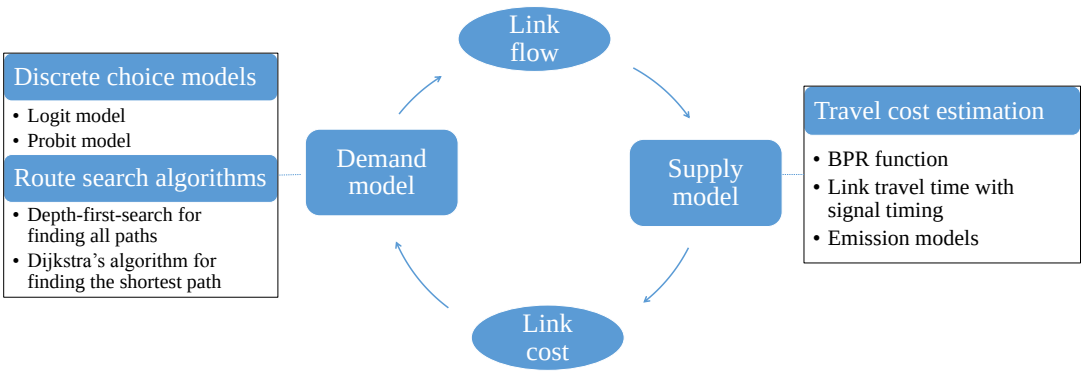

Figure 2.5.: Structure of traffic assignment models.

Figure 2.6.: The transfer between steady state delay and deterministic delay.

distributions, and the queue performs as a queue with server vacations. Although Kimber and Hollis (1979) developed the coordinate technique, the focus of the delay model is not on signalized intersections. Hence, they did not consider periodic traffic lights. Instead, they adjusted their model by applying parameters when the signal timing is involved. For different arrival distributions, the delay models are adjusted accordingly. The delay model with regular arrivals was developed by Wardrop (1952), and the delay model with binomial arrivals was developed by Beckmann et al. (1955) (Allsop, 1972b). Pacheco et al. (2017) built their delay model in the queue with server vacations by formulating the problem with a Markov chain.

The delays of different turning movements are adjusted according to their saturation flows (HCM, 2000). The saturation flow of turning movements, i.ethat is., left turns, right turns, and through movements, can be determined by the turning radius (Kimber, 1986; Wong and Wong, 2003). In HCM (2000), more factors are considered, such as lane widths, heavy vehicles, grades, parking manoeuvres, local buses, pedestrians, area types, and lane utilization in the form of adjustment factors. The saturation flows of different turning movements is are the products of the adjustment factors and the base saturation flow. Specifically, as the saturation flow of permitted left turns is dependent on the opposing through flows, they are differently treated differently by using gap acceptance theory (Akcelik, 1980; HCM, 2000).

Emission models

There are microscopic models and macroscopic models for estimating emissions. Microscopic models are developed to obtain a higher accuracy of the emission estimation (Szeto et al., 2012; Ma et al., 2014). As the macroscopic models require less data (only link length and link travel time), it is more convenient to integrate them with other models. Penic and Penic and Upchurch (1992) developed a macroscopic model based on TRANSYT-7F calibration. Due to its simplification, this model is applied by Benedek and Rilett (1998); Yin and Lawphongpanich (2006) and Chen and Yang (2012). Aziz and Ukkusuri (2012) summarized air pollutants from statistic reports and concluded that carbon monoxide (CO) is the top contributor, which is consistent with the statement of

Yin and Lawphongpanich (2006).

2.4.4. Traffic assignment model integrated with signal setting optimization

Traffic assignment models can be integrated with signal setting optimization. When determining signal control strategies, traffic managers would like to see how drivers react to the strategies and make decisions considering the benefits to the drivers. This meets the assumption of the Stackelberg game, which consists of a leader and a follower. The follower reacts to the leader's action by optimizing their benefits, and the leader makes a final decision considering the reaction from the follower. Hence, this problem is usually formulated as bi-level programming: in the upper level, the signal setting is optimized, and in the lower level, traffic assignment models are applied.

The signal optimization method involved is usually the stage-based method. The stages are given and the green duration or split for each stage is optimized (Smith, 1979b; Yang and Yagar, 1995). Smith (1979b) only considered unsaturated networks in his simple example, whereas Yang and Yagar (1995) apprached the problem in saturated networks. For signal coordination, a common cycle length is also optimized by Chiou (2014). In additional to green duration and cycle length, the start of green, which is relevant to the signal sequence, can also be determined Chiou (2014). Different from previous research, Zhao et al. (2016a) integrated signal setting optimization using the lane-based method with traffic assignment models, but how the capacity of each turning movement changes with the lane allocation was not mentioned.

Traffic assignment models combining signal setting optimization, can be either a UE model (Yang and Yagar, 1995; Chiou, 2014) or a SUE model (Cipriani and Fusco, 2004; Cascetta et al., 2006).

3. Research framework

3.1. Overall methods

This chapter introduces the overall methods of this thesis. Traffic flow distribution forecasting and signal setting optimization are the main issues to be addressed. Traffic assignment models (see Section 2.4) describe how traffic demand distributes in the network. The traffic assignment models are thereby used to forecast traffic flow distribution after left turn prohibition. The signal setting optimization method determines the cycle length, which is the time duration of a complete signal operation; the green duration, which is the time duration of vehicles which turn a direction having the right of way; the start of green, which is the time point when a signal light turns green; and the other intermediate decision variables (see relevant definitions in Section 2.3.1).

The research scope is first clarified, and then the proposed method is explained in a flow chart. The general problem formulation is briefly introduced and its details are expalined in the following chapters. Finally, the notation of decision variables and parameters are summarized.

3.1.1. Research scope

Left turn prohibition is usually applied for a specific period of the day (Koonce et al., 2008). Prohibiting left turns for fixed times can ensure that the vast majority of drivers are aware of this information in advance, and perform their route search accordingly, avoiding unexpected detours. Thus, this thesis concentrates on the long-term decision of the left turn prohibition at a fixed time of day for planning purposes.

The demand distribution is estimated with traffic assignment model. Traffic assignment models do not capture the dynamics of traffic flow. In consideration of a realistic traffic flow distribution, a stochastic user equilibrium (SUE) is applied, because in a SUE model, drivers choose routes according to perceived travel times. In the SUE model used, each link is assumed to have enough capacity for queues. In other words, queues have no physical dimensions.

The signal timing optimization is only applied for the traffic flows of private cars, thus public transportation, cyclists, and pedestrians are thereby excluded. A fixed-time signal control strategy is considered in this work. The traffic flows that influence signal settings are the average values in the fixed-time period. The signal settings of each intersection are locally optimized. For each intersection, a cycle length is optimized, but the largest cycle length is selected as the common cycle length in the network for coordination. However, the signal offsets are not considered in optimization. In the stage-based method, the lanes

of the prohibited left turns are assumed to be assigned for through movements. In the networks studied, there are only signalized intersections, and no unsignalized intersections.

Moreover, as some similar concepts are differently expressed in traffic assignment models and signal setting optimization in previous studies, these concepts are pre-clarified. In traffic assignment models, a network consists of links and nodes. The links represent the movements and the nodes represent intersections in signal setting optimization models. They have the following relationships (see Figure 3.1):

- A network in a traffic assignment model consists of external links and nodes.
- A node in a traffic assignment model includes internal nodes and internal links.
- A node in a traffic assignment model is the same as an intersection in signal setting optimization models.
- Internal links in traffic assignment models are the same as movements in signal setting optimization models.
- An external or internal link may have multiple lanes.
- A movement may be assigned to multiple lanes.
- A lane can be either an approaching lane or an exit lane.
- A lane can be occupied by multiple movements/links.

3.1.2. Proposed method

The objective of this left turn prohibition problem is to minimize the total travel time in the network. Several optimization/decision-making phases are involved in this process: a SUE and signal setting optimization (See Figure 3.2). A SUE, with the objective to minimize the perceived travel time of vehicles in the network, decides the link flows and link travel times. Signal setting optimization, with the objectiveto maximize the reserved capacity or minimize the delay, decides cycle length, green durations, and signal sequences.

The method starts by prohibiting left turns from being selected with a genetic algorithm. Decision variables that decide which left turn is prohibited and meet the relevant constraints are considered to be feasible decision variables. Only the selected feasible decision variables are checked. Given the feasible decision variables, the network is initialized with link free-flow travel times, where the link travel time of prohibited left turns is infinite. The constraints and selection algorithm are explained in Chapter 4.

A SUE runs with two different ways to update link travel time: a BPR function and the travel time based on signal timing. A SUE with a BPR function is applied to see the reaction of drivers to the left turn prohibition. When left turns are prohibited, the original signal settings are not suitable for the network without these left turns, because new signal settings have not been optimized. The new signal settings are optimized with the link flows from a SUE with a BPR function. After completing a SUE with travel time based on signal timing, there is adequate signal timing reflecting the left turn prohibition states. Thus, the reaction of drivers to the corresponding signal settings can be observed. The route choice model used is the multinomial logit model. The details are explained in Chapter 5.

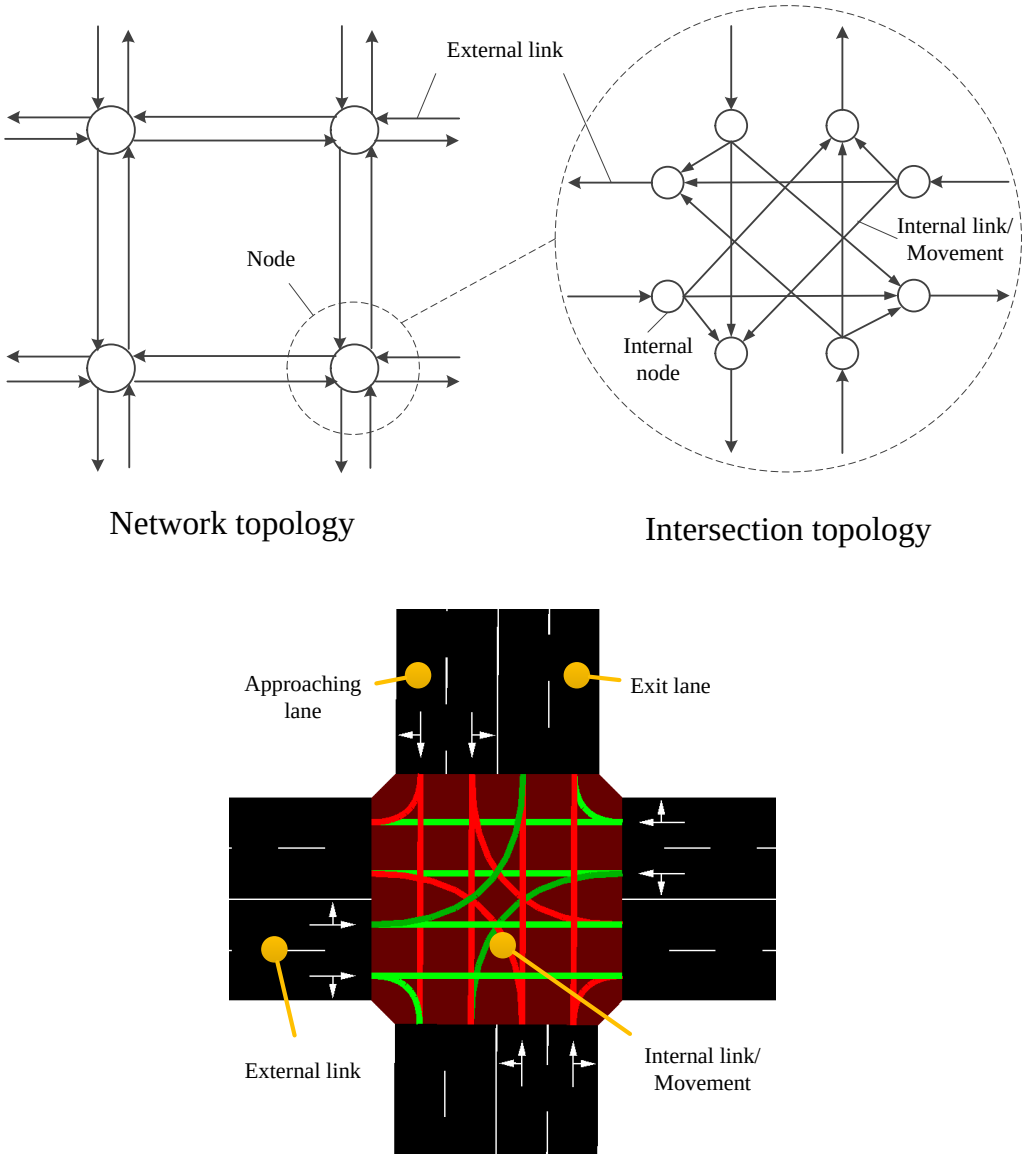

Figure 3.1.: Network and intersection representation.

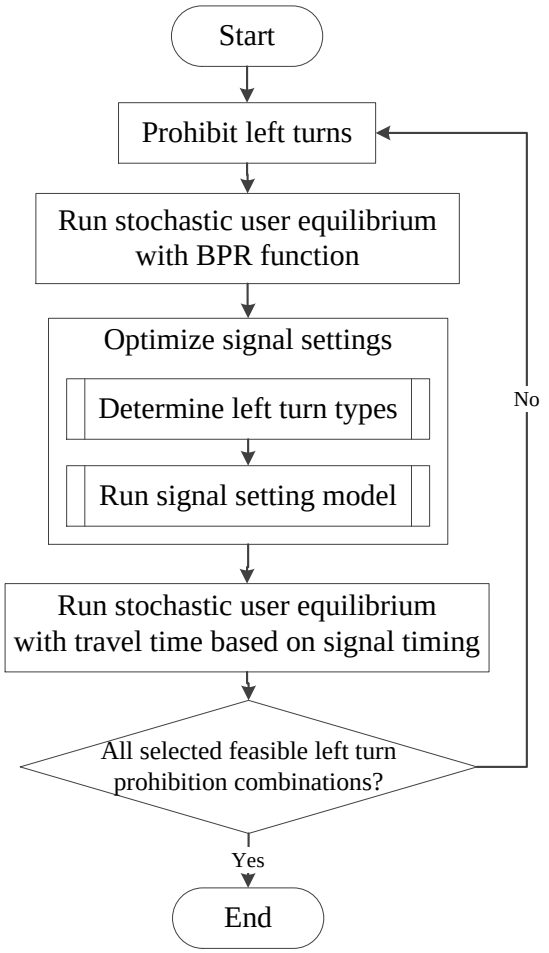

Figure 3.2.: Flow chart of the left turn prohibition problem.

Before signal settings are optimized, left turn phasing types, which refer to permitted left turns and protected left turns, should be determined for non-prohibited left turns because the change of traffic flows causes the change of left turn types. According to the left turn phasing types, the conflict matrices and saturation flows of each lane are adjusted for preparation of the signal optimization. With left turn phasing types, signal settings can be optimized or determined based on lane-based or stage-based method. This study used both the lane-based method, because it can better assign lane markings, and the stage-based method, because this method is widely applied in practice. After optimizing signal settings, green durations, starts of green, cycle length and lane assignments, travel costs can be estimated. The details are explained in Chapter 6.

3.1.3. Evaluation

The proposed method is theoretically evaluated on artificial networks and an actual network from the south of Hanover in Germany. The total travel time without left turn prohibition is used as a benchmark for comparison with the total travel time with left

turn prohibition. The signal timing plans before and after the left turn prohibition are also presented to give insight into the left turn prohibition problem.

Further, the optimal left turn prohibition combination is evaluated with the VISSIM simulation tool. The total travel time, delays, and number of stops at intersections before and after the left turn prohibition in the VISSIM model are compared.

3.2. Problem formulation

The general formulation of the problem is presented here to provide an overview of the problem, relevant decision/optimization processes, and the interaction of the decision variables.

3.2.1. Left turn prohibition

As mentioned, the objective of the left turn prohibition is to minimize the total travel time. The total travel time is defined as the sum of link travel times multiplied by the link flows. The overall formulation of this problem is presented in Eq. (3.1), where link flows $\mathbf{q}$ and link travel times $\mathbf{t}(\mathbf{q}, \eta)$ are obtained by solving the SUE with travel time based on the signal settings:

$$\min TT(\mathbf{q}, \mathbf{t}(\mathbf{q}, \eta), \mathbf{x}), \tag{3.1}$$

subject to

$$h(\mathbf{q}, \mathbf{t}(\mathbf{q}, \eta), \mathbf{x}) \leq \mathbf{0}, \tag{3.2}$$

where

$TT(\mathbf{q}, \mathbf{t}(\mathbf{q}, \eta), \mathbf{x})$	is the total travel time of networks;
$\mathbf{q}$	is the vector of link flows,
$\mathbf{t}(\mathbf{q}, \eta)$	is the vector of link travel costs,
η	is the vector of signal settings,
$\mathbf{x}$	is the vector of left turn prohibition indicators, and
$h(\mathbf{q}, \mathbf{t}(\mathbf{q}, \eta), \mathbf{x})$	is the related constraints.

3.2.2. Stochastic user equilibrium

The SUE describes how traffic flows distribute in the network while considering the probability of route choices. The goal of a SUE model is to minimize the perceived travel time. In the SUE, drivers repeatedly choose their route based on perceived travel time until any route change would cause higher travel costs for all vehicles. The SUE includes a demand model and a supply model. The demand model, which distributes the traffic demand, is relevant to route choice. The probabilities of route choices are calculated by the logit model, which assumes that the utilities of all the route choices are identically and independently distributed. The path flows are then calculated as the probabilities of each path multiplying the traffic demand between OD pairs. The supply model is to estimate travel costs by applying cost estimation functions: a BPR function and the travel time with signal settings.

Although the SUE model includes an objective function, this is not directly optimized. The flow pattern that minimizes the objective function is the one that generates the overall travel time at the SUE state. Thus, when solving the SUE model, algorithms usually simulate the processes to reach the equilibrium state.

For a SUE with a BPR function with left turn prohibition $\mathbf{x}$ from "Prohibit left turns" in Figure 3.2, the link flows $\mathbf{q}'$ and link travel times $\mathbf{t}(\mathbf{q}')$ are obtained.

$$\min PT'(\mathbf{q}', \mathbf{t}(\mathbf{q}'), \mathbf{x}), \tag{3.3}$$

subject to

$$f(\mathbf{q}', \mathbf{t}(\mathbf{q}'), \mathbf{x}) = \mathbf{0}, \tag{3.4}$$

where

$PT'(\mathbf{q}', \mathbf{t}(\mathbf{q}'), \mathbf{x})$	is the path travel time from the "SUE with BPR function" in Figure 3.2, and
$f(\mathbf{q}', \mathbf{t}(\mathbf{q}'), \mathbf{x})$	is the related constraints.

For the SUE with travel time based on signal settings, with signal settings η from "Optimize signal settings" in Figure 3.2 and left turn prohibition $\mathbf{x}$ from "Prohibit left turns" in Figure 3.2, link flows $\mathbf{q}$ and link travel times $\mathbf{t}(\mathbf{q}, \eta)$ are obtained for each OD pair.

$$\min PT(\mathbf{q}, \mathbf{t}(\mathbf{q}, \eta), \mathbf{x}), \tag{3.5}$$

subject to

$$f(\mathbf{q}, \mathbf{t}(\mathbf{q}, \eta), \mathbf{x}) = \mathbf{0}, \tag{3.6}$$

where

$PT(\mathbf{q}, \mathbf{T}(\mathbf{q}, \eta), \mathbf{x})$	is the path travel time from "SUE with travel time based on signal settings", and
$f(\mathbf{q}, \mathbf{T}(\mathbf{q}, \eta), \mathbf{x})$	is the related constraints.

3.2.3. Signal setting optimization

Signal settings η are defined as cycle length, green durations and starts of green in this thesis. In the lane-based method, lane assignment is a part of signal settings as well. The values could be locally obtained from the lane-based method or the stage-based method. $\mathbf{q}'$ is obtained from "SUE with BPR function" in Figure 3.2 and $\mathbf{x}$ are from "Prohibit left turns" in Figure 3.2:

$$\min TC(\mathbf{q}', \eta, \mathbf{x}), \tag{3.7}$$

subject to

$$g(\mathbf{q}', \eta, \mathbf{x}) \leq \mathbf{0}, \tag{3.8}$$

and

$$g'(\mathbf{q}', \eta, \mathbf{x}) = \mathbf{0}, \tag{3.9}$$

where

$TC(\mathbf{q}', \eta, \mathbf{x})$	is the total costs of intersections in networks, and
$g(\mathbf{q}', \eta, \mathbf{x}), g'(\mathbf{q}', \eta, \mathbf{x})$	are the related constraints.

3.3. Notation

3.3.1. Network and intersection representation

The relationships between traffic assignment models and signal setting optimization models are mentioned in Section 3.1.1. Thus, the internal links in traffic assignment models are expressed as the movements in the signal setting optimization problem. At each intersection, a movement is a turning direction from an arm. If the intersection index is z, the arm index is i and the direction index is j, then the movement (z, i, j) is the turning direction j in arm i at intersection z. The turning directions include left turns, right turns and through movements. U-turns are not considered. Left turns could also be expressed as permissive left turns and protected left turns. The number of approaching lanes of an arm i at intersection z is represented as $N_{L,z,i}$, and the number of exit lanes of movement (z, i, j) is represented as $N_{E,z,i,j}$. Details are listed below:

Network and intersection	**Notations**
External link set	E
External link index	$a \in E$
Number of intersections	N_Z
Intersection index	$z = 1, ..., N_Z$
Number of arms	$N_{A,z}, \forall z = 1, ..., N_Z$
Arm index	$i = 1, ..., N_{A,z}$
Through movement	TH
Right turn	RT
Left turn	LT
Turning direction set	$M = \{TH, RT, LT\}$
Direction index	$j \in M$
Protected left turn	$protLT$
Permitted left turn	$permLT$
Number of approaching lanes	$N_{L,z,i}, \forall z = 1, ..., N_Z, i = 1, ..., N_{A,z}$
Number of approaching lanes for movement	$N_{L,z,i,j}, \forall z = 1, ..., N_Z, i = 1, ..., N_{A,z}, j \in M$
Lane index	$k = 1, ..., N_{L,z,i}$
Number of exit lanes	$N_{E,z,i,j}, \forall z = 1, ..., N_Z, i = 1, ..., N_{A,z}, j \in M$
Stage index	$p, p' = 1, ..., N_{S,z}, \forall z = 1, ..., N_Z$
Origin set	O
Origin index	$o \in O$
Destination set	D
Destination index	$r \in D$
Path set	$P_{o,r}, \forall o \in O, r \in D$
Path index	$\kappa \in P_{o,r}$

3.3.2. Decision variables

The decision variables in the left turn prohibition problem are left turn prohibition indicators. The decision variables of the SUE model are link flows and link travel times.

However, as two signal setting optimization methods are applied, the decision variables in these two methods have a slight difference. Overall, the signal settings are defined as common cycle length c, green duration for movement $g_{z,i,j}$,and start of green for movement $\theta_{z,i,j}$.

In the lane-based method, lane permission indicators $\delta_{z,i,j,k}$, which are relevant to the lane assignment, indicate whether a movement is permitted on the lane. To linearize the lane-based model, one should decide upon the inverse of cycle length and green split, rather than cycle length and green durations. The cycle length and green durations need to be adjusted as $c = 1/\xi$ and $g_{z,i,j} = c \cdot \theta_{z,i,j}$, respectively. For similar purposes, the start of green $\theta_{z,i,j}$ in the lane-based method is in the interval of $[0, 1]$. The actual start of green should be $c\theta_{z,i,j}$. Successor indicators, which are relevant to the signal sequence, indicate whether a movement is the successor of others. Assigned flows, $f_{z,i,j}$, referring to the flow of a movement being assigned for a lane, are used to decide the green durations. The reserved capacity, μ, which indicates the capacity usage at intersections, is also important in the lane-based method.

In the stage-based method, the lane permission indicators are given. Cycle length and green durations of stages are directly calculated based on traffic manuals. Then the green duration of stages can be translated to green duration for movement, in order to estimate travel time per movement later on. The starts of green of stages are decided based on signal sequence optimization, and then are translated for each movement.

For all $a \in E, z = 1, ..., N_Z, i = 1, ..., N_{A,z}, l = 1, ..., N_{A,z}, j \in M, m \in M, k = 1, ..., N_{L,z,i}$, the following decision variables are decided in this thesis:

Decision variables	**Notations**	**Domain**
Left turn prohibition indicator	$x_{z,i}$	$x_{z,i} \in \{0, 1\}$
Link flow from "SUE with BPR function"	$q'_a, q'_{z,i,j}$	$q'_a, q'_{z,i,j} \in [0, \infty)$
Link travel time from "SUE with BPR function"	$t'_a, t'_{z,i,j}$	$t'_a, t'_{z,i,j} \in [0, \infty)$
Signal setting	$\eta_z = \{c, g_{z,i,j}, \theta_{z,i,j}\}$	$\eta_z \in \eta$
Lane permission indicator	$\delta_{z,i,j,k}$	$\delta_{z,i,j,k} \in \{0, 1\}$
Successor indicator	$\Omega_{z,i,j,l,m}$	$\Omega_{z,i,j,l,m} \in \{0, 1\}$
Number of stages	$N_{S,z}$	$N_{S,z} \in [1, \infty)$
Green duration for stage (s)	$g_{z,p}$	$g_{z,p} \in [g_{min,z,p}, c]$
Green split for lane	$\Phi_{z,i,k}$	$\Phi_{z,i,K} \in [g_{min,z,i,j}/c_z, 1]$
Green split for movement	$\phi_{z,i,j}$	$\phi_{z,i,j} \in [g_{min,z,i,j}/c_z, 1]$
Green duration for movement (s)	$g_{z,i,j}$	$g_{z,i,j} \in [g_{min,z,i,j}, \infty)$
Green duration for lane (s)	$g_{z,i,k}$	$g_{z,i,k} \in [g_{min,z,i,k}, \infty)$
Start of green for lane	$\Theta_{z,i,k}$	$\Theta_{z,i,k} \in [0, 1]$
Start of green for movement	$\theta_{z,i,j}$	$\theta_{z,i,j} \in [0, 1]$
Assigned flow (veh/h)	$f_{z,i,j}$	$f_{z,i,j} \in [0, \infty)$
Cycle length per intersection (s)	c_z	$c_z \in [c_{min}, c_{max}]$
Common cycle length (s)	c	$c \in [c_{min}, c_{max}]$
Inverse of cycle length (s)	ξ_z	$\xi_z \in [1/c_{max}, 1/c_{min}]$

Decision variables	**Notations**	**Domain**
Reserved capacity	μ_z	$\mu \in (0, \infty)$
Link flow from "SUE with travel time based on signal settings"	$q_a, q_{z,i,j}$	$q_a, q_{z,i,j} \in [0, \infty)$
Link travel time from "SUE with travel time based on signal settings"	$t_a, t_{z,i,j}$	$t_a, t_{z,i,j} \in [0, \infty)$

Once the values of the decision variables are determined, the values of the intermediate variables can be obtained. The list of intermediate variables is displayed below:

Intermediate variables	**Notations**
Number of paths	$N_{P,o,r}$
Capacity per lane (veh/h)	$\mu_{z,i,k}$
Capacity per movement (veh/h)	$\mu_{z,i,j}$
Degree of saturation per lane	$\rho_{z,i,k}$
Degree of saturation per movement	$\rho_{z,i,j}$
Delay per lane	$d_{z,i,k}$
Delay per movement	$d_{z,i,j}$

3.3.3. Parameters

The values of the parameters should be given before testing the proposed method.

Parameters	**Notations**
OD demand	$q_{o,r}$
Scale parameter in logit model	γ
Parameter in BPR function	α
Parameter in BPR function	β
Free flow travel time	$t_{0,a}, t_{0,z,i,j}$
Saturation flow per lane(veh/h)	$s_{z,i,k}$
Saturation flow per movement(veh/h)	s_j
Observation time (h)	T
Last number of iterations	N_I
Convergence criteria of SUE	ϵ
Conflict matrix	Ψ_z
Maximum cycle length (s)	c_{max}
Minimum cycle length (s)	c_{min}
Minimum green duration for movement (s)	$g_{min,z,i,j}$
Minimum green duration for stage (s)	$g_{min,z,p}$
Arbitrary large positive constant	H
Difference between actual green time and effective green time (s)	e
Clearance time (s)	$\omega_{z,i,j,l,m}$
Intergreen time (s)	$\omega_{z,p,p'}$

4. Left turn prohibition

4.1. Overall

In this chapter, the way that feasible left turn prohibition combinations are selected is explained. In the beginning, the detailed composition of the objective function is presented, followed by the relevant constraints. As the lane assignment is used in the lane-based method but not in the stage-based method, the constraints are slightly different. Finally, the algorithm to select left turn prohibition combinations is explained.

4.2. Objective function

As mentioned in the previous section, the objective of the left turn prohibition problem is to minimize the total travel time of networks. To be more specific, the total travel time is the sum of the total travel time of external links and the total travel time of internal links (see Eq. (4.2)). The values of left turn prohibition indicators, $x_{z,i}$, are assigned here.

For all $z = 1, ..., N_Z, i = 1, ..., N_{A,z}$,

$$x_{z,i} = \begin{cases} 1, & \text{left turn in arm } i \text{ at intersection } z \text{ is prohibited and} \\ 0, & \text{if otherwise} \end{cases} \tag{4.1}$$

Thus, if a left turn is prohibited, the relevant travel time is infinite. The prohibited left turn flow is redistributed to other links, so the link flows and link travel times of other links may change.

$$\begin{aligned} \min TT = & \sum_{a \in E} q_a \cdot t_a(q_a) + \\ & \sum_{z=1}^{N_Z} \sum_{i=1}^{N_{A,z}} \sum_{j \in M/\{LT\}} q_{z,i,j} \cdot t_{z,i,j}(q_{z,i,j}, \eta_z) + \\ & \sum_{z=1}^{N_Z} \sum_{i=1}^{N_{A,z}} (1 - x_{z,i}) \cdot q_{z,i,LT} \cdot t_{z,i,LT}(q_{z,i,LT}, \eta_z). \end{aligned} \tag{4.2}$$

The link flows are obtained from the SUE model with travel time based on signal settings. The link travel times of the internal links are the sum of the free flow travel time and the link delay, which is the function of link flows and signal settings. The delay formula is explained in Section 5.

For all $z = 1, ..., N_Z, i = 1, ..., N_{A,z}, j \in M$

$$t_{z,i,j} = t_{0,z,i,j} + d_{z,i,j}(q_{z,i,LT}, \eta_z). \tag{4.3}$$

If a left turn is prohibited, the link travel time goes to infinity. Therefore, no vehicles would select the prohibited left turn link. The method to adjust the travel times of left turn links is:

$\forall z = 1, ..., N_Z, i = 1, ..., N_{A,z},$

$$t_{z,i,LT} = \begin{cases} +\infty, \text{ if } x_{z,i} = 1 \text{ and} \\ t_{z,i,LT}, \text{ if } x_{z,i} = 0 \end{cases} . \tag{4.4}$$

4.3. Constraints

4.3.1. For the lane-based method and the stage-based method

The left turn prohibition combinations should confirm the connectivity of networks between each OD pair. For example, in Figure 4.1, if both left turns in red are prohibited, vehicles cannot go from the origin to the destination. The left turn prohibition combination is therefore not feasible. Vehicles should find at least one path from one origin to one destination. The left turn prohibition combinations must ensure that the number of paths between one OD pair is greater than or equal to 1. The number of paths is the function of left turn prohibition combinations.

For all $o \in O, r \in D, z = 1, ..., N_Z, i = 1, ..., N_{A,z}$, the constraint below holds:

$$N_{P,o,r} \geq 1. \tag{4.5}$$

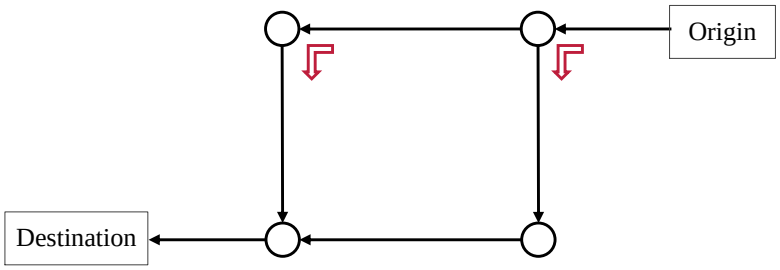

Figure 4.1.: Example of connectivity between an OD pair.

4.3.2. For stage-based method only

In the stage-based method, the connectivity of networks is still ensured (See Eq. (4.5)). The stage-based method requires lane markings, but the lane markings of the prohibited left turns are not available anymore. The lane markings of the prohibited left turns

should be used for other movements. In this thesis, the lane markings of the prohibited left turns are assigned for through movements. This causes another problem: the number of approaching lanes for through movements may be more than the number of exit lanes for through movements (Figure 4.2). Once the number of exit lanes is less than the number of approaching lanes, safety problems may be generated when vehicles merge into one lane. Thus, after the lanes of the prohibited left turns turn to through movements, the number of exit lanes must be larger. Otherwise, these left turns cannot be prohibited.

For all $z = 1, ..., N_Z, i = 1, ..., N_{A,z}$,

$$N_{L,z,i,TH} \leq N_{E,z,i,TH}. \tag{4.6}$$

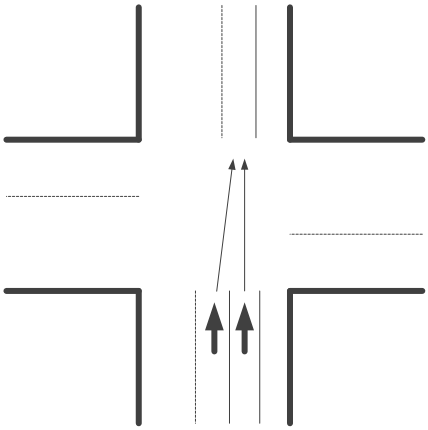

Figure 4.2.: Example of a smaller number of exit lanes than approaching lanes.

4.4. Algorithms

The left turn prohibition combinations are selected by a genetic algorithm. A genetic algorithm is inspired by natural selection. The chromosome represents the decision variables. After selection, crossover, and mutation, the chromosomes with adequate fitness values are finally selected (Figure 4.3).

The left turn prohibition indicators, $x_{z,i}, \forall z = 1, ..., N_Z, i = 1, ..., N_{A,z}$, are encoded as 0/1 binary variables. The size of a chromosome is the number of left turns. The fitness function is the objective function in Eq. (4.2). The left turn prohibition combinations with smaller total travel times are selected for the next generation.

The genetic algorithm is implemented using the Java genetic algorithm package (Jgap) (Meffert and Rotstan, 2015). The default configuration of Jgap is applied. The crossover rate is 35% and the mutation rate is 1/12. The top 90% of the user-specified population size is treated as elites and remains in the next generation.

4.5. Performance criteria

The total travel time of the optimal left turn prohibition result is compared to the total travel time without left turn prohibition. The change of the total travel time before and after left turn prohibition is calculated as

$$\Delta = \frac{TT_{optimal} - TT_0}{TT_0}, \tag{4.7}$$

where Δ is the change of the total travel time as a percent, $TT_{optimal}$ is the optimal total travel time, and TT_0 is the total travel time without left turn prohibition.

The change of the total travel time Δ is expressed as a percent. If Δ is negative, it indicates a reduction in the total travel time. If Δ is positive, it indicates an increase in the total travel time.

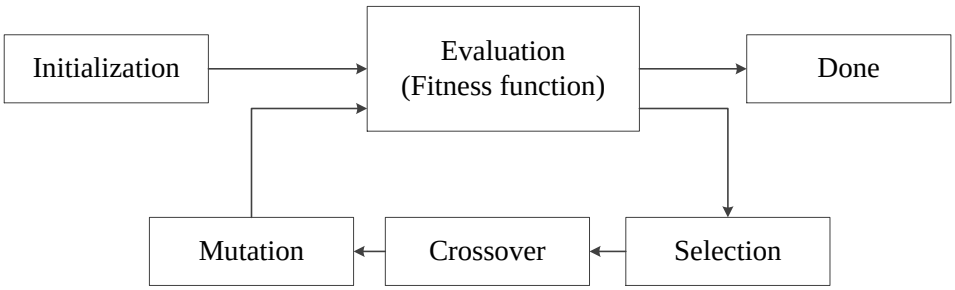

Figure 4.3.: Processes of genetic algorithm.

5. Stochastic user equilibrium

5.1. Overall

This chapter presents the route choice model being used and the methods of travel time estimation. It is necessary to decide lane flows and to adjust saturation flows for better estimations of travel time. The methods of lane flow calculation and saturation adjustment are also explained. Finally, the algorithm of solving the SUE model is stated.

5.2. Route choice

The route choice model is a multinomial logit model, as this thesis does not focus on the development of discrete choice models. The key to the multinomial logit model is the composition of the utility function. The independent variables involved must have linear relationships with the utility. Although the utility function could contain many factors such as users' requirements and preferences, the path travel time is expressed as the utility. A longer path travel time means a lower probability of a path being chosen.

For all $o \in O, r \in D$,

$$\mathcal{P}_\kappa = \frac{Exp(-\gamma \cdot t_\kappa)}{\sum_{\kappa' \in P_{o,r}} Exp(-\gamma \cdot t_{\kappa'})}, \tag{5.1}$$

where

$\mathcal{P}_\kappa$ is the probability of path κ being chosen, and
t_κ is the travel time of path κ.

Given the OD demand, $q_{o,r}, \forall o \in O, r \in D$, the path flows can be calculated:

$$q_{o,r,\kappa} = q_{o,r} \cdot \mathcal{P}_\kappa. \tag{5.2}$$

When the link-path matrix of OD pairs multiplies the path flows, the link flows are obtained. A link-path matrix records whether a link is on a path. If a link is on a path, the relevant value is 1; if the link is not on the path, the value is 0. Eq. 5.3 shows the method to obtain link flows.

$$q_a = \Lambda_{o,r} \cdot q_{o,r,\kappa}, \forall a \in E, o \in O, d \in D, \tag{5.3}$$

where $\Lambda_{o,r}$ is the link-path matrix of OD pair o, r.

5.3. Travel time with the BPR function

Before the signal settings are optimized, they are not available. The BPR function is thereby applied to both external and internal links. In a BPR function, link travel times increase as link flows increase. The increasing trend becomes apparent when the link flows are closed to the capacity. The capacity of a link is the product of the saturation flow and the number of lanes. The parameters α and β can be obtained by data calibration:

$\forall a \in E, z = 1, ..., N_Z, i = 1, ..., N_{A,z}, j \in M$

$$t_a(q_a) = t_{0,a} \cdot \left(1 + \alpha \cdot \left(\frac{q_a}{Q_a}\right)^{\beta}\right), \tag{5.4}$$

and

$$t_{z,i,j}(q_{z,i,j}) = t_{0,z,i,j} \cdot \left(1 + \alpha \cdot \left(\frac{q_{z,i,j}}{Q_{z,i,j}}\right)^{\beta}\right). \tag{5.5}$$

5.4. Travel time with signal timing

After signal settings are optimized, travel time with signal timing is suitable. As mentioned in the previous section, link travel time is the sum of the free-flow travel time of the link and link delay. As the link delay is generated by signal settings, only internal links are considered. For external links, the BPR function is applied as in Eq. 5.4:

$\forall z = 1, ..., N_Z, i = 1, ..., N_{A,z}, j \in M$

$$t_{z,i,j} = t_{0,z,i,j} + d_{z,i,j}(q_{z,i,LT}, \eta_z). \tag{5.6}$$

The delay formula developed by Akcelik (1980) is used in this thesis. The delay formula consists of uniform delay and incremental delay. The uniform delay is generated by periodic red lights. The incremental delay is caused by stochastic arrivals of vehicles:

$\forall z = 1, ..., N_Z, i = 1, ..., N_{A,z}, j \in M,$

$$d_{z,i,j} = d_{1.z,i,j} + d_{2,z,i,j}, \tag{5.7}$$

where $d_{1.z,i,j}$ is the uniform delay of internal link (i, j) at intersection z, and $d_{2,z,i,j}$ is the incremental delay.

However, an internal link may have multiple lanes. As the queue lengths in different lanes could vary, the waiting times of vehicles in different lanes are different. Hence, the link delay is the average delay of the relevant lanes if the internal link is on the lanes (see Eq. 5.8 and Eq. 5.9).

Let $\delta_{z,i,j,k}$ be the lane permission indicator. If $\delta_{z,i,j,k} = 1$, the internal link (i, j) at intersection z is on lane k; if $\delta_{z,i,j,k} = 0$, it is not on lane k. Note that $\delta_{z,i,j,k}$ are the

decision variables in the lane-based method, whereas the values of network configuration are given in the stage-based method.

For all $z = 1, ..., N_Z, i = 1, ..., N_{A,z}, j \in M, k = 1, ..., N_{L,z,i}$,

$$d_{1,z,i,j}(\eta) = \frac{\sum_{k=1}^{L_{z,i}} \delta_{z,i,j,k} \cdot q_{z,i,j,k} \cdot d_{1,z,i,k}(\eta)}{q_{z,i,j}}, \tag{5.8}$$

and

$$d_{2,z,i,j}(\eta) = \frac{\sum_{k=1}^{L_{z,i}} \delta_{z,i,j,k} \cdot q_{z,i,j,k} \cdot d_{2,z,i,k}(\eta)}{q_{z,i,j}}. \tag{5.9}$$

Therefore, the delay per lane should be calculated in order to calculate the link delay. The uniform delay and the incremental delay of a lane are calculated using Eq. (5.10) and (5.11).

For all $z = 1, ..., N_Z, i = 1, ..., N_{A,z}, k = 1, ..., N_{L,z,i}$,

$$d_{1,z,i,k}(\eta) = \frac{0.5c \cdot (1 - g_{z,i,k}/c)^2}{1 - \min(1, \rho_{z,i,k}) \cdot g_{z,i,k}/c}, \tag{5.10}$$

and

$$d_{2,z,i,k}(\eta) = \begin{cases} 900T \left[(\rho_{z,i,k} - 1) + \sqrt{(\rho_{z,i,k} - 1)^2 + \dfrac{12(\rho_{z,i,k} - \rho_{0,z,i,k})}{s_{z,i,k} \cdot g_{z,i,k} \cdot T/c}} \right] & \text{if } \rho_{z,i,k} \geq \rho_{0,z,i,k} \\ 0, \text{ if otherwise} \end{cases}, \tag{5.11}$$

where

$$\rho_{0,z,i,k} = 0.67 + \frac{s_{z,i,k} \cdot g_{z,i,k}}{600}. \tag{5.12}$$

In the delay function, the values of lane flow, lane saturation flows, and signal settings should be prepared for delay estimation. Signal settings are from signal setting optimization, but lane flows need to be calculated, and saturation flows need to be adjusted.

In a SUE model, it takes several iterations to find the equilibrium state. In different iterations, drivers may choose different lanes of a link, and then the lane flows of each iteration may be different and would need to be calculated. Saturation flows for certain turning direction are fixed, but the saturation flows of lanes are influenced by the flow compositions of different turning directions. Thus, for each iteration, the saturation flows on shared lanes should also be determined. With both lane flows and saturation flows of lanes, the delay estimation can proceed.

5.4.1. Lane flow calculation

A lane can either be shared by multiple movements or not. $q_{z,i,j,k}$ is the flow of movement (i,j) on lane k at intersection z. The link flow of the movement (i,j) is the sum of all vehicles turning (i,j) in different lanes:

$$q_{z,i,j} = \sum_{k=1}^{N_{L,z,i}} q_{z,i,j,k}, \forall z = 1, ..., N_Z, i = 1, ..., N_{A,z}, j \in M, \tag{5.13}$$

where $q_{z,i,j,k}$ is the flow of movement (i,j) to lane k.

When a movement occupies multiple lanes, vehicles have to choose one lane. They intend to choose the lane with a shorter queue. In the signal setting optimization model, lane allocation can be optimized from the lane-based method or obtained from the stage-based method. The lane permission indicators $\delta_{z,i,j,k}$ mentioned in Chapter 3 refer to whether a movement is permitted on a lane. Drivers who intend to turn (i,j) can only choose the lanes where that movement (i,j) is permitted.

In order to know how drivers will choose lanes, $\delta'_{z,i,j,k}$ is assigned as the indicator representing whether drivers turning (i,j) choose lane k. If $\delta'_{z,i,j,k} = 1$, drivers turning movement (i,j) select lane k; if $\delta'_{z,i,j,k} = 0$, they select a different lane. The initial values of $\delta'_{z,i,j,k}$ are equal to $\delta_{z,i,j,k}$ because all permitted lanes can be chosen.

If no turning drivers (i,j) select lane k, $q_{z,i,j,k}$ should be 0. For all $lz = 1, ..., N_Z, i = 1, ..., N_{A,z}, j \in M, k = 1, ..., N_{L,z,i}$, if $\delta'_{z,i,j,k} = 0$,

$$q_{z,i,j,k} = 0. \tag{5.14}$$

If one movement occupies multiple lanes, the flow ratios of adjacent lanes tend to be equal. Vehicles tend to select the lane with the shorter queue, so the flow ratios of different lanes should be equal. Then Eq. (5.15) holds.

For all $z = 1, ..., N_Z, i = 1, ..., N_{A,z}, j \in M, k = 1, ..., N_{L,z,i} - 1$, if $\delta'_{z,i,j,k} = 1$ and $\delta'_{z,i,j,k+1} = 1$,

$$\sum_{j \in M} \frac{q_{z,i,j,k}}{s_{j,k}} - \sum_{j \in M} \frac{q_{z,i,j,k+1}}{s_{j,k+1}} = 0. \tag{5.15}$$

By solving linear equations (5.13) through (5.15), $q_{z,i,j,k}$ are determined. The equations are solved with JAMA (Java Matrix Package), a package created to solve linear equations (Hicklin et al., 2012).

However, although the flow ratios tend to be identical, it is possible that no matter how drivers choose lanes, the flow ratios cannot be equal. In Figure 5.1, the example shows how this case happens. Through movement is permitted in both Lane 1 and Lane 2. As there are many right turn vehicles in Lane 1, the possibility that the through vehicles will choose Lane 1 is very low because a long queue means a long waiting time. The value of $\delta'_{z,i,TH,1}$ should be 0 because no through vehicles would want to choose this lane. If this

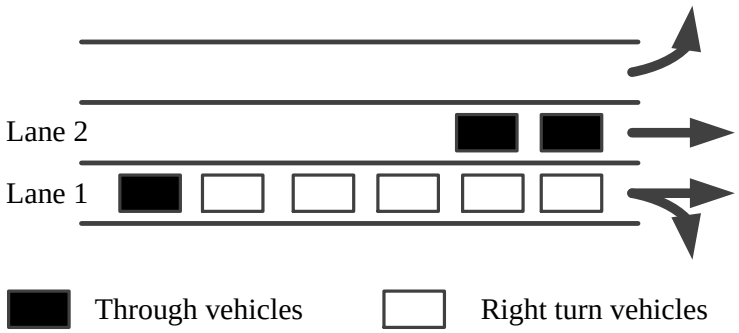

Figure 5.1.: Example of non-equal flow ratios in adjacent lanes.

case is ignored, the value of $q_{z,i,TH,1}$ must be negative to reduce the flow ratio of Lane 1. The negative value is not feasible for a traffic flow.

If the flow ratios of adjacent lanes are not equal, drivers will choose the lane with a shorter queue. In this case, the value of $\delta'_{z,i,j,k}$ changes to 0 to represent the real choice behaviour of drivers. The flow chat in Figure 5.2 below shows the processes of calculating $q_{z,i,j,k}$. After solving the linear equations, all $\delta'_{z,i,j,k}$ with negative $q_{z,i,j,k}$ are assigned to be 0. The linear equations are solved again until no $q_{z,i,j,k}$ is negative.

Finally, the flow of lane k, $q_{z,i,k}$ can be calculated by:

$$q_{z,i,k} = \sum_{j \in M} q_{z,i,j,k}, \forall z = 1, ..., N_Z, i = 1, ..., N_{A,z}. \tag{5.16}$$

5.4.2. Adjustment of saturation flows

A lane could be occupied by multiple internal links or movements. The lane saturation flow, which is the important input of the lane delay in Eq. (5.11), should be a weighted value of the saturation flows of relevant movements if these movements share lanes (HBS, 2001). Eq. (5.17) must be calculated in every iteration because $q_{z,i,j,k}$ changes in every iteration.

For all $z = 1, ..., N_Z, i = 1, ..., N_{A,z}, i = 1, ..., N_{L,z,i}$,

$$s_{z,i,k} = \frac{1}{\sum_{j \in M} \frac{(q_{z,i,j,k}/q_{z,i,k}) \cdot \delta_{z,i,j,k}}{s_{j,k}}}, \tag{5.17}$$

where $s_{j,k}$ is the saturation flow of turning direction j on exclusive lane k.

Saturation flows are relevant to turning radius (Kimber, 1986; Wong and Heydecker, 2011), so the saturation flows of different turning directions should be different. Although in HCM (2000), saturation flows are also influenced by area type, lane widths, parking,

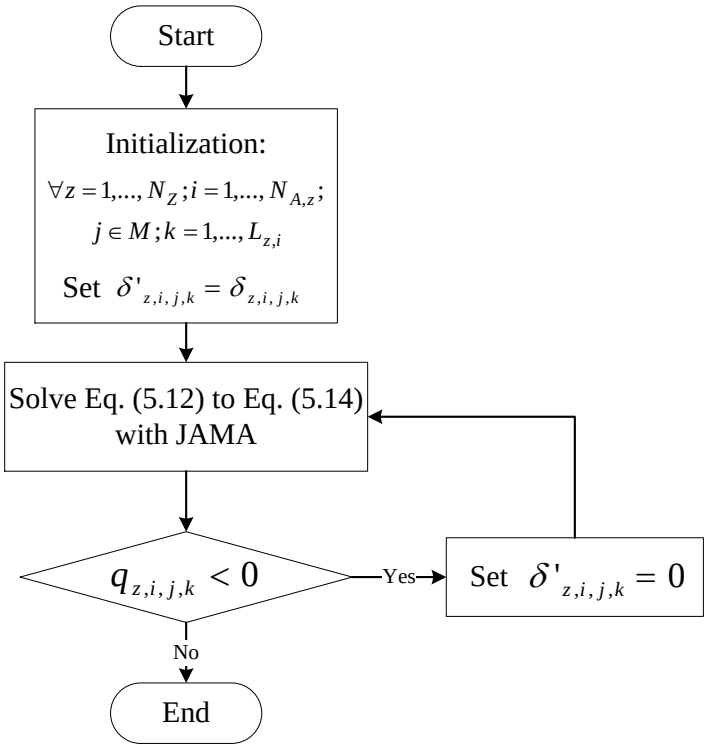

Figure 5.2.: Flow chat of calculation of the flow of vehicles choosing a lane.

grade, and bus blockage, which are highly relevant to network and road geometry, these factors are not considered for planning purposes. In the model, only turning direction influences the saturation flows.

Let $s_{j,k}$ be the saturation flow of exclusive lanes per movement. The saturation flows of through movements, right turns and protected left turns per lane in HCM (2000) are adjusted by a base saturation flow multiplying adjustment factors:

$\forall k = 1, ..., N_{L,z,i}, z = 1, ..., N_Z,$

$$s_{TH,k} = s_{0,k}, s_{RT,k} = 0.85 s_{0,k}, s_{protLT,k} = 0.95 s_{0,k}, \tag{5.18}$$

where $s_{0,k}$ is the base saturation flow of lane k (veh/h), $s_{TH,k}$ is the saturation flow of through movements (veh/h), $s_{RT,k}$ is the saturation flow of right turns (veh/h), and $s_{protLT,k}$ is the saturation flow of protected left turns (veh/h).

Permitted left turns are interrupted by opposing through movements, so the saturation flow of permitted left turns is dependent on the flow of opposing through movements. To obtain the saturation flow of permitted left turns, one needs to calculate the filtered saturation flow. The filtered saturation flow is developed from gap acceptance theory, so the possible number of gaps is estimated. However, the saturation flow is also influenced by the signal settings. In the green duration, opposing through vehicles are cleared first,

and the rest of green duration is used by permitted left turn vehicles. Therefore, signal settings play a role in saturation flow adjustment of permitted left turns. At the end of the green duration, the left turn vehicles in the waiting area can go through the intersection, which is an extra capacity. The method of adjustment on permitted left turn saturation flow follows Akcelik (1980).

For all $z = 1, ..., N_Z, i = 1, ..., N_{A,z}$,

$$s_{filtered} = \frac{q_{z,i,TH} \cdot Exp(-q_{z,i,TH} \cdot t_c)}{1 - Exp(-q_{z,i,TH} \cdot t_f)}, \tag{5.19}$$

where $s_{filtered}$ is the filtered saturation flow (veh/s), $q_{z,TH}$ is the flow of through movement (veh/s), t_c is the critical gap with a value of 4.5 s, and t_f is the follow-up headway with a value of 2.5 s. Then, the saturation flow of permitted left turns is calculated:

$\forall k = 1, ..., N_{L,z,i}, i = 1, ..., N_{A,z}, z = 1, ..., N_Z$,

$$s_{permLT,k} = s_{TH,k} \frac{s_{filtered} \cdot g_u + n_f}{0.5 g_{z,i,LT}}, \tag{5.20}$$

where

$s_{permLT,k}$	is the saturation flow of permitted left turns (veh/h),
$g_u = \max(0, \frac{s_{TH,k} g_{i,permLT} - f_{THC}}{s_{TH,k} - q_{z,i,TH}})$	is the unsaturated part of the green period for the opposing through movement (s), and
n_f	is the number of vehicles passing during the amber period.

The value of n_f is is predefined as 1.5 veh in Akcelik (1980) and HCM (2000).

5.5. Algorithms

5.5.1. Method of successive averages

The SUE model is solved using the method of successive averages (MSA). This algorithm describes the process of how drivers choose routes and react to different path travel times. After repeating the simulated process of choosing routes in several iterations, the link flows in the network go to convergence. In every iteration, the convergence is checked until the link flows to meet the convergence criteria. The criteria with adjustment to this problem is based on Sheffi (1985):

$$\frac{\sqrt{\sum_{a \in E} (\overline{q}_a^{n+1} - \overline{q}_a^n)^2 + \sum_{z=1}^{N_Z} \sum_{i=1}^{N_{A,z}} \sum_{j \in M} (\overline{q}_{z,i,j}^{n+1} - \overline{q}_{z,i,j}^n)^2}}{\sum_{a \in E} \overline{q}_a^n + \sum_{z=1}^{N_Z} \sum_{i=1}^{N_{A,z}} \sum_{j \in M} \overline{q}_{z,i,j}^n} \leq \epsilon, \tag{5.21}$$

where $\overline{q}_a^n, \overline{q}_{z,i,j}^n$ is the average value over the last N_I iteration of the iteration n. $\overline{q}_a^n$ is calculated in Eq. (5.22):

$$\overline{q}_a^n = \frac{1}{N_I} \sum_{m=0}^{N_I - 1} q_a^{n-m}, \forall a \in E. \tag{5.22}$$

Although Eq. (5.22) only refers to the external links, it is also applicable to internal links.

The pseudo code of the MSA is displayed in Algorithm 1. In the MSA, stochastic loading is applied to calculate the link flows. The relevant algorithm is the STOCH algorithm which is explained in the next section.

Algorithm 1 Method of successive averages

Require: $t_{0,a}, t_{z,i,j}, \eta, \gamma, \alpha, \beta, \epsilon, N_I$
Ensure: $q_a, q_{z,i,j}$
function MSA
  $t_a^0 \leftarrow t_{0,a}$, $t_{z,i,j}^0 \leftarrow t_{0,z,i,j}$
  $q_a^1 \leftarrow$ STOCH algorithm, $q_{z,i,j} \leftarrow$ STOCH algorithm
  $y \leftarrow 0$
  for Eq. (5.21) **do**
    $n \leftarrow n + 1$
    $t_a^n \leftarrow$ Eq. (5.4), $t_{z,i,j}^n \leftarrow$ Eq. (5.5) or Eq. (5.6)
    $y_a^n \leftarrow$ STOCH algorithm
    $q_a^{n+1} \leftarrow (1/n)(y_a^n - q_a^n) + q_a^n$
  end for
  return $q_a, q_{z,i,j}$
end function

5.5.2. The STOCH algorithm

The STOCH algorithm is also called Dial's algorithm (Dial, 1971). This algorithm can be applied in networks with a multinomial logit route choice model. In the STOCH algorithm, path enumeration is avoided, and only reasonable paths between OD pairs are considered. This is believed to be more efficient than path enumeration.

The reasonable paths in a STOCH algorithm are relevant to the shortest paths between OD pairs. As Dijkstra's algorithm can be used in the graph with positive link weights and cycles, it is suitable to find the shortest path in STOCH algorithm. The details of Dijkstra's algorithm are found in papers by Dijkstra (1959) and Sedgewick (1988).

In addition to the shortest route search, the upstream links and downstream links must also be defined. A link a has a *start* node and an *end* node. The notation $\mathcal{U}_{node}$ is used to denote the set of upstream links of a node, and $\mathcal{D}_{node}$ as the set of downstream links of a node. In Figure 5.3, $\mathcal{U}_{start}$ includes "Link 1" and "Link 2", $\mathcal{U}_{end}$ includes "Link 3" and "Link 4", and $\mathcal{D}_{end}$ includes "Link 5" and "Link 6". $\mathcal{U}_{start}, \mathcal{U}_{end}, \mathcal{D}_{end}$ are important in the STOCH algorithm.

Link likelihoods, link weights and link flows are sequentially calculated with Eq. (5.23), Eq. (5.24), and Eq. (5.25), respectively. All of these three equations are applicable to $L_{z,i,j}, w_{z,i,j}, q_{z,i,j}$ as well.

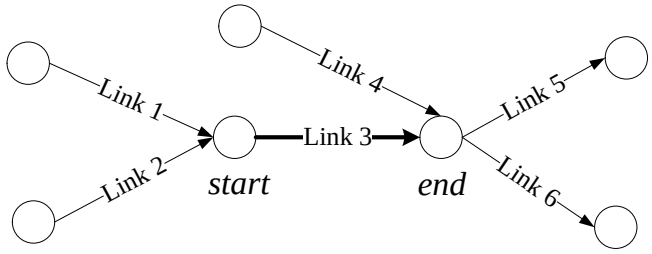

Figure 5.3.: Definition of upstream links and downstream links.

For all $o \in O, r \in D, a \in E$,

$$L_a = \begin{cases} Exp(\gamma \cdot (t_{o,end} - t_{o,start} - t_a)), & \text{if } t_{o,start} < t_{o,end} \text{ and } t_{start,r} > t_{end,r} \text{ and} \\ 0, & \text{if otherwise} \end{cases}, \quad (5.23)$$

where

L_a	is the likelihood of link a,
γ	is the scale parameter in the multinomial logit model,
$t_{o,end}$	is the shortest travel time from origin o to the end node of link a,
$t_{o,start}$	is the shortest travel time from origin o to the start node of link a,
$t_{start,r}$	is the shortest travel time from the start node of link a to destination r, and
$t_{end,r}$	is the shortest travel time from the end node of link a to destination r.

$$w_a = \begin{cases} L_a, & \text{if } start = o \text{ and} \\ L_a \sum_{a' \in \mathcal{U}_{start}} w_{a'} & \text{if otherwise} \end{cases}, \quad (5.24)$$

where w_a is the link weight of link a; $\mathcal{U}_{start}$ is the set of upstream links of the start node of link a.

$$y_a = \begin{cases} q_{o,r} \dfrac{w_a}{\sum_{a' \in \mathcal{U}_{end}} w_{a'}}, & \text{if } end = r \text{ and} \\ \sum_{a' \in \mathcal{D}_{end}} y_{a'} \dfrac{w_a}{\sum_{a' \in \mathcal{U}_{end}} w_{a'}}, & \text{if otherwise} \end{cases}, \quad (5.25)$$

where

y_a	is the flow of link a from stochastic loading,
$\mathcal{D}_{end}$	is the set of downstream links of the end node of link a, and
$\mathcal{U}_{end}$	is the set of upstream links of the end node of link a.

The pseudo code of the STOCH algorithm is displayed in Algorithm 2. As Eq. (5.24) and Eq. (5.25) are linear equations, they are solved with JAMA.

Algorithm 2 STOCH algorithm

Require: $t_a, t_{z,i,j}$
Ensure: $y_a, y_{z,i,j}$
1: **function** STOCHA
2: $t_{o,end}, t_{o,start} \leftarrow$ Dijkstra's algorithm
3: $L_a, L_{z,i,j} \leftarrow$ Eq. (5.23)
4: $w_a, w_{z,i,j} \leftarrow$ Eq. (5.24) with JAMA
5: $\sum_{a' \in \mathcal{U}_{end}} w_{a'} \leftarrow 0$
6: **for** $a' \in \mathcal{U}_{end}$ **do**
7: $\sum_{a' \in \mathcal{U}_{end}} w_{a'} \leftarrow \sum_{a' \in \mathcal{U}_{end}} w_{a'} + w_{a'}$
8: **end for**
9: $y_a, y_{z,i,j} \leftarrow$ Eq. (5.25) with JAMA
10: **return** $y_a, y_{z,i,j}$
11: **end function**

6. Signal setting optimization

6.1. Overall

This chapter first introduces the method of left turn phasing. Then, the lane-based method is explained in detail. The stage-based method is explained at the end. Signal setting optimization is applied for each intersection. Pedestrians, cyclists and railway transportation are not considered, and only vehicle flows are considered in the signal setting models. Left turn prohibition indicators, $x_{z,i}$, and link flows, $q'_a, q'_{z,i,j}$ are inputs of the signal setting optimization models. As in the lane-based method, the signal settings of lanes are optimized, and in the stage-based method, the signal settings of stages are optimized. The consistency between the signal settings of lanes and stages are made by assigning values to the signal settings of movements. Details are explained at the beginning of each section.

6.2. Left turn phasing

The types of left turn phasing affect the saturation flows of left turns and conflict matrices. As opposing through movements interrupt the permitted left turn vehicles, the saturation flows decrease, compared with the saturation flows of protected left turns.

A conflict matrix records the conflicts between the movements of different arms. If two movements conflict with each other, they will not be in the same green duration. The conflict matrix is denoted as $\Psi_z, \forall z = 1, ..., N_Z$. Then, the conflict state $\psi_{z,i,j,l,m} \in \Psi_z$ indicates whether movement (i, j) and movement (l, m) conflict with each other.

For all $z = 1, ..., N_Z, i = 1, ..., N_{A,z}, j \in M, l = 1, ..., N_{A,z}, m \in M$,

$$\psi_{z,i,j,l,m} = \begin{cases} 1, & \text{if the'movement } (i,j) \text{ conflicts with movement } (l,m) \text{ and} \\ 0, & \text{if otherwise} \end{cases}. \tag{6.1}$$

If left turns are protected, $\psi_{z,i,LT,l,TH} = 1$ and $\psi_{z,i,TH,l,LT} = 1$ if l is the opposing arm of i, so left turns and opposing through movements will not be in the same green durations. If left turns are permitted, $\psi_{z,i,LT,l,TH} = 0$ and $\psi_{z,i,TH,l,LT} = 0$, so left turns and opposing through movements could be in the same green duration. Note that it is possible for left turns to also not be in the same green duration as the opposing through movement even if $\psi_{z,i,LT,l,TH} = 0$ and $\psi_{z,i,TH,l,LT} = 0$. In this case, the left turns are treated as protected because the left turn flows are not interrupted by the opposing through movements.

In order to determine whether left turns need to be protected, one can apply recommendations from different guidelines. The criteria applied in this thesis are volume conditions

where the types of left turn phasing depend on left turn flows, opposing through flows, and the number of opposing lanes. If a left turn has no opposing through movement, it is unnecessary to consider its left turn phasing type. In HCM (2000), any of the following conditions leads to protected left turns:

For all $z = 1, ..., N_Z, i = 1, ..., N_{A,z}, l = 1, ..., N_{A,z}$ and l is the opposing arm of i,

- $q_{z,i,LT} > 240$
- if $N_{L,z,l,TH} = 1$, $q_{z,i,LT} \cdot q_{z,l,TH} > 50000$
- if $N_{L,z,l,TH} = 2$, $q_{z,i,LT} \cdot q_{z,l,TH} > 90000$
- if $N_{L,z,l,TH} \geq 3$, $q_{z,i,LT} \cdot q_{z,l,TH} > 110000$

where

$N_{L,z,l,TH}$	is the number of opposing through lanes,
$q_{z,i,LT}$	is the left turn flow in arm i at intersection z(veh/h), and
$q_{z,l,TH}$	is the opposing through flow in arm l at intersection z (veh/h).

Once the types of left turn phasing are determined, the values of $\psi_{z,i,LT,l,TH}$ and $\psi_{z,i,TH,l,LT}$ are adjusted accordingly. Then the conflict matrix Ψ_z is used in the signal setting optimization models.

6.3. Lane-based method

The contents of this section were published in

Q. Tang. Lane-based optimization of signal timing including left turn prohibition in communication scenarios. In *Intelligent Transportation Systems (ITSC), 2016 IEEE 19th International Conference on*, pages 2071-2076. IEEE, 2016. (Tang, 2016)

The model is further developed by adding constraints (6.24) and (6.17).

6.3.1. Objective function

Reserved capacity is represented by the common multiplier indicating capacity usage on lanes at an intersection (Allsop, 1972a). The multiplier μ' is the ratio of the capacity to the flow, and the capacity takes the maximum acceptable degree of saturation into consideration. Therefore, the practical capacity of a movement or lane is $\mu' q$ if μ and q are the mutipler and the flow of the movement or lane, respectively, according to the definition of Allsop (1972a). When the multiplier μ' is calculated for each lane, the maximum μ' is selected as the common multipler μ. If $\mu > 1$, the intersection has a reserved capacity with the given traffic demand; if $\mu < 1$, the intersection is overloaded. A large reserved capacity indicates better capacity usage. Reserved capacity maximization, is the objective of this lane-based method. This problem is formulated as a mixed-integer-linear-program (MILP)(Improta and Cantarella, 1984; Wong and Wong, 2003; Wong and Heydecker, 2011). With this objective, demand fluctuations can be properly treated.

For all $z = 1, ..., N_Z$,

$$\max \quad \mu_z. \tag{6.2}$$

6.3.2. Decision variables

The decision variables in the lane-based method are different from the decision variables in the stage-based method. Although these decision variables are mentioned in Chapter 3, for a better understanding of the lane-based method, the decision variables are clarified below.

Decision variables	**Notations**	**Domain**
Lane permission indicator	$\delta_{z,i,j,k}$	$\delta_{z,i,j,k} \in \{0,1\}$
Successor indicator	$\Omega_{z,i,j,l,m}$	$\Omega_{z,i,j,l,m} \in \{0,1\}$
Green split for lane	$\Phi_{z,i,k}$	$\Phi_{z,i,K} \in [0, g_{z,i,j,min}/c_z]$
Green split for movement	$\phi_{z,i,j}$	$\phi_{z,i,j} \in [0, g_{z,i,j,min}/c_z]$
Start of green for lane	$\Theta_{z,i,k}$	$\Theta_{z,i,k} \in [0,1]$
Start of green for movement	$\theta_{z,i,j}$	$\theta_{z,i,j} \in [0,1]$
Assigned flow (veh/h)	$f_{z,i,j}$	$f_{z,i,j} \in [0,\infty)$
Inverse of cycle length (s)	ξ_z	$\xi_z \in [1/c_{max}, 1/c_{min}]$
Reserved capacity	μ_z	$\mu \in (0,\infty)$

After obtaining the values of ξ_z, $\phi_{z,i,j}$ and $\Phi_{z,i,k}$, the cycle length of intersection z and the relevant green durations can be calculated by Eq. (6.3), Eq. (6.4) and Eq. (6.5). When maximization of the reserved capacity is the objective, the optimal cycle length is always equal to the maximum cycle length according to the results of Wong and Wong (2003), so the common cycle length among all intersections is equal to the maximum cycle length.

For all $z = 1, ..., N_Z, i = 1, ..., N_{A,z}, j \in M, k = 1, ..., N_{L,z,i}$,

$$c_z = \frac{1}{\xi_z}, \tag{6.3}$$

and

$$c = c_z, \tag{6.4}$$

and

$$g_{z,i,j} = \phi_{z,i,j} \cdot c;\ g_{z,i,k} = \Phi_{z,i,k} \cdot c. \tag{6.5}$$

6.3.3. Constraints

The constraints used in this study are originally from Wong and Wong (2003) and Wong and Heydecker (2011). In order to adjust the lane-based method into a left turn prohibition problem, constraints (6.6), and (6.19) are modified. To narrow the search space, constraint (6.24) is added. Constraint (6.17) is also different from the original constraints because the sum of the start of green for a movement and its duration should be less than the cycle length. The modifications of constraint (6.17) and constraint (6.24) are the improvement on the original lane-based method.

Left turn prohibition

If the left turn on the arm i is prohibited, the left turn is never permitted on any lanes of the arm. Only if the left turn is not prohibited is the left turn movement possible to

be permitted on some of the lanes. Please note the difference between lane permission indicators and left turn prohibition indicators. The lane permission indicators are used for lane marking assignment. That means they decide, whether the lane marking of a movement is drawn on a lane. Any lane markings of the movements could be assigned to a lane if they meet the design rules. The left turn prohibition indicators decide whether the left turn is prohibited. If a left turn is prohibited, it cannot be one option of the movements drawn as lane markings. The "permission" and "prohibition" in this context are not antonyms.

This constraint is applied on the arm with left turns. If the arm has no left turn, this constraint is skipped.

For all $z = 1, ..., N_Z, i = 1, ..., N_{A,z}, j = LT, k = 1, ..., N_{L,z,i}$

$$0 \leq \delta_{z,i,j,k} \leq 1 - x_{z,i}, \tag{6.6}$$

where $\delta_{z,i,j,k}$ is the lane permission indicator.

$$\delta_{z,i,j,k} = \begin{cases} 1, & \text{if the movement } (i,j) \text{ is permitted on the lane } k \text{ and} \\ 0, & \text{if otherwise} \end{cases}. \tag{6.7}$$

With constraint (6.6), if the left turn is prohibited, that is, if $x_{z,i} = 1$, the values of $\delta_{z,i,j,k}, \forall k = 1, ..., N_{L,z,i}$ must be 0, meaning that no lanes could be assigned for left turns. If the left turn is not prohibited, that is, if $x_i = 0$, the values of $\delta_{z,i,j,k}, \forall k = 1, ..., N_{L,z,i}$ can be either 0 or 1, so the lane k could be assigned for either left turns or other movements.

Minimum permitted movement

Each lane must be permitted for at least one movement because idle lanes waste the capacity of roads. The sum of $\delta_{z,i,j,k}$ by turning direction j is the number of movements sharing lane k. This number must be equal to or more than 1.

For all $z = 1, ..., N_Z, i = 1, ..., N_{A,z}, k = 1, ..., N_{L,z,i}$,

$$\sum_{j \in M} \delta_{z,i,j,k} \geq 1. \tag{6.8}$$

Maximum permitted lanes

For the safety reasons, the number of permitted lanes for each movement (i, j), is no more than the number of exit lanes of the movement. Otherwise, vehicles will conflict with each other when merging into one lane. The sum of $\delta_{z,i,j,k}$ for lane k is the number of lanes occupied by movement (i, j). This number must be equal to or less than the number of exit lanes $N_{E,z,i,j}$.

For all $z = 1, ..., N_Z, i = 1, ..., N_{A,z}, j \in M$,

$$\sum_{k=1}^{N_{L,z,i}} \delta_{z,i,j,k} \leq N_{E,z,i,j}. \tag{6.9}$$

Conflict elimination on adjacent lanes

To eliminate the internal conflicts on adjacent lanes, once a movement is permitted on a lane, the left adjacent lane cannot be occupied by conflicting movements. For example, in Figure 6.1, if a left turn is permitted on lane $k = 2$, right turns and through movements are not permitted on lane $k = 3$. Otherwise, the right turn and the through movement would conflict with the left turn.

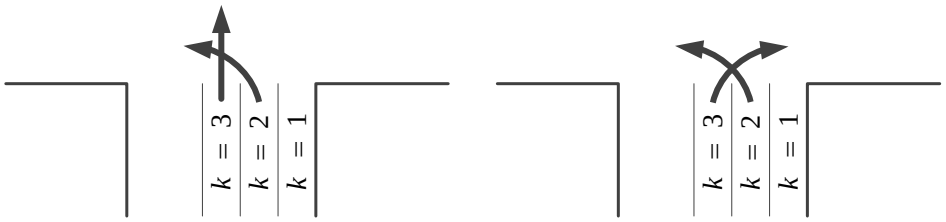

Figure 6.1.: Conflicts with adjacent lanes

Let M' be the subset of M. For $j \in M$, if $j = LT$, $M' = \{LT\}$; if $j = TH$, $M' = \{LT, TH\}$;if $j = RT$, $M' = \{LT, TH, RT\}$. If $\delta_{z,i,j,k+1} = 1$, which means that movement (i, j) is permitted on lane $k + 1$, $\delta_{z,i,m,k} = 0$, meaning that movement (i, m) cannot be permitted on lane k.

For all $z = 1, ..., N_Z, i = 1, ..., N_{A,z}, j \in M, m \in M', k = 1, ..., N_{L,z,i} - 1$,

$$\delta_{z,i,m,k+1} + \delta_{z,i,j,k} \leq 1. \tag{6.10}$$

Maximum amount of traffic increase

The maximum amount of traffic increase, that maintains the reasonable performance of intersections, is the product of the reserved capacity μ_z and the link flow $q'_{z,i,j}$ from the SUE model with a BPR function. The maximum amount is equal to the sum of traffic flows of movement (i, j) being assigned to all lanes on arm i.

For all $lz = 1, ..., N_Z, i = 1, ..., N_{A,z}, j \in M$,

$$\mu_z q'_{z,i,j} = \sum_{k=1}^{N_{L,z,i}} f_{z,i,j,k}. \tag{6.11}$$

where $f_{z,i,j,k}$ is the assigned flow of movement (i, j) on lane k.

Assigned flow of non-permitted lanes

If a movement (i, j) is not permitted on lane k, then no vehicles turning j will choose lane k. Thus, the assigned flow $f_{z,i,j,k}$ should be 0. If $\delta_{z,i,j,k} = 0$, the values of $f_{z,i,j,k}$ must be 0.

For all $z = 1, ..., N_Z, i = 1, ..., N_{A,z}, j \in M, k = 1, ..., N_{L,z,i}$,

$$0 \leq f_{z,i,j,k} \leq H \cdot \delta_{z,i,j,k}. \tag{6.12}$$

where H is an arbitrary large positive constant.

Identical flow factor of adjacent lanes being occupied by a movement

Flow factor is defined as the lane flow divided by the lane saturation flow. Let $b_{z,i,k}$ be the flow factor of lane k on arm i.

For all $z = 1, ..., N_Z; i = 1, ..., N_{A,z}; k = 1, ..., N_{L,z,i}$,

$$b_{z,i,k} = \frac{\sum_{j \in M} f_{z,i,j,k}}{s_{z,i,k}}, \tag{6.13}$$

where $s_{z,i,k}$ is the saturation flow of lane k being calculated with Eq. (5.17), but using $f_{z,i,j,k}$ as inputs.

If a movement occupies multiple lanes, the flow factor of each lane must be the same. The reason is that drivers are not willing to be on the lane with longer waiting time. Considering this, the lane permission indicators should manage to equalize the flow factor of adjacent lanes. If movement (i, j) is permitted on both lane k and $k + 1$, i.e. $\delta_{z,i,j,k} = 1, \delta_{z,i,j,k+1} = 1$, $b_{z,i,k}$ is equal to $b_{z,i,k+1}$.

For all $z = 1, ..., N_Z, i = 1, ..., N_{A,z}, k = 1, ..., N_{L,z,i}$,

$$-H \cdot (2 - \delta_{z,i,j,k} - \delta_{z,i,j,k+1}) \leq b_{z,i,k} - b_{z,i,k+1} \leq H \cdot (2 - \delta_{z,i,j,k} - \delta_{z,i,j,k+1}). \tag{6.14}$$

Maximum acceptable degree of saturation

The degree of saturation should be no more than the maximum acceptable degree of saturation. As the degree of saturation is relevant to green split, this constraint ensures that the degree of saturation is not too large, and that, the green split is large enough. $\rho_{z,i,k}$ is denoated as the degree of saturation on lane k.

For all $z = 1, ..., N_Z, i = 1, ..., N_{A,z}, k = 1, ..., N_{L,z,i}$,

$$\rho_{z,i,k} = \frac{b_{z,i,k}}{\Phi_{i,k} + e\xi_z} \leq \rho_{max,i,k}, \tag{6.15}$$

where $\Phi_{z,i,k}$ is the green split of lane k, ξ_z is the inverse of the cycle length, e is the difference between the actual green time and the effective green time, and $\rho_{max,i,k}$ is the maximum acceptable degree of saturation.

Cycle length, start of green and duration of green

Cycle length $1/\xi_z$ is in the interval $[c_{min}, c_{max}]$, where c_{min} and c_{max} are the minimum and maximum cycle lengths, respectively. The start of green and the green split are ratios smaller than 1. Specially, for left turns, if a left turn is prohibited, the green split is 0 (Eq. (6.19)).

For all $z = 1, ..., N_Z, i = 1, ..., N_{A,z}, j \in M$,

$$1/c_{max} \leq \xi_z \leq 1/c_{min}, \tag{6.16}$$

$$0 \leq \theta_{z,i,j} + \phi_{z,i,j} \leq 1. \tag{6.17}$$

where $\theta_{z,i,k}$ is the start of green for movement (i, j) and $\phi_{i,k}$ is the green split for movement (i, j).

For all $z = 1, ..., N_Z, i = 1, ..., N_{A,z}, j \in \{TH, RT\}$,

$$g_{min,z,i,j} \cdot \xi_z \leq \phi_{z,i,j} \leq 1. \tag{6.18}$$

and $\forall j \in \{LT\}$,

$$(1 - x_{z,i}) \cdot g_{min,z,i,j} \cdot \xi_z \leq \phi_{z,i,j} \leq 1 - x_{z,i}, \tag{6.19}$$

where $g_{min,z,i,j}$ is the minimum green time.

Identical signal settings of movements on shared lanes

When multiple movements share one lane, the signal settings of these movements are identical, to avoid internal conflicts on the lane. For example, in Figure 6.2, if the start of green and the green split of the through movement are different from those of right turn, vehicles turning different directions will block each other. As Lane 2 is also permitted for the through movement, the signal setting of Lane 2 is the same as that of Lane 1, because it is not reasonable that the through movement has two signal settings on different lanes. Thus, constraints (6.20) and (6.21) ensure the identical signal settings on shared lanes, and the identical signal settings of one movement on multiple lanes.

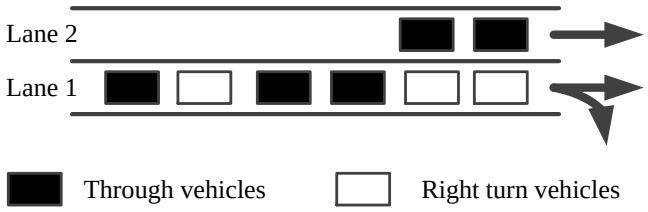

Figure 6.2.: Identical signal settings on shared lanes.

For all $z = 1, ..., N_Z, i = 1, ..., N_{A,z}, j \in M, k = 1, ..., N_{L,z,i}$,

$$-H \cdot (1 - \delta_{z,i,j,k}) \leq \Theta_{z,i,k} - \theta_{z,i,j} \leq H \cdot (1 - \delta_{z,i,j,k}), \tag{6.20}$$

and

$$-H \cdot (1 - \delta_{z,i,j,k}) \leq \Phi_{z,i,k} - \phi_{z,i,j} \leq H \cdot (1 - \delta_{z,i,j,k}), \tag{6.21}$$

where $\Theta_{z,i,k}$ is the start of green for lane k and $\Phi_{i,k}$ is the green split for lane k.

Signal sequence

If two movements conflict with each other, they cannot be in the same green durations. The conflict states, $\psi_{z,i,j,l,m}$, are defined in Section 6.2. Thus, one movement can be either the predecessor or the successor of another movement. The successor indicators $\Omega_{z,i,j,l,m}$ indicate whether a movement is the successor of other movements. This constraint is only applicable for movements that conflict with each other. Constraint (6.23) says that two movements cannot be the successors of each other at the same time. Although in some signal sequence practices a signal group could appear twice in a cycle, a phenomena that makes constraint (6.23) incorrect, it is important to note that many signal sequences could be equivalent and they are excluded in this thesis. An example is in Figure 6.3 and more equivalent sequence examples can be found in Memoli et al. (2017). Constraint (6.24) further limits the search space of the feasible area. When movement (i, j) is the predecessor of movement (l, m) and movement (l, m) is the predecessor of movement (u, v), movement (i, j) must be the predecessor of movement (u, v).

For all $z = 1, ..., N_Z, i = 1, ..., N_{A,z}, j \in M, l = 1, ..., N_{A,z}, m \in M$,

$$\Omega_{z,i,j,l,m} = \begin{cases} 1, & \text{if the movement } (i,j) \text{ is the successor of movement } (l,m), \text{and} \\ 0, & \text{if otherwise} \end{cases}. \tag{6.22}$$

If $\psi_{z,i,j,l,m} = 1$, the following equations hold:

$$\Omega_{z,i,j,l,m} + \Omega_{z,l,m,i,j} = 1. \tag{6.23}$$

For all $u = 1, ..., N_{A,z}, v \in M$, if $\psi_{z,i,j,l,m} = 1, \psi_{z,l,m,u,v} = 1$ and $\psi_{z,i,j,u,v} = 1$,

$$\Omega_{z,i,j,l,m} + \Omega_{z,l,m,u,v} - 1 \leq \Omega_{z,i,j,u,v} \leq \Omega_{z,i,j,l,m} + \Omega_{z,l,m,u,v}. \tag{6.24}$$

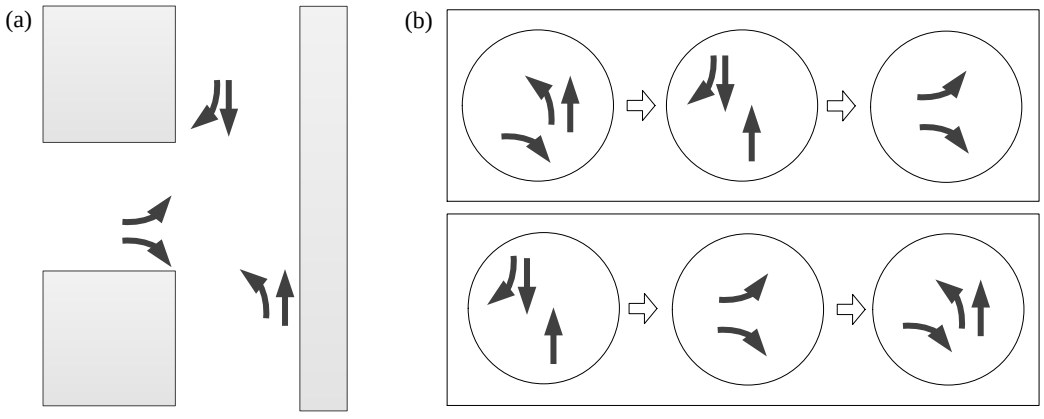

Figure 6.3.: (a) Layout of an example intersection. (b) Two equivalent signal sequences of the example intersection.

Start of green for successor movements

It is necessary to have intergreen time between two conflict movements for safety. Without intergreen time, the vehicles passing the stop line may conflict with the vehicles from conflicting movements. Then, the start of green for successor movements must be later than the end of the predecessor movements plus the intergreen time.

For all $z = 1, ..., N_Z, i = 1, ..., N_{A,z}, j \in M, l = 1, ..., N_{A,z}, m \in M$,

$$\theta_{z,i,j} + \phi_{z,i,j} + \omega_{z,i,j,l,m} \cdot \xi_z \leq \theta_{z,l,m} + \Omega_{z,i,j,l,m}. \tag{6.25}$$

6.3.4. Algorithms

The optimization problem is a standard MILP. The MILP problem is solved by IBM ILOG Cplex using a standard branch-and-bound algorithm.

6.4. Stage-based method

Generally, in the stage-based method, the stage composition and the stage sequence are given. In this thesis, the stage-based method starts from stage generation and then stage sequence optimization. As the prohibited left turns are not in the stages, new stages without prohibited left turns should be generated. The stage sequence may also change after adding the new stages. When the stage compositions and the stage sequence are available, the signal timing of each stage is adjusted.

6.4.1. Decision variables

As opposed to the lane-based method, lane permission indicators $\delta_{z,i,j,k}, \forall z = 1, ..., N_Z, i = 1, ..., N_{A,z}, j \in M, k = 1, ..., N_{L,z,i}$ are given in the stage-based method. Hence, they are parameters. If a left turn is prohibited, $\delta_{z,i,LT,k}$ does not exist anymore; instead, $\delta_{z,i,TH,k} = 1$ because the lanes of the prohibited left turn are assigned for through movements. Once a left turn is prohibited, the prohibited left turn is not involved in stage generation.

The decision variables in the stage-based method are:

Decision variables	**Notations**	**Domain**
Movement-stage indicator	$h_{z,p,i,j}$	$h_{z,p,i,j} \in \{0, 1\}$
Lane-stage indicator	$h_{z,p,i,k}$	$h_{z,p,i,k} \in \{0, 1\}$
Stage selection indicator	$h'_{z,p}$	$h'_{z,p} \in \{0, 1\}$
Number of optimal stages	$N_{S,z}$	$N_{S,z} \in [1, \infty)$
Successor indicator for stages	$\Omega'_{z,p,p'}$	$\Omega'_{z,p,p'} \in \{0, 1\}$
Green duration for stage (s)	$g_{z,p}$	$g_{z,p} \in [g_{min,z,p}, c_z]$
Cycle length (s)	c_z	$c_z \in [c_{min}, c_{max}]$

The first four decision variables are relevant to stage generation. Let $h_{z,p,i,j}$ be the movement-stage indicator, which indicates whether movement (i, j) is related to stage p.

$$h_{z,p,i,j} = \begin{cases} 1, & \text{if movement } (i,j) \text{ is related to stage } p \text{ and} \\ 0, & \text{if otherwise} \end{cases}. \tag{6.26}$$

The stage selection indicator $h'_{z,p}$ represents whether a feasible stage is selected as one of the optimal stages.

Once the stages are available, the stage sequence is optimized. The successor indicators of the stages, $\Omega'_{z,p,p'}$, are defined as:

$\forall z = 1, ..., N_Z, p = 1, ..., N_{S,z}, p' = 1, ..., N_{S,z}, p \neq p'$,

$$\Omega'_{z,p,p'} = \begin{cases} 1, & \text{if the stage } p \text{ is the } \textbf{direct} \text{ successor of stage } p' \text{ and} \\ 0, & \text{if otherwise} \end{cases}. \tag{6.27}$$

For all $i = 1, ..., N_{A,z}, j \in M, l = 1, ..., N_{A,z}, m \in M$, if movement (i,j) is in stage p and movement (l,m) is in stage p',

$$\Omega_{z,i,j,l,m} = \Omega'_{z,p,p'}. \tag{6.28}$$

The difference between the successor indicators of stages and movements is that the stage p directly follows the stage p' without any other stages in-between. The successor indicators of movements allow other movements in-between.

The cycle length for each intersection $c_z, \forall z = 1, ..., N_Z$ is adjusted and the largest cycle length is selected as the common cycle length in the network c. The green durations for each stage, $g_{z,p}$, are adjusted. A stage contains the information about movement (i,j) and lane k. Thus, in the stage-based method, the green durations for movements and the green durations for lanes can be obtained from the green durations for stages.

For all $z = 1, ..., N_Z, i = 1, ..., N_{A,z}, j \in M, k = 1, ..., N_{L,z,i}, p = 1, ..., N_{S,z}$, if $h_{z,p,i,j} = 1$ and $h_{z,p,i,k} = 1$,

$$g_{z,i,j} = g_{z,p}, \tag{6.29}$$

and if $\delta_{z,i,j,k} = 1$,

$$g_{z,i,k} = g_{z,i,j}. \tag{6.30}$$

6.4.2. Stage generation

Two requirements of stage generation are compatibility and completeness. Compatibility means that a stage can only include non-conflicting movements; otherwise, the conflicting movements may cause accidents. Completeness means that each movement must be included in at least one stage so that vehicles turning all directions can go through the intersection.

The requirement of compatibility is highly relevant to the conflict matrices: movements that conflict with each other cannot be compatible. The conflict matrices define the conflict between movements. However, as multiple movements may share the same lane, the conflict states should also consider the influence of lane assignments. For example, in

Figure 6.4, although the through movement on Lane 1 of Arm 1 does not conflict with the right turn on Lane 1 of Arm 3, because the left turn on Lane 2 of Arm 1 conflict with the right turn on Lane 1 of Arm 3, the right turn on Lane 1 of Arm 3 cannot be on the same stage as the through movement on Lane 2 of Arm 1. Considering the lane assignments, $\psi_{z,i,k,l,n}$ is denoted as the conflict states between lanes. The following relationship holds:

For all $z = 1, ..., N_Z, i = 1, ..., N_{A,z}, j \in M, k = 1, ..., N_{L,z,i}, l = 1, ..., N_{A,z}, m \in M, n = 1, ..., N_{L,z,l}$, if $\delta_{z,i,j,k} = 1$ and $\delta_{z,l,m,n} = 1$,

$$\psi_{z,i,k,l,n} = \psi_{z,i,j,l,m}. \tag{6.31}$$

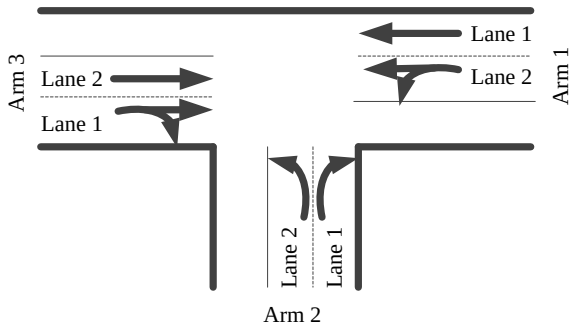

Figure 6.4.: Effect of lane assignments on conflict states.

With the conflict states between lanes, a feasible set of stages can be generated. A feasible set would be one that contains different stages with non-conflicting movements. It is equivalent to the problem of finding all cliques in graph theory. A clique is a subset of nodes in an undirected graph. The nodes in the clique can connect to each other; that is to say, the nodes are adjacent. In graph theory, the adjacent matrices, which record the connectivity between nodes, are similar to the conflict matrices. The cliques constructed by connected nodes are equivalent to the stages.

If $\psi_{z,i,k,l,n} = 1$, for each stage p,

$$h_{z,p,i,k} + h_{z,p,l,n} = 1. \tag{6.32}$$

For movement (i, j) and (l, m), if $\delta_{z,i,j,k} = 1$ and $\delta_{z,l,m,n} = 1$,

$$h_{z,p,i,j} + h_{z,p,l,m} = 1. \tag{6.33}$$

There are usually many feasible stages. To decrease the intergreen time, one should use the minimal number of stages that include all movements in the signal timing plan. The stage selection is formulated as a 0/1 integer-programming problem, the objective of which is to minimize the number of stages (Eq. (6.34)). The decision variables describe whether a stage should be selected and the constraints represent the requirement that each movement must be included at least in one stage - that is, the requirement of completeness (Constraint (6.35)). Consequently, the minimum number of stages including all movements is generated.

Let $h'_{z,p}$ be the indicator of whether stage p is selected as one of the optimal stages. $h'_{z,p} = 1$ means that stage p is selected; $h'_{z,p} = 0$ means, otherwise.

$$N_{S,z} = \min \sum_{p=1}^{N_{FS,z}} h'_{z,p}, \tag{6.34}$$

subject to

$\forall i = 1, ...N_{A,z}, j \in M,$

$$\sum_{p=1}^{N_{FS,z}} h'_{z,p} \cdot h_{z,p,i,j} \geq 1, \tag{6.35}$$

where

$N_{S,z}$ is the optimal number of stages, and
$N_{FS,z}$ is the number of stages in a feasible set.

When the stages are generated, one movement may be shared by multiple stages. For example, in the numerical example by Memoli et al. (2017), two stages share the through movement. Sharing a movement across multiple stages influences the stage sequence and green duration of these stages. The issue of stages sharing the same movements is further addressed in Section 6.4.3 and Section 6.4.4.

6.4.3. Stage sequence optimization

Between two sequential conflicting movements, intergreen time is required for safety reasons. The most favourable stage sequence is determined by the total transition times that lead to shortest cycle time (RiLSA, 1992). However, this manner ignores the situation in which the stages share the same movements. Once the stages may share the same movements, these stages have the potential to be sequential so that in the intergreen time, the movements can keep green and obtain extra green duration. When the total transition time is minimized, the green duration of movements in multiple stages could be interrupted by other stages, and the movements could not have an extra green duration (Figure 6.5(a)). Therefore, when determining the stage sequence, one should consider the potential gain of extra green time (Figure 6.5(b)).

In this thesis, the objective of stage sequence optimization is to minimize the total intergreen time between lanes. To consider the possibility of stages sharing the same movements, the total intergreen time among lanes related to the two stages needs to be calculated first. Once the conflict matrices between lanes are obtained, the intergreen time matrices recording the intergreen between conflict movements can be also obtained according to the intersection geometry and pedestrian flows. In the intergreen time matrices, the compatible movements have no intergreen time, whereas the incompatible movements do. The total intergreen time matrices, which have the total intergreen time among lanes related to the two stages, are determined based on the intergreen time among lanes and the composition of the stages. In this regard, if the stages sharing the same movements are sequential, the total intergreen time between each stage is shorter than the total intergreen time among non-sequential stages sharing the same movements.

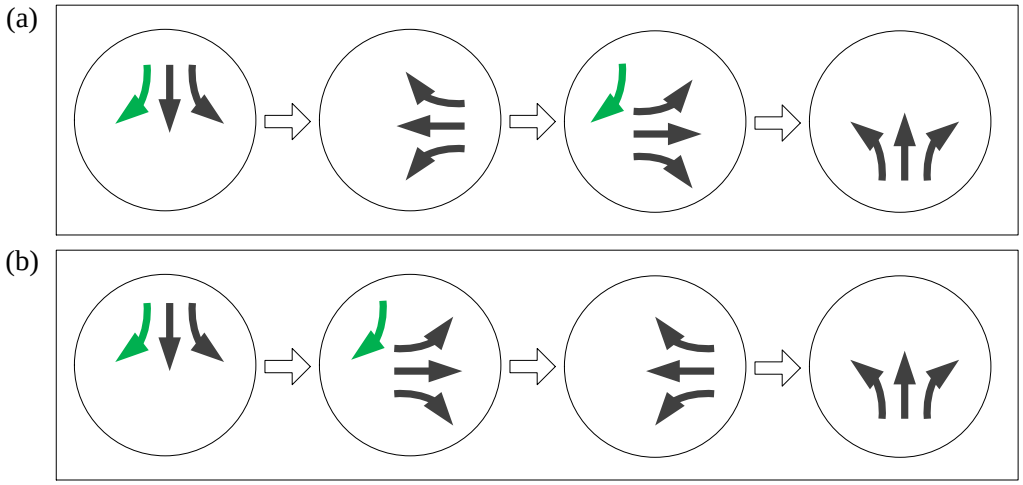

Figure 6.5.: (a) Non-sequential stages sharing the same movements. (b) Sequential stages sharing the same movements.

Set formally, for intersection z, if lane k in arm i is related to stage p and lane n in arm l is related to stage p' , then the total intergreen time among lanes related to both stages can be expressed as follows:

$\forall z = 1, ..., N_Z, p = 1, ..., N_{S,z}, p' = 1, ..., N_{S,z},$

$$\omega'_{z,p,p'} = \sum_{i=1}^{N_{A,z}} \sum_{k=1}^{N_{L,z,i}} \sum_{l=1}^{N_{A,z}} \sum_{n=1}^{N_{L,z,i}} h_{z,p,i,k} \cdot h_{z,p',l,n} \cdot \omega_{z,i,k,l,n}, \tag{6.36}$$

where

$\omega'_{z,p,p'}$ is the total intergreen time among lanes being related to stage p and stage p' and
$\omega_{z,i,k,l,n}$ is the intergreen time between lane k and n.

With the total intergreen time among lanes being related to both stages, the stage sequence optimization can be formulated as 0/1 integer programming with the objective of minimization of the total intergreen time. The successor indicators between stages can decide the minimal intergreen time (Eq. (6.37)). Constraint (6.38) requires that each stage p be the successor of stage p' and that stage p is the only successor. Constraint (6.39) requires that each stage p' be the predecessor of stage p and that stage p' is the only predecessor. Let $\tau_{z,p}$ be the number of stages prior to stage p (including stage p) and stage p is not the first stage in the signal plan. Thus, $\tau_{z,p}$ is in the interval $[2, N_{S,z}]$. Constraint (6.40) ensures that the stage sequence is unique.

For all $z = 1, ..., N_Z$,

$$\min \sum_{p=1}^{N_{S,z}} \sum_{p'=1}^{N_{S,z}} \omega'_{z,p,p'} \cdot \Omega_{z,p,p'}. \tag{6.37}$$

subject to

$$\sum_{p=1,p\neq p'}^{N_{S,z}} \Omega'_{z,p,p'} = 1. \tag{6.38}$$

$$\sum_{p'=1,p'\neq p}^{N_{S,z}} \Omega'_{z,p,p'} = 1. \tag{6.39}$$

$$\tau_{z,p'} - \tau_{z,p} + 1 \leq (N_{S,z} - 1) \cdot (1 - \Omega'_{z,p,p'}). \tag{6.40}$$

The stage sequence optimization problem formulated as 0/1 integer programming is equivalent to the traveling salesman problem. In the traveling salesman problem, a traveling salesman visits cities and finaly returns to the origin in the optimal sequence with the minimum total distance. In this sequence optimization problem, the sequence of stages with a minimum total intergreen time is equivalent to the sequence of visited cities with a minimum total distance. Thus, the 0/1 integer programming can be solved with some classical algorithms of the traveling salesman problem. The traveling salesman problem is solved in this thesis by applying a backtracking algorithm.

6.4.4. Signal timing adjustment

The formulas for signal timing calculation were originally deduced by Webster (1958). By minimizing the total delay at isolated intersections, the formulas of optimal green duration and cycle length can be deduced. However, as the delay formula used by Webster (1958) is only applicable in the unsaturated situation, the cycle length formula and the green duration formula are also used when the flow rate is less than 1. Practically, cycle length has its domain, that is, maximum and minimum cycle length. When the flow ratio is large, the maximum cycle length is applied. Thus, Webster's formulas are feasible and applicable. HBS (2001) uses these formulas in its manual.

To calculate cycle length, the ratio of flow to saturation flow for each stage must be determined. As green times are determined by the lane with the maximum flow in a stage, for all lanes in the same stage, the maximum flow ratio of lanes is the flow ratio of the stage (Eq. (6.41)).

For all i, k is related to stage p at intersection z,

$$b_{z,p} = \max\left(\frac{q_{z,i,k}}{s_{z,i,k}}\right). \tag{6.41}$$

For all $\Omega'_{z,p,p'} = 1, z = 1, ..., N_Z, i = 1, ..., N_{A,z}, k = 1, ..., N_{L,z,i}, l = 1, ..., N_{A,z}, n = 1, ..., N_{L,z,l}$,

$$\omega_{z,p,p'} = \max\left(\omega_{z,i,k,l,n}\right). \tag{6.42}$$

Then cycle length of intersection z and the green durations of stage p can be calculated with the following equations:

$$c_z = \frac{1.5(\sum_{p=1}^{N_{S,z}} \sum_{\Omega'_{z,p',p=1}} \omega_{z,p,p'} + 5)}{1 - B_z}, \tag{6.43}$$

and

$$g_{z,p} = \frac{b_{z,p}}{B_z}\left(c_z - \sum_{p=1}^{N_{S,z}} \sum_{\Omega'_{z,p',p=1}} \omega_{z,p,p'}\right), \tag{6.44}$$

subject to $c_z \in [c_{min}, c_{max}]$, $g_{z,p} \in [g_{min,z,p}, c_z]$, where

$\omega_{z,p,p'}$	is the intergreen time between stage p and its predecessor stage p'(s),
$B_z = \sum_{p=1}^{N_{S,z}} b_{z,p}$	is the sum of flow ratio at one intersection,
$N_{P,z}$	is the number of phases at intersection z,
c_{min}	is the minimum cycle time (s),
c_{max}	is the maximum cycle time (s), and
$g_{min,z,p}$	is the minimum green duration of stage p (s).

Cycle length must be no less than the minimum cycle length and no longer than the maximum cycle length. Thus, if $B_z > 1 - 1.5(\sum_{p=1}^{N_{S,z}} \sum_{\Omega'_{z,p',p=1}} \omega_{z,p,p'} + 5)/c_{max}$, the cycle length is always the maximum.

Due to the constraints of minimum green times, if the green time of stage p is less than the minimum green time, the green time is equal to the minimum green time. These minimum green times are treated as the components of intergreen time. Because the value of the green time is fixed to the minimum, the green times can only be assigned for the rest of the stages. The cycle time should be recalculated because the actual sum of the intergreen times increases. The rest of the effective green time has to be accommodated according to the stage flows.

$$c_z = \frac{1.5(\sum_{p=1}^{N_{S,z}} \sum_{\Omega_{z,p,p'=0}} \omega_{z,p,p'} + \sum_{p=1}^{N_{S',z}} g_{min,z,p} + 5)}{1 - B'_z}, \tag{6.45}$$

and

$$g_{z,p} = \frac{b_{z,p}}{B'_z}\left(c_z - \sum_{p=1}^{N_{S,z}} \sum_{\Omega_{z,p,p'=0}} \omega_{z,p,p'} - \sum_{p=1}^{N_{S',z}} g_{min,z,p}\right), \tag{6.46}$$

subject to $c_z \in [c_{min}, c_{max}]$, $g_{z,p} \in [g_{min,p}, c_z]$, where $N_{S',z}$ is the number of stages with minimum green times and $B'_z = B_z - \sum_{p=1}^{N_{S',z}} b_p$.

The cycle times are first calculated for each intersection, and the largest cycle length is used as the common cycle length for the network. Green times are then recalculated using the common cycle length in Eq. (6.46). Please note that the sum of minimum green durations could be 0.

For all $z = 1, ..., N_Z$,

$$c = \max(c_z). \tag{6.47}$$

$$g_{z,p} = \frac{b_{z,p}}{B'_z}\left(c - \sum_{p=1}^{N_{S,z}} \sum_{\Omega'_{z,p',p=1}} \omega_{z,p,p'} - \sum_{p=1}^{N_{S',z}} g_{min,z,p}\right). \tag{6.48}$$

Signal timing of stages sharing movements

As mentioned, to calculate signal timing, the flows of movements or lanes in each stage should be known. However, if one movement is in two stages, it is hard to separate the movement flows into two stages beforehand, and the flow ratio then cannot be calculated. This case is neglected by HBS (2001), but considered by Pohlmann (2010).

The rule for dealing with stages sharing movements is that green times are determined by the lane with the maximum flow. When calculating the green time of stages sharing movements, two cases need to be considered: either the required green time for the movement shared in multiple stages is longer than the required green time for the other movements included in these stages, or this green time is shorter. The final green time will be the longer one of these two cases. For example, in Figure 6.6, it is assumed that each movement occupies one lane. For the movement with the flow q_3, it cannot be known in advance the number of vehicles in stages p_1 and p_2, respectively. Hence, following HBS (2001) recommendations, one cannot solve this case. As the largest flow determines the flow ratio in a stage, Pohlmann (2010) separately calculated the flow ratios for stages p_1 and p_2, as well as the combined stage p_1p_2. Individual stages only include the movement not shared by two stages, and the combined stage only includes the movement shared by two stages. In Figure 6.6, $b_{p_1} = q_1/s_1$ and $b_{p_2} = q_2/s_2$, but $b_{p_1p_2} = q_3/s_3$. The flow ratio of stages p_1 and p_2 is determined by $\max(b_{p_1} + b_{p_2}, b_{p_1p_2})$. With the same logic, the green times of stages p_1 and p_2 are determined by $\max(g_{p_1} + g_{p_2}, g_{p_1p_2})$.

$$g_{z,p_1p_2} = \frac{b_{z,p_1p_2}}{B'_z}\left(c_z - \sum_{p=1}^{N_{S,z}} \sum_{\Omega'_{z,p',p=1}} \omega_{z,p,p'} - \sum_{p=1}^{N_{S',z}} g_{min,z,p}\right). \tag{6.49}$$

If $g_{p_1p_2} > g_{p_1} + g_{p_2}$,

$$g_{z,p_1} = \frac{b_{z,p_1}}{b_{z,p_1} + b_{z,p_2}} g_{z,p_1p_2} \in [g_{min,z,p_1}, c_z], \tag{6.50}$$

and

$$g_{z,p_2} = g_{z,p_1p_2} - g_{z,p_1}, \tag{6.51}$$

if $g_{p_1p_2} \leq g_{p_1} + g_{p_2}$, g_{z,p_1} and g_{z,p_2} are calculated in Eq. 6.48, that is to say, Eq. 6.50 and Eq. 6.51 are skipped.

Pohlmann (2010) considered only two stages sharing movements. Although this is usually the case, there may be also cases involving more than two stages. Generalizing the Pohlmann method (Pohlmann, 2010) to include more than two stages is not straightforward. For example, taking into account three stages sharing movements, the following process should be performed. First, not all three stages necessarily share the same movements, and movements may be shared only by two stages, as demonstrated in Figure 6.7(a). Stage p_1 and p_2 may share the through movement, and stages p_2 and p_3 may share the left turn. Therefore, in order to calculate the green time, one should calculate $\max(b_{z,p_1} + b_{z,p_2} + b_{z,p_3}, b_{z,p_1} + b_{z,p_2p_3}, b_{z,p_1p_2} + b_{z,p_3})$. A different calculation should be carried out for the case presented in Figure 6.7(b). There, the through movement is shared by all three stages, and therefore the flow ratio would be $\max(b_{z,p_1} + b_{z,p_2} + b_{z,p_3}, b_{z,p_1p_2p_3})$. The green duration is calculated in a similar manner.

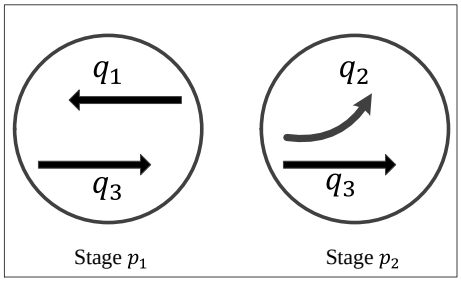

Figure 6.6.: An example of two stages sharing movements(Pohlmann, 2010).

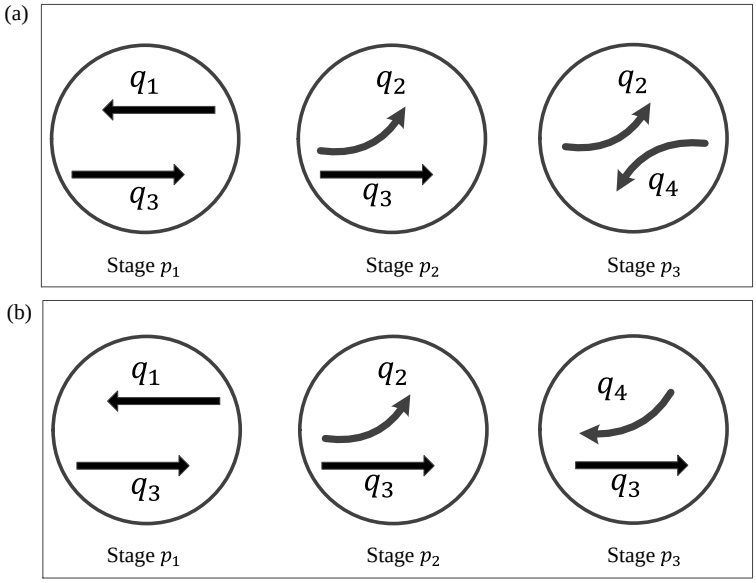

Figure 6.7.: Examples of three stages sharing movements.

6.4.5. Algorithms

The focus of this section is to explain signal timing calculation in the case of stages sharing the same movements, extended from (Pohlmann, 2010). The cycle length for each intersection is first calculated using Algorithm 3, and the largest cycle length is selected as the common cycle length. Using this, the green duration for each stage is calculated using Algorithm 4.

6.5. Performance criteria

The signal optimization methods are evaluated using three measurements. Delays at intersections are the most important measurements in many signal control systems. Then, the average degree of saturation at intersections is observed, as this measurement indicates the capacity usage at intersections. Finally, the total number of stops in the network is compared between cases with and without left turn prohibitions.

Algorithm 3 Calculation of cycle lengths for each intersection

Require: $b_{z,np}, b_{z,cp}, b_{z,sp}, B_z \triangleright b_{z,np}, b_{z,cp}, b_{z,sp}$ are the flow ratios of normal stages, stages sharing movements, and related sstages respectively.

Ensure: c_z

function CalculateCycleLength
  $B'_z \leftarrow B_z$, $\sum_{p=1}^{N'_{S,z}} g_{min,z,p} \leftarrow 0$
  repeat
    $flag \leftarrow 0$
    if $B_z > 1 - 1.5(\sum_{p=1}^{N_{S,z}} \sum_{\Omega'_{z,p',p=1}} \omega_{z,p,p'} + 5)/c_{max}$ **then**
      $c_z \leftarrow c_{max}$
    else
      $c_z \leftarrow Eq.\ (6.45)$
      if $c_z < c_{min}$ **then**
        $c_z \leftarrow c_{min}$
      end if
    end if
    for normal stages np **do**
      $g_{np} \leftarrow Eq.\ (6.46)$
      if $g_{z,np} < g_{min,z,np}$ **then**
        $g_{z,np} \leftarrow g_{min,z,np}$
        $\sum_{p=1}^{N_{S',z}} g_{min,p} \leftarrow g_{z,np}$, $B'_z \leftarrow B'_z - b_{z,np}$
        $flag \leftarrow 1$
      end if
    end for
    for stages sharing movements cp and their related stages sp **do**
      $g_{z,cp} \leftarrow Eq.\ (6.46)$, $g_{z,sp} \leftarrow Eq.\ (6.46)$
      if $g_{z,sp} < g_{min,z,sp}$ **then**
        $g_{z,sp} \leftarrow g_{min,z,sp}$
      end if
    end for
    for stages sharing movements cp and their related stages sp **do**
      if $g_{z,cp} < \sum g_{z,sp}$ and $g_{z,sp} == g_{min,z,sp}$ **then**
        $\sum_{p=1}^{N_{S',z}} g_{min,z,p} \leftarrow g_{z,p}$, $B'_z \leftarrow B'_z - b_{z,p}$
        $flag \leftarrow 1$
      end if
    end for
  until $flag == 0$
  return c_z
end function

Algorithm 4 Calculation of green durations for each stage

Require: $b_{z,np}, b_{z,cp}, b_{z,sp}, B_z, c$
Ensure: $g_{z,p}$

function CalculateGreens
  $B'_z \leftarrow B_z$
  $\sum_{p=1}^{N_{S',z}} g_{min,z,p} \leftarrow 0$
  repeat
    $flag \leftarrow 0$
    for normal stages p **do**
      $g_{z,np} \leftarrow Eq.\ (6.48)$
      if $g_{z,np} < g_{min,z,np}$ **then**
        $g_{z,np} \leftarrow g_{min,z,np}$
        $\sum_{p=1}^{N_{S',z}} g_{min,z,p} \leftarrow g_{z,np}$
        $B'_z \leftarrow B'_z - b_{z,np}$
        $flag \leftarrow 1$
      end if
    end for
    for stages sharing movements cp and their related stages sp **do**
      $g_{z,cp} \leftarrow Eq.\ (6.48)$
      $g_{z,sp} \leftarrow Eq.\ (6.48)$
      if $g_{z,sp} < g_{min,z,sp}$ **then**
        $g_{z,sp} \leftarrow g_{min,z,sp}$
      end if
    end for
    for stages sharing movements cp and their related stages sp **do**
      if $g_{z,cp} < \sum g_{z,sp}$ and $g_{z,sp} == g_{min,z,sp}$ **then**
        $\sum_{p=1}^{N_{S',z}} g_{min,z,p} \leftarrow g_{z,sp}$
        $B'_z \leftarrow B'_z - b_{z,sp}$
        $flag \leftarrow 1$
      else
        $g_{z,sp} \leftarrow \frac{b_{z,sp}}{\sum b_{z,sp}} g_{z,cp} \in [g_{min,p_1}, c]$
      end if
    end for
  until $flag == 0$
  for all stages p **do**
    $g_{z,p} \leftarrow g_{z,np}, g_{z,sp}$
  end for
  return g_p
end function

6.5.1. Delays

Although delays can be obtained from the proposed model, the delay values used for evaluation are from a VISSIM model, as the VISSIM simulation tool is widely used and reliable. It is interesting to compare delays between the lane-based method and the stage-based method, but also to compare between cases with and without left turn prohibitions.

6.5.2. Average degree of saturation

The average degree of saturation for each intersection is compared, rather than the degree of saturation for each movement. By observing the average degree of saturation at intersections, it is easier to detect how left turn prohibition influences the capacity usage of the whole intersection. The average degree of saturation is defined as:

$$\bar{\rho}_z = \frac{\sum \rho_{z,i,j} \cdot q_{z,i,j}}{\sum q_{z,i,j}}, \tag{6.52}$$

where $\bar{\rho}_z$ is the average degree of saturation of intersection z, and $\rho_{z,i,j} = \frac{\rho_{z,i,k} \cdot q_{z,i,j,k}}{q_{z,i,j}}$ if $\delta_{z,i,j,k} = 1$ is the degree of saturation of movement (i, j).

6.5.3. Total number of stops

The number of stops is another important measurement that is used in the TRANSYT, SCOOT, and MOTION signal control systems. As the total number of stops cannot be obtained from the proposed model, the values of this measurement are obtained from a VISSIM model.

7. Numerical analysis

7.1. Overall

The proposed method is tested for both an artificial network and a real network in the southern city of Hanover, Germany. The artificial network is used to evaluate the proposed method and to analyse the idea behind left turn prohibition. The real network is used to apply the proposed method in a situation of near reality.

7.2. Artificial network

7.2.1. Network configuration

The artificial network has five signalized intersections with eight origins and eight destinations. The layouts of the networks and intersections are drawn in SUMO, a simulation tool developed by the German Aerospace Centre (DLR), and are shown in Figure 7.1 and Figure 7.2, respectively. With five intersections, there are 20 left turns in total - each arm has one left turn (See Table 7.1). The lengths of external links and the number of lanes for each external link are displayed in Table 7.2. The free flow speed is 50 km/h, so the free flow travel time of each link is calculated via the link length divided by the free flow speed. The network is tested with an OD matrix in Table 7.3.

The maximum cycle length is 90 s and the minimum cycle length is 60 s for each intersection. The minimum green duration is 5 s for each movement. Intergreen times between conflict movements are 4 s. Conflict matrices of each intersection are obtained from SUMO networks. The values of relevant parameters are given in Table 7.4.

7.2.2. Results

Both the lane-based method and the stage-based method are tested using the OD matrix and the artificial network. In the proposed method with the lane-based signal setting optimization, the total travel time of the network is reduced from 120.60 h to 117.82 h, which is a 2.31% reduction. Left turn numbers 1, 2, 15, and 20 are prohibited. In the proposed method with the stage-based optimization, the total travel time without left turn prohibition is 115.49 h, and that of the optimal result is 110.02 h. Thus, it is a 4.74% reduction. Left turn numbers 9, 15, 16 and 20 are prohibited. Please note that left turns are not prohibited if no travel time reduction is gained.

The cycle length in the lane-based method before and after left turn prohibition is 90 s, and the cycle lengths in the stage-based method before and after left turn prohibition are 68 s and 61 s respectively. The stage-based method can shorten cycle length compared

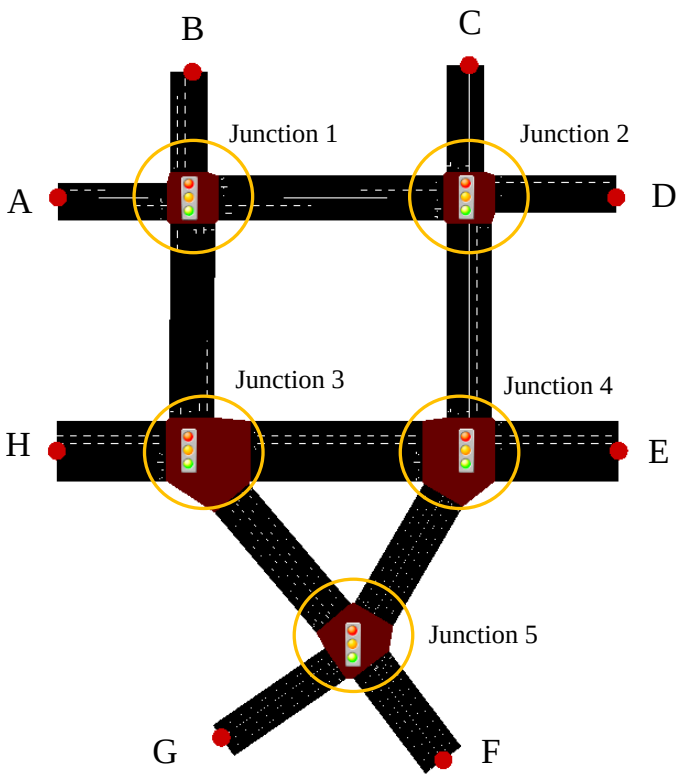

Figure 7.1.: Layouts of the artificial network.

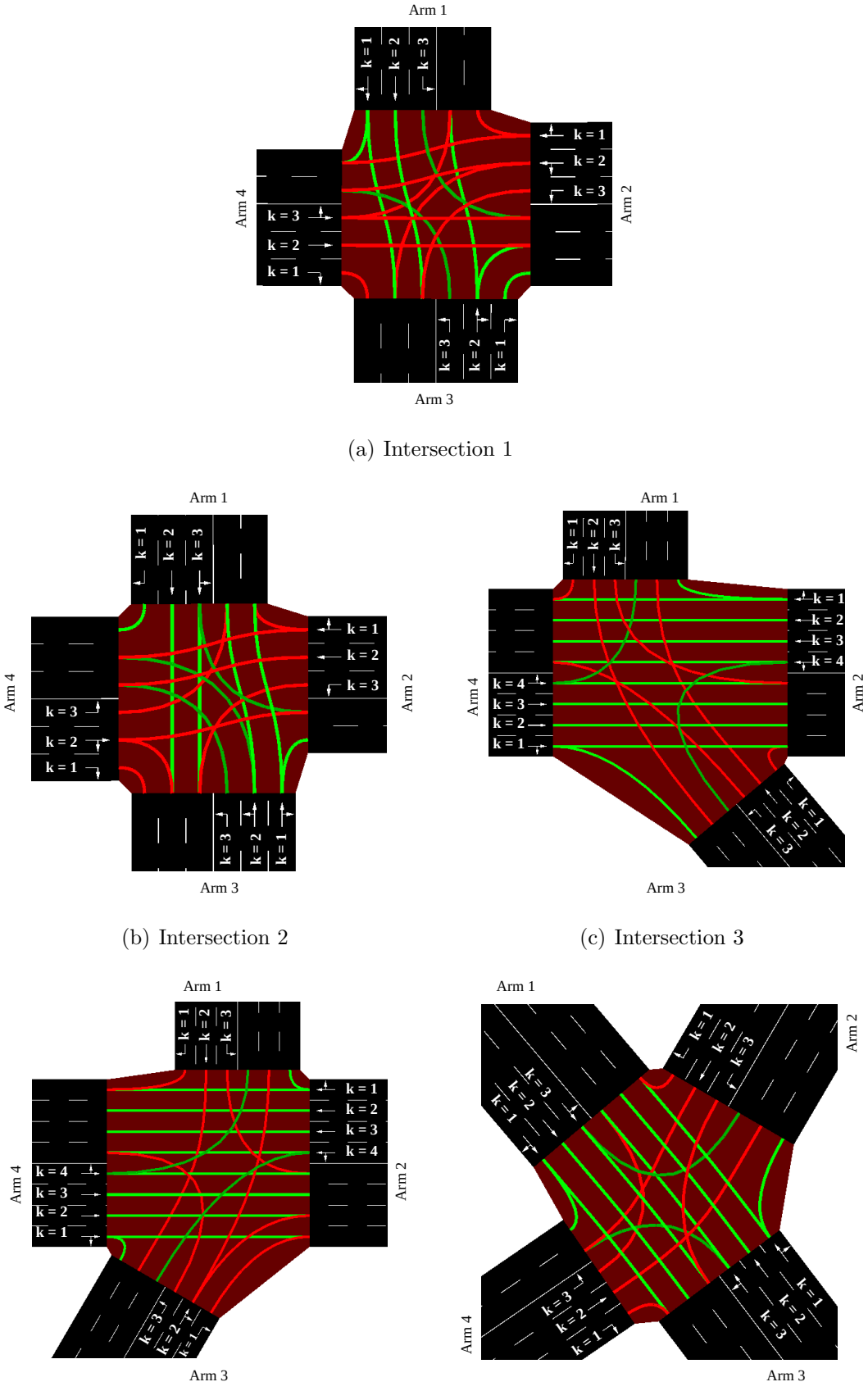

(a) Intersection 1

(b) Intersection 2

(c) Intersection 3

(d) Intersection 4

(e) Intersection 5

Figure 7.2.: Layout of intersections in the artificial network.

Table 7.1.: Left turns in the artificial network

No.	Intersection	From arm	To arm
1	1	1	2
2	1	2	3
3	1	3	4
4	1	4	1
5	2	1	2
6	2	2	3
7	2	3	4
8	2	4	1
9	3	1	2
10	3	2	3
11	3	3	4
12	3	4	1
13	4	1	2
14	4	2	3
15	4	3	4
16	4	4	1
17	5	1	2
18	5	2	3
19	5	3	4
20	5	4	1

to the lane-based method. The signal timing plans of both methods can be seen in Appendix A.

It is also interesting to observe the changes in the shortest travel times. In a SUE assignment model, the route travel times between each OD pair may not be the same in the equilibrium state because only the perceived route travel times are the same. The changes in the shortest route travel times are calculated to see the effect of left turn prohibition on the shortest travel time. In Table 7.5 and Table 7.6, the changes in the proposed model with the lane-based method and with the stage-based method are displayed respectively. Most of the shortest route travel times are reduced, but some of them increase. The shortest travel times for most of OD pairs are reduced, with the cost being that the travel times for some OD pairs increase.

7.2.3. Simulation study

The left turn prohibition results and the signal timing results are also studied in a VISSIM 8 simulation tool. The simulation study is conducted because more performance criteria before and after left turn prohibition can be compared. Further, the left turn decision can also be evaluated in a simulation model to check the correctness of the proposed model. The involved performance criteria in the simulation are:

- total travel time,

Table 7.2.: Information on external links in the artificial network

No.	From	To	Length (m)	Number of lanes
1	Origin A	Intersection 1	200	3
2	Intersection 1	Destination A	200	2
3	Origin B	Intersection 1	50	3
4	Intersection 1	Destination B	50	2
5	Intersection 1	Intersection 2	400	3
6	Intersection 2	Intersection 1	400	3
7	Intersection 1	Intersection 3	400	3
8	Intersection 3	Intersection 1	400	3
9	Origin C	Intersection 2	50	3
10	Intersection 2	Destination C	50	2
11	Origin D	Intersection 2	200	3
12	Intersection 2	Destination D	200	2
13	Intersection 2	Intersection 4	400	3
14	Intersection 4	Intersection 2	400	3
15	Origin H	Intersection 3	200	4
16	Intersection 3	Destination H	200	4
17	Intersection 3	Intersection 4	400	4
18	Intersection 4	Intersection 3	400	4
19	Origin E	Intersection 4	200	4
20	Intersection 4	Destination E	200	4
21	Origin F	Intersection 5	200	3
22	Intersection 5	Destination F	200	3
23	Origin G	Intersection 5	200	3
24	Intersection 5	Destination G	200	2
25	Intersection 3	Intersection 5	300	3
26	Intersection 5	Intersection 3	300	3
27	Intersection 4	Intersection 5	400	3
28	Intersection 5	Intersection 4	400	3

Table 7.3.: Demands between origins and destinations in the artificial network (veh/h)

Origin \ Destination	A	B	C	D	E	F	G	H	Origin total
A	0	70	90	60	100	60	50	50	480
B	100	0	30	60	40	70	90	30	420
C	80	90	0	80	90	60	70	50	520
D	40	70	40	0	80	20	60	100	410
E	60	30	70	40	0	90	40	50	380
F	90	80	90	80	70	0	50	100	560
G	60	70	100	50	80	80	0	90	530
H	90	80	40	50	0	70	60	0	390
Destination total	520	490	460	420	460	450	420	470	3690

Table 7.4.: Values of parameters in the artificial network

Parameters	Notations	Values
Scale parameter in logit model	γ	1
Parameter in BPR function	α	0.15
Parameter in BPR function	β	4
Saturation flow of through movements (veh/h)	s_{TH}	1900
Saturation flow of right turns (veh/h)	s_{RT}	1615
Saturation flow of protected left turns (veh/h)	s_{protLT}	1805
Saturation flow ofpermitted left turns (veh/h)	s_{permLT}	Eq. (5.19) and Eq. (5.20)
Observation time in delay function (h)	T	0.25
Convergence criteria of SUE	ϵ	5.0×10^{-4}
Arbitrary large positive constant	H	1.0×10^{15}
Difference between actual green time and effective green time (s)	e	1
Number of populations in genetic algorithm	-	40
Number of generations in genetic algorithm	-	60

Table 7.5.: Changes in shortest route travel time between each OD pair in the proposed model using the lane-based method (%).

Origin \ Destination	A	B	C	D	E	F	G	H
A	0.0	-5.1	2.1	2.9	7.1	- 8.0	-7.3	12.2
B	-3.9	0.0	120.1	100.8	9.5	- 8.6	-7.9	12.3
C	1.6	20.2	0.0	13.2	-4.1	- 17.1	-17.5	-31.1
D	0.2	14.9	-19.7	0.0	11.4	- 6.5	-6.7	-24.6
E	1.5	1.6	39.3	14.0	0.0	- 6.2	-6.5	-25.5
F	-12.5	-13.4	6.7	-4.7	0.0	0.0	-0.7	-4.9
G	-13.3	-14.3	5.9	-4.1	0.1	0.0	0.0	-5.6
H	-10.0	-11.1	-4.2	-3.3	0.0	29.0	26.4	0.0

Table 7.6.: Changes in shortest route travel time between each OD pair in the proposed model using the stage-based method (%).

Origin \ Destination	A	B	C	D	E	F	G	H
A	0.0	-2.8	-4.2	-3.6	12.5	- 8.9	-8.9	5.3
B	-4.4	0.0	-5.6	-4.8	-0.7	- 9.1	-9.1	4.4
C	-4.6	-5.5	0.0	-6.0	-5.5	- 3.3	-3.3	1.1
D	-3.2	-3.8	-4.2	0.0	-2.4	- 1.3	-1.2	0.6
E	-4.8	-5.3	-5.0	-5.5	0.0	- 5.4	-5.4	-6.0
F	1.0	2.9	-0.3	-0.9	1.4	0.0	-3.1	-10.0
G	-3.2	-1.7	-1.2	-1.7	0.1	- 2.5	0.0	-14.6
H	-9.3	-7.8	-8.3	-6.9	0.0	- 9.7	-9.6	0.0

- average delays, and
- total number of stops.

The layout configuration of the network, including the external link length, the number of lanes, and the lane markings, stays consistent in the simulation model. The demands are from Table 7.3 and with default stochastic arrivals. The simulation period is 900 s. The random seed is 42 with an increment value of 1. The number of runs is 30.

The signal timing plan is the same as the proposed model. The priority rule is set between left turns and their opposing through vehicles if the left turns are permitted. For different turning movements, a reduced area is applied: 25 km/h is applied for left turns and 15 km/h is applied for right turns. Thus, the saturation flow for different movements can be adjusted. The turning rates of different movements are calculated based on the link flows at equilibrium states from the proposed model. The link flows of internal links and their turning rates can be found in Appendix B.1. The Wiedemann (1974) car-following model is selected as the simulation model.

A comparison of link delays can be found in Appendix B.3. The link delays in both the proposed model and the VISSIM model generally match well, except for some of the permitted left turns. The delays of the permitted left turns in the proposed models are obviously larger than the delays in the VISSIM model. The main reason behind this is the different capacity estimations of permitted left turns in these two models.

7.2.4. Evaluation

The effects of left turn prohibition are evaluated using the same VISSIM model and the proposed model. The link flows and link delays of the case with the lane-based method without left turn prohibition are compared. The travel times, delays, and the number of stops are observed in the VISSIM model, and the degree of saturation is observed in the proposed model.

Total travel time

The travel time data are read from the vehicle performance in VISSIM. In the proposed method with lane-based signal optimization, the total travel time in 900 s is 113,913.4 s in the case without left turn prohibition and 111,367.1 s in the optimal case, which is a 2.2% reduction. In the models with stage-based signal settings, the total travel time changes from 113,683.5 s to 107,698.6 s - a 5.3% reduction. Prohibiting left turns reduces the total travel time in the VISSIM model as well.

Average delays

The average delay is also read from the vehicle performance. In the VISSIM model with lane-based signal optimization, the average delay of the network is 55.5 s/veh in the case without left turn prohibition and 57.2 s/veh in the optimal case, which is a 3.1% increase in delays. In the VISSIM model with stage-based signal settings, the average delays without and with left turn prohibition are 61.5 s/veh and 55.8 s/veh respectively, so the delay increases by 9.3% with left turn prohibition.

The average delays of each intersection are also compared based on the data of the VISSIM model. Figure 7.3 shows the comparison between the lane-based method and the stage-based method in the case without left turn prohibition, and the comparison between the cases without and with left turn prohibition in the lane-based method and in the stage-based method. Generally, in the lane-based method, the average delays of the intersections are smaller. In Figure 7.3(b), the delay at Intersection 2 after left turn prohibition becomes smaller, whereas the delays at the rest of the intersections become larger. In Figure 7.3(c), the delay at Intersections 1 and 2 increases after left turn prohibition and the delays at the rest of the intersections decrease. Therefore, left turn prohibition reduces the total delays with the cost being that delays increase at some of the intersections.

Number of stops

The total number of stops in the network is recorded in Table 7.7. The total number of stops increases in both the lane-based method and the stage-based method. Prohibiting left turns does not reduce the number of stops.

Table 7.7.: Total number of stops in the VISSIM model without and with left turn prohibition

Method	Without left turn prohibition	Optimal result	Reduction
Lane-based	1,447	1,444	0.2%
Stage-based	1,846	1,763	4.5%

Degree of saturation

The average degrees of saturation for each intersection are first compared between the proposed model with the lane-based method and the proposed model with the stage-based method (See Figure 7.4(a)). The degrees of saturation of the proposed model with the lane-based method for all intersections are smaller those of the proposed model with the stage-based method, which indicates that the lane-based method has a better capacity usage than the stage-based method.

The average degree of saturation for each intersection also changes. In the proposed method with the lane-based optimization, the average degrees of saturation before and after left turn prohibition are shown in Figure 7.4(b), and those of the stage-based optimization are shown in Figure 7.4(c). In the proposed model with the lane-based method, the average degree of saturation for Intersections 1, 2, and 3 decreases after left turns are prohibited, whereas the average degree of saturation for Intersections 4 and 5 slightly increases. In the proposed model with the stage-based method, only the average degree of saturation at Intersection 4 decreases. Left turn prohibition forces vehicles to reach uncongested intersections.

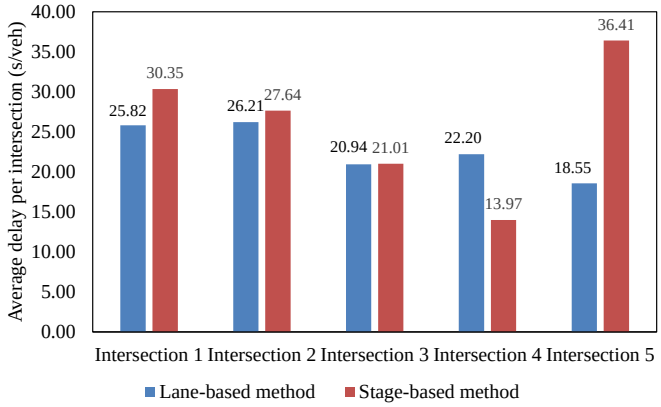

(a) Comparison of the lane-based method and the stage-based method

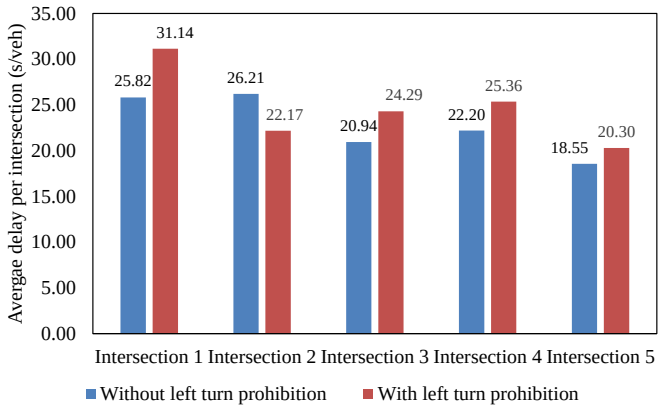

(b) Comparison between the cases without and with left turn prohibition in the lane-based method

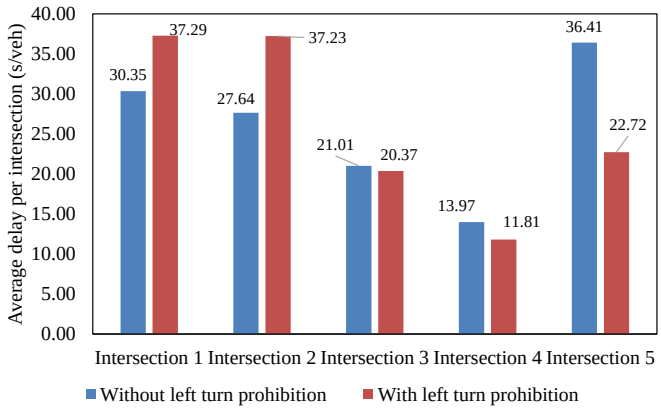

(c) Comparison between the cases without and with left turn prohibition in the stage-based method

Figure 7.3.: Comparison of average delays in the VISSIM model.

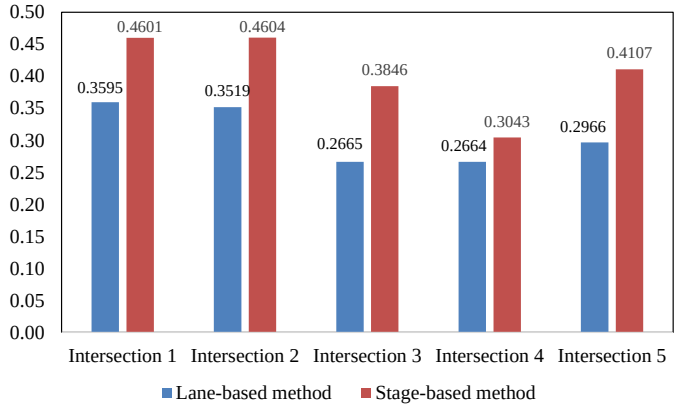

(a) Comparison of the lane-based method and the stage-based method

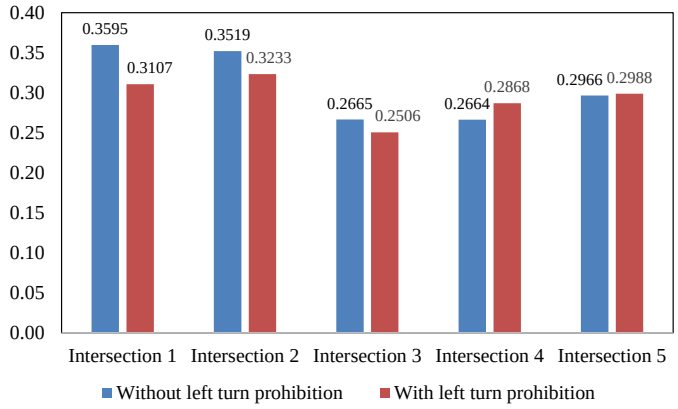

(b) Comparison between the cases without and with left turn prohibition in the lane-based method

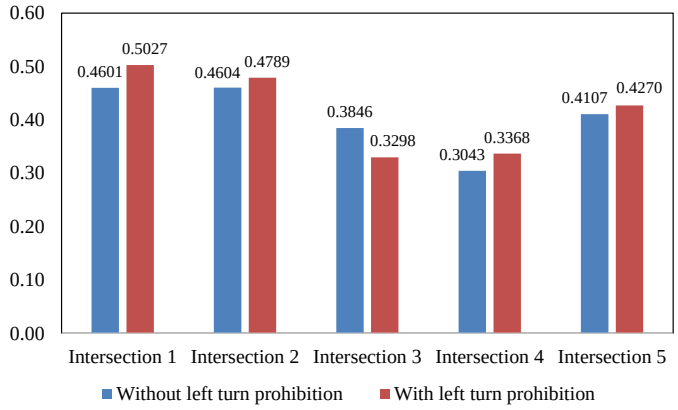

(c) Comparison between the cases without and with left turn prohibition in the stage-based method

Figure 7.4.: Comparison of average degrees of saturation in the proposed model.

7.3. Hanover South network

7.3.1. Network configuration

The proposed method is also tested with a network from the southern city of Hanover, Germany. This test network has 16 origins and 16 destinations. There are 14 signalized intersections. In reality, Intersection 9 and Intersection 12 are unsignalized. However, as the proposed model does not consider the delay estimation at unsignalized intersections, these two intersections are set as signalized intersections. That is why this test network is a "like-real" network rather than a real network. The network has 56 left turns. The details of external links and the OD matrix can be found at Github[1].

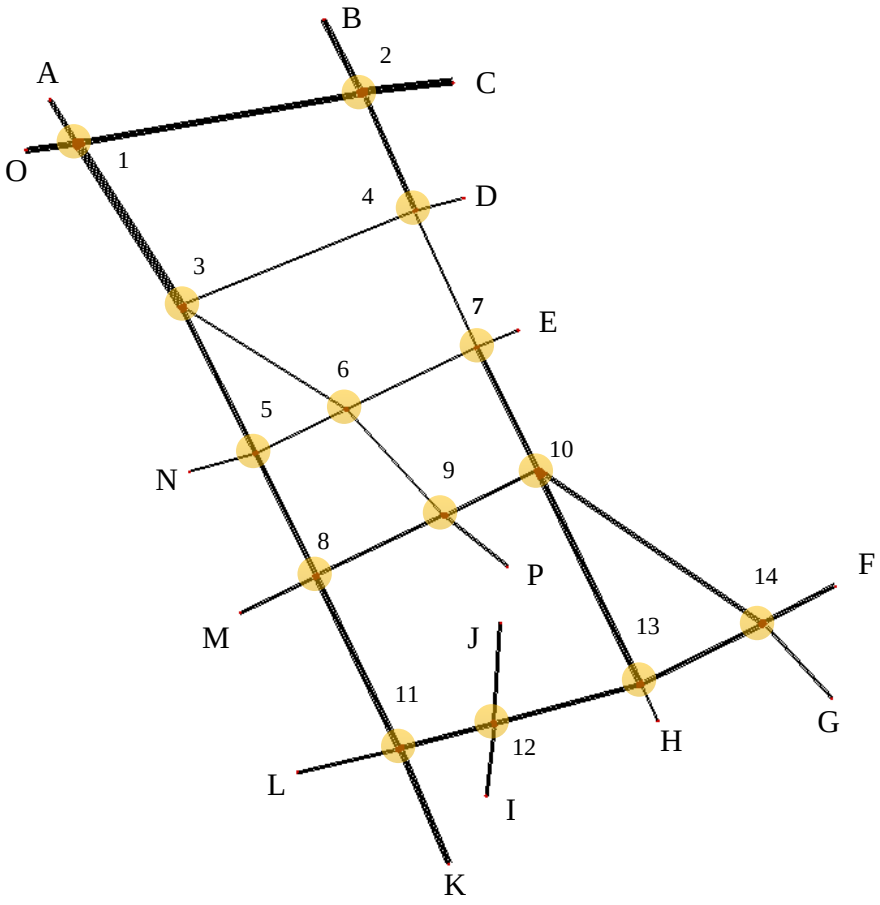

Figure 7.5.: Layout of the Hanover South network.

7.3.2. Results

In the proposed method with the lane-based optimization, the total travel times before and after left turn prohibition are 6,327.95 h and 5,593.31 h respectively, and 18 left turns are prohibited. The total travel time reduction is 11.6%. With the stage-based

[1] https://github.com/yemayet/HannoverSuedNetwork.git

optimization, the total travel times before and after left turn prohibition are 7,008.39 h and 4,690.75 h respectively - a reduction of 33.1% - and 21 left turns are prohibited.

The changes in the shortest route between each OD pair are recorded in Table 7.8 and Table 7.9 for both the lane-based method and the stage-based method, respectively. Similarly, prohibiting left turns lengthens some of the route travel times, but overall it reduces the total travel time.

7.4. Analysis of prohibited left turns

All analysis of prohibited left turns is conducted with the artificial network. The influence of demand variance and, the influence of left turn types are analysed in this section.

7.4.1. Influence of demand variance

Whether left turn prohibition results can stand up to changeable demands is tested in this section. With the stochastic arrivals of vehicles, traffic demands are not always stable. If left turn prohibition cannot deal with the variance of demands, it is hard to apply them in practice. Thus, it is necessary to observe the influence of demand variance.

In order to test the influence of demand variance, eight OD matrices are generated based on the OD matrix in Table 7.3. The demands in the base OD matrix are the mean values and the test OD matrices are generated by randomly adding the variance in the interval $[-5, 5]$, $[-10, 10]$, $[-15, 15]$, $[-20, 20]$, $[-25, 25]$, $[-30, 30]$, $[-35, 35]$ and $[-40, 40]$. The test OD matrices can be found in Appendix C. The optimal left turn prohibition results in the proposed model with the lane-based method and the stage-based method are fixed when the OD matrices with demand variance are tested.

The testing results are shown in Figure 7.6. The horizon axis is the demand variance. The vertical axis is the total demand change between the case with and without left turn prohibition. In the proposed model with the lane-based method, the optimal left turn prohibition combination can deal with only half of the different demand variances. When the OD matrices are tested with the stage-based method, the optimal combination can deal with all of the different OD matrices, but the reductions of the OD matrices with high variances are not large.

7.4.2. Analysis of factors influencing left turn prohibition

More OD matrices are tested for the purpose of analysing the factors influencing left turn prohibition. The idea behind this is determining whether a traffic manager can roughly determine the effects of left turn prohibition based on the data from a network without left turn prohibition. For example, left turns with minor flows might be best to prohibit, or left turns with major opposing flows might be best to prohibit. To explore the factors influencing left turn prohibition, more tests should be done.

In the literature review (Section 2.2.6), several factors that may influence left turn prohibition are mentioned. The factors are left turn flows, opposing through flows, and

Table 7.8.: Changes in shortest route travel time of Hanover South network in the proposed model with the lane-based method (%).

Ori \ Des	A	B	C	D	E	F	G	H	I	J	K	L	M	N	O	P
A	0.0	-2.0	0.0	-28.6	-27.1	0.0	-19.0	-20.6	-36.1	0.0	-37.1	-39.8	0.0	-47.8	-25.9	-26.1
B	-65.5	0.0	0.0	0.0	0.0	0.0	0.0	0.0	-35.0	0.0	0.0	0.0	0.0	-40.0	-72.9	-22.7
C	0.0	0.0	0.0	0.0	29.2	0.0	-25.1	-18.4	-26.8	0.0	-24.3	-26.4	-29.8	-29.8	-49.5	-22.9
D	-14.3	0.0	0.0	1.9	0.0	0.0	-15.1	0.0	-19.2	0.0	-6.6	0.0	0.0	0.9	0.0	-14.0
E	-27.0	0.0	0.0	0.0	0.0	0.0	-9.0	0.0	-18.2	-18.2	-15.2	0.0	-16.4	-30.2	-32.2	-7.7
F	-3.4	0.0	-3.0	-3.0	9.9	-8.8	980.3	0.0	-30.7	-30.6	-25.5	0.0	-15.9	-23.0	-6.4	38.7
G	-2.8	0.0	-2.4	-2.4	11.5	0.0	0.0	0.0	0.0	0.0	0.0	0.0	0.0	0.0	0.0	43.0
H	-2.5	-11.0	-8.5	0.0	0.0	0.0	0.0	0.0	225.8	223.4	91.8	0.0	116.0	43.2	-7.4	21.0
I	21.5	-8.9	-6.6	-6.7	-0.6	-1.3	0.0	58.8	-3.4	0.0	0.0	71.3	0.0	83.3	15.2	20.8
J	-1.5	0.0	0.0	0.0	0.0	-2.9	0.0	41.4	0.7	0.0	0.0	0.0	0.0	0.0	0.0	-10.8
K	-23.3	-28.0	-29.4	-26.7	-6.8	13.5	0.0	61.3	52.8	0.0	-12.1	0.0	-22.9	-14.2	-29.0	-12.2
L	-21.4	-26.7	-28.1	0.0	-5.5	0.0	0.0	0.0	0.0	0.0	0.0	0.0	-14.5	0.0	-27.2	-8.7
M	0.0	0.0	-20.8	0.0	-22.6	0.0	0.0	13.7	-10.7	0.0	6.4	-7.3	0.0	0.0	-6.6	0.0
N	-23.2	-29.0	-30.9	-27.5	-10.4	-6.0	0.0	7.3	-8.1	0.0	-0.2	-5.7	0.0	-30.3	-31.0	-9.1
O	2264.6	0.2	-25.1	0.0	-25.4	0.0	-17.4	-19.1	-34.5	0.0	-35.4	-38.1	-43.3	-45.6	-28.0	-24.1
P	-10.8	-21.1	-18.9	-19.4	-20.2	-7.2	-5.2	3.3	-16.9	-16.8	13.0	13.2	170.7	30.8	-16.4	0.0

Note: "Ori" is short for "Origin" and "Des" is short for "Destination".

Table 7.9.: Changes in shortest route travel time of Hanover South network in the proposed model with the stage-based method (%).

Ori \ Des	A	B	C	D	E	F	G	H	I	J	K	L	M	N	O	P
A	0.0	76.0	0.0	46.1	16.2	0.0	-29.3	-28.2	-40.6	0.0	-41.2	-37.6	0.0	-48.0	-30.0	-24.1
B	-36.2	0.0	0.0	0.0	0.0	0.0	0.0	0.0	-44.1	0.0	0.0	0.0	0.0	-54.7	-36.3	-32.4
C	0.0	0.0	0.0	0.0	22.5	0.0	-47.1	-43.1	-49.0	0.0	-47.0	-44.1	-51.0	-54.5	-36.3	-32.3
D	-49.3	0.0	0.0	-14.9	0.0	0.0	-48.1	0.0	-50.1	0.0	-47.4	0.0	0.0	-54.2	0.0	-34.6
E	-17.7	0.0	0.0	0.0	0.0	0.0	8.8	0.0	-7.7	-7.7	3.3	0.0	-13.5	-19.7	-5.1	9.1
F	-49.6	0.0	-58.8	-60.7	-58.0	93.7	56.3	0.0	9.3	9.2	23.7	0.0	-50.8	-49.1	-39.2	-44.1
G	-46.0	0.0	-55.6	-57.4	-52.7	0.0	0.0	0.0	0.0	0.0	0.0	0.0	0.0	0.0	0.0	-34.4
H	-31.3	-37.7	-37.4	0.0	0.0	0.0	0.0	0.0	-8.3	-8.2	11.5	0.0	-17.9	-21.9	-19.0	17.6
I	-17.7	-31.5	-31.2	-32.3	-20.0	48.1	0.0	20.6	37.7	0.0	0.0	599.8	0.0	28.1	-1.8	31.4
J	-25.7	0.0	0.0	0.0	0.0	8.1	0.0	-7.2	-45.2	0.0	0.0	0.0	0.0	0.0	0.0	-11.0
K	-47.7	-43.4	-43.1	-44.2	-21.7	4.5	0.0	-5.0	-19.6	0.0	-9.2	0.0	-19.5	-0.7	-38.3	-8.3
L	-48.6	-44.3	-44.0	0.0	-24.7	0.0	0.0	0.0	0.0	0.0	0.0	0.0	-20.4	0.0	-39.2	-8.3
M	0.0	0.0	-45.9	0.0	-35.5	0.0	0.0	-8.0	-24.0	0.0	-25.0	-16.1	0.0	0.0	-39.0	0.0
N	-36.7	-14.9	-15.8	-15.5	-45.4	-34.4	0.0	-27.7	-43.7	0.0	-44.6	-39.2	0.0	-14.1	-17.3	-35.7
O	-1.5	-7.8	13.6	0.0	21.2	0.0	-43.7	-37.5	-47.6	0.0	-48.3	-44.4	-54.3	-61.6	-29.9	-30.7
P	-59.1	-53.7	-53.2	-55.2	-30.3	-39.9	-39.4	-24.0	-44.3	-44.0	2.8	0.0	-79.6	13.9	-47.9	0.0

Note: "Ori" is short for "Origin" and "Des" is short for "Destination".

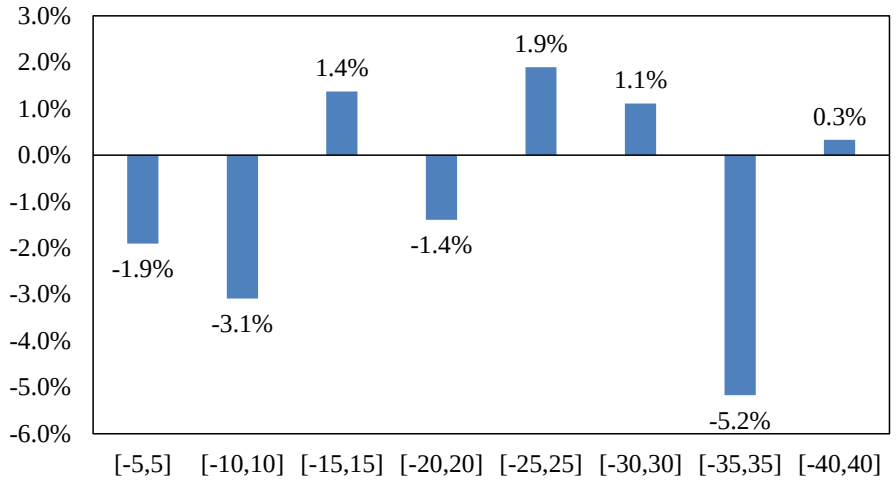

(a) Total travel time reduction in the proposed model with the lane-based method

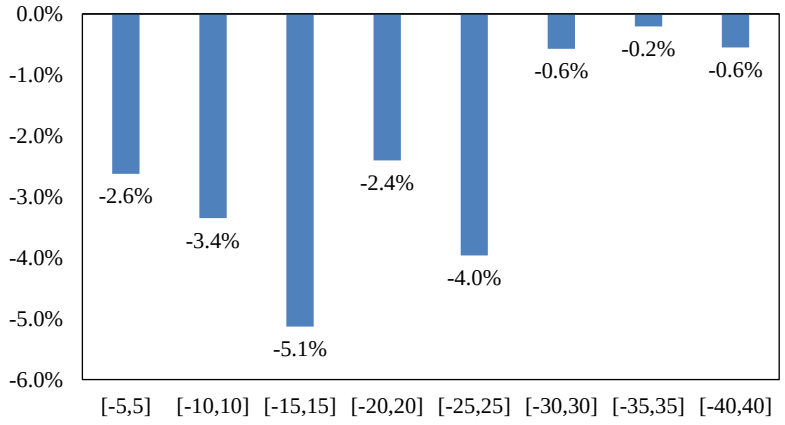

(b) Total travel time reduction in the proposed model with the stage-based method

Figure 7.6.: Influence of demand variance in proposed model with the lane-based and the stage-based methods.

the average degree of saturation at the intersection. Although turning capacity is also mentioned, this factor is found at unsignalised intersections and is similar to the degree of saturation, so it is not analysed in this thesis. According to the findings in previous research, left turns with small flows, left turns with large opposing through flows, and left turns at congested intersections should be prohibited. However, in the early study of this thesis, left turns with minor flows are not always prohibited. Thus, left turn phasing types, which are not mentioned in previous studies, are considered. Left turn prohibition might be relevant to left turn phasing types in that the permitted left turns with large flows cause high delays and the protected left turns with small flows reduce the effective green time. It is interesting to observe whether the data matches the three factors mentioned, and whether left turn phasing types influence left turn prohibition.

The data are collected from the proposed model without left turn prohibition because the goal of this analysis is to roughly decide which left turns would potentially be prohibited. Then, the optimal left turn prohibition combination is recorded from the proposed model with left turn prohibition. As the average degrees of saturation at intersections of the base OD matrix are small, it is better to use larger demands and observe how left turn prohibition changes with larger demands. The artificial network is then tested with the OD demands generated based on the OD matrix in Table 7.3 by adding the random demand in the interval $[-10, 0]$, $[0, 10]$, $[10, 20]$, $[20, 30]$, $[30, 40]$, $[40, 50]$, $[50, 60]$ and $[60, 70]$. Thus, nine OD matrices are tested including the base OD matrix. Because the artificial network has 20 left turns, in total, 180 left turn data points are collected for each signal optimization method. The proposed model is tested with the lane-based method and the stage-based method.

In the proposed model with the lane-based method, 57 of 180 left turns are prohibited; in the proposed model with the stage-based method, 36 of 180 left turns are prohibited. The small flows are defined as the flows smaller than the average values. Table 7.10 shows the average flows of different left turns. The average flow of the prohibited left turn case is much smaller than the average flow of the case with left turns not prohibited in the proposed model with the lane-based and the stage-based methods. Thus, left turns with minor flows are likely to be prohibited.

The average flow of protected left turns is usually larger than the average flow of permitted left turns. The average flow of prohibited protected left turns is smaller than the average flow of all protected left turns, so protected left turns with minor flows are likely to be prohibited. However, permitted left turns with large flows only partially support the hypothesis because the average flow of prohibited permitted left turns with the lane-based method is even smaller than the average flow of permitted left turns.

Table 7.11 shows the average flow of opposing through movements of different left turns. Overall, the average flow of prohibited left turns, whether the left turn is permitted or protected, is larger than the average flow of all left turns. Left turns with large flows of opposing through movements, are the best candidates for prohibition.

In Table 7.12, the average degrees of saturation at the intersection are summarized, rather than the degrees of saturation of left turns. Although previous studies say that left turns

Table 7.10.: Average flows of different left turns (veh/h).

Left turns	With lane-based method	With stage-based method
All left turns	169.30	172.93
Prohibited left turns	98.81	98.42
Permitted left turns	88.42	95.27
Protected left turns	246.67	198.81
Prohibited permitted left turns	72.74	96.67
Prohibited protected left turns	155.28	100.17

Table 7.11.: Average flows of opposing through movements of different left turns (veh/h).

Opposing through movements of	With lane-based method	With stage-based method
All left turns	282.08	281.82
Prohibited left turns	304.46	336.00
Permitted left turns	262.39	276.67
Protected left turns	300.98	283.74
Prohibited permitted left turns	293.59	317.17
Prohibited protected left turns	328.00	300.83

at intersections with higher degrees of saturation should be prohibited, the data does not support this finding because the average degree of saturation for prohibited left turns is larger than that for all left turns. However, if left turn phasing types are considered, in the proposed model with the lane-based method and with the stage-based method, permitted left turns at the intersections with a higher average degree of saturation are likely to be prohibited. For protected left turns, the data from the proposed model with the stage-based method still supports this finding, but the data from the model with the lane-based method does not support this finding.

Table 7.12.: Average degree of saturation at the intersection for different left turns.

Average degree of saturation	With lane-based method	With stage-based method
All left turns	0.5216	0.6285
Prohibited left turns	0.4888	0.6032
Permitted left turns	0.4518	0.4741
Protected left turns	0.5455	0.6532
Prohibited permitted left turns	0.4763	0.5153
Prohibited protected left turns	0.5015	0.6861

In summary, according to the data from the numerical example, left turns with minor flows, protected left turns with minor flows, left turns having opposing through movements with large flows, and permitted left turns at the intersections with a high degree of saturation are likely to be prohibited.

7.5. Discussion

The goal of this thesis is to minimize the total travel time of networks by prohibiting left turns. After left turns are prohibited, the total travel time is reduced. Through an analysis of prohibited left turns, it is found that left turn prohibition is related to left turn flows, left turn phasing types, opposing through flows, and the average degree of saturation at the intersections. This study could potentially lead to useful insights regarding congestion management and the options for left turn treatment.

7.5.1. Left turn prohibition

Although left turn prohibition makes some intersections more congested and lengthens some of the route travel time, the overall travel time of the network is reduced. Left turn prohibition assigns traffic flows at some intersections to other intersections so that the overall capacity usage of the network is improved. Hence, the precondition of successful application of left turn prohibition is that the capacity of some intersections can handle the prohibited left turn flows. If the whole network is over congested, prohibiting left turns hardly reduces the total travel time.

Prohibiting left turns can reduce delays at intersections with prohibited left turns, and in turn, the corresponding travel time. The main reasons for this are that left turn prohibition reduces the number of conflict points and increases the lane capacity of through movements.

Prohibiting left turns reduces the number of conflict points at intersections. There are intergreen times between all conflict movements for safety reasons. After left turns are prohibited, the intergreen time between left turns and other movements is transferred to effective green time. In the proposed model with the lane-based method, all movements at that intersection could benefit from a longer effective green time. The number of movements sharing lanes is not as high as that before left turn prohibition, so the lane assignment for movements is more flexible. For this reason, more movements can be assigned individually rather than colonially as signal groups. The signal timing is then more specifically adjusted. As a result, vehicles can access the intersection with shorter delays. In the proposed model with the stage-based method, due to the reduction of conflict points, the number of stages decreases so that the intergreen time between two movements decreases. More movements are in multiple stages, which also lengthens effective green times for those movements. Even if the number of stages does not decrease, because the prohibited left turns do not share lanes with the through movements, the saturation flows of the lanes increases. With the same green time and cycle time, the capacity of the lanes increases.

The re-usage of left turn lanes is another reason why prohibiting left turns reduces the total travel times. More lanes could be used for the rest movements, causing the capacities of the movements to increase. Due to the increase in the capacities, vehicles can pass the intersection in question more quickly.

7.5.2. Factors influencing left turn prohibition

In the last section, some factors influencing left turn prohibition are found. Left turns with minor flows, especially for protected left turns, are likely to be prohibited. The large opposing through flows also influence left turn prohibition. Permitted left turns at relatively congested intersections have a high potential to be prohibited.

Left turns with minor flows should be prohibited because the prohibited traffic flows have fewer influences on the network, and these influences are usually treated as negative. More precisely, protected left turns with minor flows should be prohibited, as more effective green times can be achieved by prohibiting small protected left turn flows. However, although permitted left turn flows are usually smaller than protected left turn flows, permitted left turn flows have no obvious influences. The delays of permitted left turns are highly dependent on the opposing through flows. Even if the permitted left turn flows are small, the delays of the permitted left turns could be large if the opposing through flows are large. Thus, permitted left turns with large flows are not always prohibited. Large opposing through flows influence left turn prohibition, whether the left turns are protected or permitted. As mentioned, large opposing through flows can make the permitted left turns congested, so permitted left turns with large opposing through flows should be prohibited. Protected left turns are also influenced by large opposing through flows, which to some degree indicate greater capacity requirements for the through movements. The capacity being assigned to the protected left turns then might not be enough. Permitted left turns at intersections with a high average degree of saturation have a similar issue. If the average degree of saturation of the intersection is high, it is better that through movements are not interrupted by permitted left turns.

The findings regarding the factors influencing left turn prohibition can contribute to the heuristic algorithm development of the left turn prohibition problem. Once the relevant data of the test network are obtained, only the left turns with these factors are tested to be prohibited, so the search space of left turn prohibition combinations is narrowed. If the findings are proven to be solid, it is also possible to build up a guideline to be used in operations.

However, the findings are based on the results of one artificial network. With different test OD matrices, the findings may be different. All analyses about turning movement restriction only focused on the descriptive area to the best of my knowledge. There is no analysis for forecasting left turn or other turning movement prohibition. The difficulty is in collecting enough data from the real world, because the influences of left turn prohibition on real road networks are not well studied. It would be interesting to study these in the future.

7.5.3. Comparison between lane-based and stage-based signal optimization

As was mentioned in previous sections, the lane-based method is suitable for left turn prohibition problem because this method can handle the lane assignment in the absence of left turns. The stage-based method is widely used in practice, so it is also valuable

for use. The applications of the lane-based method and the stage-based method, to my knowledge, have not been compared by previous researchers. Thus, in this section, the advantages and disadvantages of these methods are compared.

A most important advantage of the lane-based method is that it can better assign the lanes of the prohibited left turns through optimization, rather than assign the lanes through assumptions like the stage-based method. Due to this advantage, applying the lane-based method to a network can allow a better usage of capacity, especially when the traffic demands are high. The average degree of saturation at intersections is smaller if the lane-based method is applied. However, a network using the stage-based method has fewer delays. Only when the traffic demands are large is the network using the lane-based method less congested. Thus, the stage-based method is suitable for a network with small demands, and the lane-based method is suitable for a network with increasing demands, which supports the statements of Allsop (1972a).

However, the lane-based method sometimes may have unreasonable green durations, and the stage-based method meets common sense more. The lane-based method determines green durations according to the flows of movements. When the flows are very small, the relevant green durations are also small, even if the movements in the same green time have longer durations. In practice, this is not common, because the green duration is determined by the movement with the largest flows in the same green time, like the stage-based method. Considering the stochastic arrivals of vehicles, this uncommon green duration may not be that convenient for vehicles. In order to better apply the lane-based method, the way of determining green durations should be improved.

Moreover, the stage sequence optimization of this thesis may have bias in favour of signal groups having many lanes. If there are many lanes for a particular movement, the intergreen time will be counted multiple times. If a movement only occupies one lane, the intergreen time is only counted once. The total intergreen time between two signal groups differentiates much.

8. Conclusions

8.1. Summary

The purpose of this dissertation is to investigate whether prohibiting left turns can improve efficiency in an urban signalized network. After prohibiting left turns, the proposed method forecasts traffic flows using the SUE model, for which link flows are the inputs of signal setting optimization. The left turn prohibition combination and signal settings on the networks are tested by the SUE again by calculating the total travel time of the network. As mentioned in Chapter 1, the following tasks are finished in this dissertation:

- Prohibiting left turns by minimizing the total travel times in urban networks.

Prohibiting left turns can reduce the total travel time in networks. The reason is that prohibiting left turns decreases the conflicts at intersections. Fewer conflicts lead to shorter clearance times and higher capacities, which thereby reduce the delays at intersections. However, as vehicles have to detour due to left turn prohibition, some parts of the network become more congested. Therefore, whether left turn prohibition can reduce total travel times highly depends on traffic demands and network configurations.

- Forecasting demands in networks using the stochastic user equilibrium model.

The traffic demands after introducing the left turn prohibition are estimated with the SUE while taking into consideration realistic route choice behaviour. The link flow distribution resulting from the SUE model shows how drivers respond to changes in the network. In the equilibrium state, the perceived path travel times for each OD are the same, but as drivers do not have sufficient knowledge regarding the actual travel times, the actual travel times may not be exactly the same. After left turn prohibition, the shortest path travel time between different ODs may be longer because the flow of prohibited left turn vehicles is assigned to other parts of the network. In sum, prohibiting left turns increases the overall efficiency but lengthens some of the individual path travel times.

- Optimizing signal settings by improving the lane-based method and the stage-based method in consideration of left turn phasing types.

The focus of this dissertation is to optimize signal settings, including left turn prohibition. The signal settings are decentralized and optimized intersection by intersection. Then, in order to evaluate the overall gain, the total travel time of the network is calculated. The stage-based method and the lane-based method are applied because the stage-based method is frequently used in practice, whereas the lane-based method can better handle lane assignment for planning purposes. In the lane-based method, lane assignment, signal sequence, and signal timing are locally optimized by maximizing the reserved capacity.

The cycle length for each intersection corresponds to the maximum reserved capacity. The original lane-based method is improved by avoiding conflicts in the next signal cycle. The movement restriction is also considered in the lane-based method, so that the improved method can be applied to any movement restriction problem, rather than to left turn prohibition alone. The stage-based method first determines the minimum number of stages of all movements and then optimizes the stage sequence by minimizing the total intergreen time. The cycle length and green durations are adjusted with the formulas in Webster (1958) and HBS (2001). Intersections are coordinated using the common cycle length, but the offset optimization is not studied in this thesis. The stage-based method is improved by examining the stages sharing the same movements both in the stage sequence optimization and then also during the signal timing adjustment.

As the computing complexity is exponential, the algorithms should be properly applied. The left turn prohibition combinations are randomly searched using the genetic algorithm. The genetic algorithm can select favourable individuals in each generation and quickly find the meta-optimal results. The stochastic loading part of the SUE model is efficiently solved with the STOCH algorithm, which does not need to enumerate all paths between each OD. If all paths between each OD are enumerated, the memory requirement is very high, and it is difficult to run the SUE in large networks. The lane-based method is formulated as a MILP, and this formulation does not require many computing resources. The optimization models in the stage-based method also do not consume memory and running time. The proposed model makes use of all these algorithms.

8.2. Outlook

Prohibiting left turns has both theoretical and practical implications. It provides insight into network design and congestion management in urban road networks. The signal setting optimization methods are enhanced to handle the absence of left turns. Left turn treatment can be extended to protected, permitted, and prohibited left turns rather than just protected and permitted left turns. The observation of the features of prohibited left turns contributes to solving turning movement restriction problems more quickly.

Left turn prohibition provides a new solution to congestion management in urban road networks. To solve congestion problems, traffic managers take many measures to improve the design of networks, for example, constructing new types of intersections and broadening and constructing roads. However, restricting some movements is seldom analysed, and especially the combination between network design problems and signal control problems. In practice, although left turns are prohibited at some intersections, the decisions are made according to historical accident data. The intersections with prohibited left turns are not analysed as part of the network, and then the effects of left turn prohibition on networks are left unclear. Prohibiting left turns supports the idea that the capacity of the prohibited left turns can be taken advantage of for other movements. This research supplies the network design problem and builds a theoretical basis for the application of left turn prohibition in practice.

Signal setting optimization methods are enhanced to handle the absence of left turns. Left turn prohibition influences traffic demand, conflict matrices, and lane assignment,

and significantly affects signal setting optimization results. All these elements are not considered by many signal control methods. Therefore, a signal setting solution is needed to deal with the signal control problem after left turn prohibition. This research improves the existing methods to solve the signal setting optimization problem in the absence of left turns. Focusing on the theoretical implications, signal setting optimization including left turn prohibition is achieved using the lane-based method; on the practical side, the problem is achieved with the stage-based method. Hence, both theoretical and practical applications are considered.

Left turn treatment options are extended to prohibiting left turns. In previous left turn treatments, left turns are treated as permitted or protected left turns, or combinations of the two. Prohibiting left turns is an extra option for left turn treatment. Further, the left turn type is also analytically determined in the proposed model. Compared with previous studies focusing on guidelines or isolated intersections, the proposed model can handle network scenarios. It is believed to be a superior method to determine left turn types.

The analysis of the factors influencing left turn prohibition contributes to solving turning movement restriction problems quickly. Left turn prohibition is not only relevant to left turn flows, but also to their phasing types, their opposing flows, and the average degree of saturation of the intersection. These findings may be applied in the algorithm development for the left turn prohibition problem.

As prohibiting left turns has both theoretical and practical implications, future works could improve upon this research. First, this dissertation concentrated on mathematical modelling rather than on algorithm development, so there are many research gaps for algorithm development. Left turn prohibition combinations can be selected with other algorithms, and in the case of non-linear objectives (e.g., minimization of the total delay) in the lane-based method, new algorithms would be interesting to explore. Second, the data generated from the proposed model may be used to analyse the network. With this data, the statistic or data mining method can be used to support some decisions on networks. Third, it is worth considering the adaptive scenario, in addition to fixed-time planning, . If left turn prohibition is applied in dynamic cases, a dynamic process should be employed in the traffic assignment model and adaptive traffic controls should be used in the signal setting optimization. A comparison between a fixed-time planning scenario and an adaptive scenario is also an interesting topic.

Bibliography

K. R. Agent. Guidelines for the Use of Protected/permissive Left-turn Phasing. Technical Report No. UKTRP-85-19, Kentucky Transportation Research Program, College of Engineering,University of Kentucky, 1985.

K. R. Agent and R. C. Deen. Warrants for Left-Turn Signal Phasing. Technical Report 505, Division of Research, Bureau of Highways, Department of Transportation, Commonwealth of Kentucky, 1978.

R. Akcelik. Time-Dependent Expressions for Delay , Stop Rate and Queue Length at Traffic Signals. Technical report, 1980.

A. F. Al-Kaisy and J. A. Stewart. New approach for developing warrants of protected left-turn phase at signalized intersections. *Transportation Research Part A: Policy and Practice*, 35(5):561–574, 2001.

R. Allsop. Estimating the traffic capacity of a signalized road junction. *Transportation Research*, 6:245–255, 1972a.

R. Allsop. Delay at a Fixed Time Traffic Signal-I: Theoretical Analysis. *Transportation Science*, 6(3):260–285, 1972b.

H. M. Aziz and S. V. Ukkusuri. Integration of environmental objectives in a system optimal dynamic traffic assignment model. *Computer-Aided Civil and Infrastructure Engineering*, 27(7):494–511, 2012.

J. G. Bared and E. Kaisar. Median U-turn design as an alternative treatment for left turns at signalized intersections. *ITE Journal (Institute of Transportation Engineers)*, 72(2):50–54, 2002.

M. J. Beckmann, C. B. McGuire, and C. B. Winsten. *Studies in the Economics of Transportation.* Yale University Press, 1955.

M. Ben-Akiva, M. Bierlaire, and E Frejinger. Expanded path size attribute for route choice models including sampling correction. In *Proceedings of the International Choice Modelling Conference*, 2009.

M. E. Ben-Akiva and S. R. Lerman. *Discrete choice analysis: theory and application to travel demand*. MIT press, 1985.

C. M. Benedek and L. R. Rilett. Equitable traffic assignment with environmental cost functions. *Journal of transportation engineering*, 124(1):16–22, 1998.

C. Bielefeldt and F. Busch. Motion-a new on-line traffic signal network control system motion. 1994.

G. T. Bowen and R. D. Bretherton. Latest developments in scoot-version 3.1. 1996.

E. Cascetta. *Transportation Systems Analysis: Models and Applications*. Springer, 2009.

E. Cascetta, M. Gallo, and B. Montella. Models and algorithms for the optimization of signal settings on urban networks with stochastic assignment models. *Annals of Operations Research*, 144(1):301–328, may 2006.

H. Ceylan and M. G. H. Bell. Reserve capacity for a road network under optimized fixed time traffic signal control. *Journal of Intelligent Transportation Systems*, 8(2):87–99, 2004a.

H. Ceylan and M.G.H Bell. Traffic signal timing optimisation based on genetic algorithm approach, including drivers' routing. *Transportation Research Part B: Methodological*, 38(4):329–342, may 2004b.

L. Chen and H. Yang. Managing congestion and emissions in road networks with tolls and rebates. *Transportation Research Part B: Methodological*, 46(8):933–948, 2012.

S. Chiou. Optimal signal-setting for road network with maximum capacity. *Information Sciences*, 273:287–303, 2014.

M. Chowdhury, N. Derov, and P. Tan. Evaluating the effects of prohibiting left turns and the resulting U-turn movement. Technical Report FHWA/OH-2003/001, University of Dayton,Ohio Department of Transportation,Federal Highway Administration, 2003.

M. Chowdhury, N. Derov, P. Tan, and C. Stemen. A Survey of State Practices for Restricting Direct Left Turns from Driveways. *ITE journal*, 2004.

M. Chowdhury, N. Derov, and P. Tan. Prohibiting left-turn movements at mid-block unsignalized driveways: Simulation analysis. *Journal of transportation engineering*, 131(4):279–285, 2005.

E. Cipriani and G. Fusco. Combined signal setting design and traffic assignment problem. *European Journal of Operational Research*, 155(3):569–583, jun 2004.

C. F. Daganzo and M. Kusnic. CTwo properties of the nested logit model. *Transportation Science*, 27(4):395–400, 2004.

G. Davis and H. Xiong. Access to destinations: travel time estimation on arterials. Technical Report No. MN/RC 2007-35, Minnesota Department of Transportation, the USA, 2007.

E. W. Dijkstra. A note on two problems in connexion with graphs. *Numerische mathematik*, 1(1):269–271, 1959.

F. Donati, V. Mauro, G. Roncolini, and M. Vallauri. A hierarchical-decentralized traffic light control system. the first realization: "progetto torino". *IFAC Proceedings Volumes*, 17(2):2853–2858, 1984.

D. R. Drew, L. R. LaMotte, J. H. Buhr, and J. A. Wattleworth. Gap acceptance in the freeway merging process. *Highway research record*, 208:1–36, 1967.

J. L. Farges, I. Khoudour, and J. B. Lesort. Prodyn: On site evaluation. In *Road Traffic Control, 1990., Third International Conference on*, pages 62–66. IET, 1990.

L. R. Foulds, D. C. Duarte, H. A. do Nascimento, H. J. Longo, and B. R. Hall. Turning restriction design in traffic networks with a budget constraint. *Journal of Global Optimization*, 60(2):351–371, 2014.

B. Friedrich. Models for adaptive urban traffic control. *Proceedings of the 8th Metting of the Euro Working Group on Transportation, Rome, Italy*, 2000.

S. Gallivan and B. Heydecker. Optimising the control performance of traffic signals at a single junction. *Transportation Research Part B*, 22(5):357–370, 1988.

N. H. Gartner. Opac: Strategy for demand-responsive decentralized traffic signal control. *IFAC Proceedings Volumes*, 23(2):241–244, 1990.

N. H. Gartner. Implementation of the OPAC adaptive control strategy in a traffic signal network. In *Intelligent Transportation Systems Conference Proceedings*, pages 195–200, 2001. ISBN 0780371941.

X. Guang and L. Wu. A model of the urban road intersection left-turning restriction. *Journal of Theoretical and Applied Information Technology*, 48(3), 2013.

S. Gyawali. *A New Decision Making Approach for Indirect Left Turn Treatments by Utilizing Decision Assistance Curves*. PhD thesis, 2014.

A. Hajbabaie, J. C. Medina, and R. F. Benekohal. Effects of ITS-Based Left Turn Policies on Network Performance. *IEEE Conference on Intelligent Transportation Systems, Proceedings, ITSC*, pages 80–84, 2010.

B. Han. A new comprehensive sheared delay formula for traffic signal optimisation. *Transportation Research Part A: Policy and Practice*, 30(2), 1996.

HBS. *Handbuch für die Bemessung von Strassenverkehrsanlagen (HBS, German Highway Capacity Manual)*. Road and Transport Association, Cologne, Germany, 2001.

HCM. *Highway Capacity Manual. Chapter 16: Signalized Intersections.* Transportation Research Board (TRB), Washington, DC, the USA, 2000.

Jean-Jacques Henry, Jean Loup Farges, and J Tuffal. The prodyn real time traffic algorithm. *IFAC Proceedings Volumes*, 16(4):305–310, 1983.

B. G. Heydecker, C. Cai, and C. K. Wong. Adaptive dynamic control for road traffic signals. In *Networking, sensing and control, 2007 ieee international conference on*, pages 193–198. IEEE, 2007.

J. Hicklin, C. Moler, P. Webb, R. Boisvert, B. Miller, R. Pozo, and K. Remington. Jama : A java matrix package. `http://math.nist.gov/javanumerics/jama/`, November 23 2012.

A. Horni, K. Nagel, and K. W. Axhausen. *The multi-agent transport simulation MATSim.* London: Ubiquity Press, 2016.

P. B. Hunt, D. I. Robertson, R. D. Bretherton, and R. I. Winton. Scoot-a traffic responsive method of coordinating signals. Technical report, 1981.

G. Improta and G. E. Cantarella. Control system design for an individual signalized junction. *Transportation Research Part B*, 18(2):147–167, 1984.

J. H. Kell and I. J. Fullerton. *Manual of traffic signal design*. Prentice Hall, 1991.

R. M. Kimber. The prediction of saturation flows for road junctions controlled by traffic signals. *TRRL Research Report*, 67, 1986.

R. M. Kimber and E. M. Hollis. Traffic Queues and Delays at Road Junctions. Technical Report No. LR909 Monograph, Transport and Road Research Laboratory, 1979.

P Koonce, L Rodegerdts, K Lee, and S Quayle. Traffic signal timing manual. page 273, 2008.

M. Koshi. Cycle time optimization in traffic signal coordination. *Transportation Research Part A: General*, 23(1):29–34, 1989.

S. Lee and S. C. Wong. Group-based approach to predictive delay model based on incremental queue accumulations for adaptive traffic control systems. *Transportation Research Part B: Methodological*, 98:1–20, 2017.

J. Leng, H. Zhao, and Q. Zhang. Research on the Impact of U-turn Location on Operation Efficiency at Intersection. *IEEE International Conference on Measuring Technology and Mechatronics Automation*, 2009.

A. Z. Li, X. S. Song, X. H. Song, and B. H. Wu. Traffic volume condition for left-turn forbidden on urban road unsignalized T-intersection. *IEEE International Conference on Computational Intelligence and Software Engineering*, 2009.

W. Lin and C. Wang. An enhanced 0-1 mixed-integer lp formulation for traffic signal control. *IEEE Transactions on Intelligent transportation systems*, 5(4):238–245, 2004.

H. K. Lo. A novel traffic signal control formulation. *Transportation Research Part A: Policy and Practice*, 33(6):433–448, 1999.

H. K. Lo. A cell-based traffic control formulation: strategies and benefits of dynamic timing plans. *Transportation Science*, 35(2):148–164, 2001.

J. Long, Z. Gao, H. Zhang, and W. Y. Szeto. A turning restriction design problem in urban road networks. *European Journal of Operational Research*, 206(3):569–578, 2010.

J. Long, W. Y. Szeto, and H. J. Huang. A bi-objective turning restriction design problem in urban road networks. *European Journal of Operational Research*, 237(2):426–439, 2014.

P. R. Lowrie. The Sydney coordinated adaptive traffic system - principles, methodology, algorithms. *International Conference on Road Traffic Signalling, London, United Kingdom*, 1982.

J. Lu, S. Dissanayake, L. Xu, and K. Williams. Safety evaluation of right-turns followed by U-turns as an alternative to direct left turns: Crash data analysis. Technical report, 2001a.

J. Lu, S. Dissanayake, H. Zhou, and X. K. Yang. Operational evaluation of right turns followed by u-turns as an alternative to direct left turns. *the report based on "Methodology to quantify the effects of access management on roadway operation and safety"*, III, 2001b.

J. Lu, S. Dissanayake, L. Xu, and K. Williams. Safety evaluation of right truns followed by U-turns at signalized intersections(6 or more lanes) as an alternative to direct left turns - conflict analysis. Technical report, 2005.

X. Ma, J. Jin, and W. Lei. Multi-criteria analysis of optimal signal plans using microscopic traffic models. *Transportation Research Part D: Transport and Environment*, 32:1–14, 2014.

V. Mauro and C. di Taranto. Utopia. *IFAC Proceedings Volumes*, 23(2):245–252, 1990.

K. Meffert and N. Rotstan. Jgap: Java genetic algorithm package. `http://jgap.sourceforge.net/`, July 3 2015.

S. Memoli, G. E. Cantarella, S. de Luca, and R. Di Pace. Network signal setting design with stage sequence optimisation. *Transportation Research Part B: Methodological*, 100: 20–42, 2017.

A. Pacheco, M. L. Simoes, and P. Milheiro-Oliveira. Queues with server vacations as a model for pretimed signalized urban traffic. *Transportation Science*, 2017.

M. A. Penic and J. Upchurch. TRANSYT-7F: enhancement for fuel consumption, pollution emissions, and user costs. *Transportation Research Board*, 1360, 1992.

J. L. Pline. *Left-Turn Treatments at Intersections*. Number NCHRP Sytthesis of Highway Practice 225. Transportation Research Board, 1996.

T. Pohlmann. *New Approaches for Online Control of Urban Traffic Signal Systems*. PhD thesis, Fakultaet Architektur, Bauingenieurwesen und Umweltwissenschaften der Technischen Carolo-Wilhelmina zu Braunschweig, 2010.

T. Pohlmann and B. Friedrich. Online control of signalized networks using the cell transmission model. In *Intelligent Transportation Systems (ITSC), 2010 13th International IEEE Conference on*, pages 1–6. IEEE, 2010.

A. K. Rathi. A control scheme for high traffic density sectors. *Transportation Research Part B: Methodological*, 22(2):81–101, 1988.

RiLSA. Guidelines for Traffic Signals RiLSA. Technical report, Cologne, Germany, 1992.

D. I. Robertson. Transyt: a traffic network study tool. 1969.

D. I. Robertson. Research on the transyt and scoot methods of signal coordination. *ITE journal*, 56(1), 1986.

R. P. Roess, E. S. Prassas, and W. R. McShane. *Traffic engineering*. Prentice Hall, 2004.

B. Roudsari, R. Kaufman, and R. Nirula. Comparison of mid-block and intersection-related left turn collisions. *Traffic injury prevention*, 8(4):393–397, 2007.

R. Sedgewick. *Algorithms*. Pearson Education India, 1988.

Y. Sheffi. *Urban transportation networks*. Prentice Hall, 1985.

J.P. Silcock. Designing signal-controlled junctions for group-based operation. *Transportation Research Part A: Policy and Practice*, 31(2):157–173, 1997.

A. G. Sims. The sydney coordinated adaptive traffic system. In *Engineering Foundation Conference on Research Directions in Computer Control of Urban Traffic Systems, 1979, Pacific Grove, California, USA*, 1979.

A. G. Sims and A. B. Finlay. Scats, splits and offsets simplified (sos). *Australian Road Research*, 12(4), 1984.

A. Skabardonis and R. Dowling. Improved speed-flow relationships for planning applications. *Transportation Research Record: Journal of the Transportation Research Board*, (1572):18–23, 1997.

M. J. Smith. Optimum network control using traffic signals. In *UK Developments in Road Traffic Signalling, IEE Colloquium on*, pages 8–1. IET, 1988.

M.J. Smith. The existence, uniqueness and stability of traffic equilibria. *Transportation Research Part B: Methodological*, 13(4):295–304, 1979a.

M.J. Smith. Traffic control and route-choice: a simple example. *Transportation Research Part B: Methodological*, 13(4):289–294, 1979b.

H. Spiess. Technical Note: Conical Volume-Delay Functions. *Transportation Science*, 24 (2):153–158, 1990.

N. Stamatiadis, K. Agent, and Bizakis A. Guidelines for left-turn phasing treatment. *Transportation Research Record: Journal of the Transportation Research Board*, 1605: 1–7, 1997.

N. Stamatiadis, A. Hedges, and A. Kirk. A simulation-based approach in determining permitted left-turn capacities. *Transportation Research Part C: Emerging Technologies*, 55:486–495, 2015.

W. Y. Szeto, X. Jaber, and S. C. Wong. Road network equilibrium approaches to environmental sustainability. *Transport Reviews*, 32(4):491–518, 2012.

Q. Tang. Lane-based optimization of signal timing including left turn prohibition in communication scenarios. In *Intelligent Transportation Systems (ITSC), 2016 IEEE 19th International Conference on*, pages 2071–2076. IEEE, 2016.

Q. Tang and B. Friedrich. Minimization of travel time in signalized networks by prohibiting left turns. *Transportation Research Procedia*, 14:3446–3455, 2016.

J. G. Wardrop. Some theoretical aspects of road traffic research. *Inst Civil Engineers Proc London/UK/*, 1(2):325–378, 1952.

F. V. Webster. Traffic signal settings. Technical Report Road Research Technical Paper, No.39, Road Research Laboratory, London, 1958.

C. H. Wen and F. S. Koppelman. The generalized nested logit model. *Transportation Research Part B: Methodological*, 9(7):627–641, 2001.

R. Wiedemann. Simulation des strassenverkehrsflusses. 1974.

H. C. Williams. On the formation of travel demand models and economic evaluation measures of user benefit. *Environment and planning A*, 9(3):285–344, 1977.

C. K. Wong and B. G. Heydecker. Optimal allocation of turns to lanes at an isolated signal-controlled junction. *Transportation Research Part B: Methodological*, 45(4):667–681, may 2011.

C. K. Wong and Y. Y. Lee. Convergence study of minimizing the nonconvex total delay using the lane-based optimization method for signal-controlled junctions. *Discrete Dynamics in Nature and Society*, 2012:1–8, 2012.

C. K. Wong and S. C. Wong. Lane-based optimization of signal timings for isolated junctions. *Transportation Research Part B: Methodological*, 37(1):63–84, 2003.

C. K. Wong, S. C. Wong, and C. O. Tong. a Lane-Based Optimization Method for the Multi-Period Analysis of Isolated Signal-Controlled Junctions. *Transportmetrica*, 2(1): 53–85, 2006.

S. C. Wong. Group-based optimisation of signal timings using the transyt traffic model. *Transportation Research Part B: Methodological*, 30(3):217–244, 1996.

H. Yang and S. Yagar. Traffic assignment and signal control in saturated road networks. *Transportation Research Part A: Policy and Practice*, 29(2):125–139, 1995.

Y. Yin and S. Lawphongpanich. Internalizing emission externality on road networks. *Transportation Research Part D: Transport and Environment*, 11(4):292–301, 2006.

J. Zhao, W. Ma, K. L. Head, and X. Yang. Dynamic Turning Restriction Management for Signalized Road Network. *Transportation Research Record*, (2487):96–111, 2015a.

J. Zhao, W. Ma, K. L. Head, and X. Yang. Optimal operation of displaced left-turn intersections: A lane-based approach. *Transportation Research Part C: Emerging Technologies*, 61:29–48, 2015b.

J. Zhao, Y. Liu, and P. Li. A network enhancement model with integrated lane reorganization and traffic control strategies. *Journal of Advanced Transportation*, 50(6): 1090–1110, 2016a.

J. Zhao, W. Ma, K. L. Head, and Y. Han. Improving the operational performance of two-quadrant parclo interchanges with median U-turn concept. *Transportmetrica B: Transport Dynamics*, 2(2):1–21, 2016b.

List of Figures

List of Tables

Lists of Abbreviations

OD	Origin-destination
SUE	Stochastic User Equilibrium
UE	User Equilibrium
CTM	Cell transmission model
LT	Left turn
TH	Through movement
RT	Right turn
CTM	Cell transmission model
BPR	Bureau of Public Roads
HCM	Highway Capacity Manual
HBS	German Highway Capacity Manual
MSA	Method of Successive Averages
MILP	Mixed-Integer-Linear-Programming
veh/h	Vehicle per hour
h	Hour
s	Second

A. Signal settings of artificial network

A.1. Lane-based method

A.1.1. Without left turn prohibition

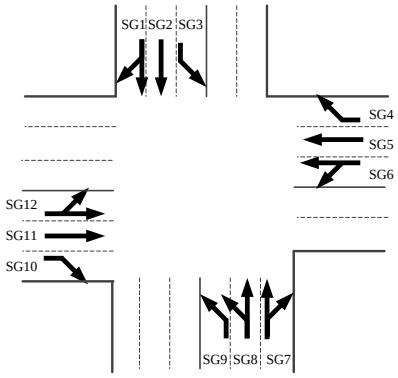

(a) Intersection 1

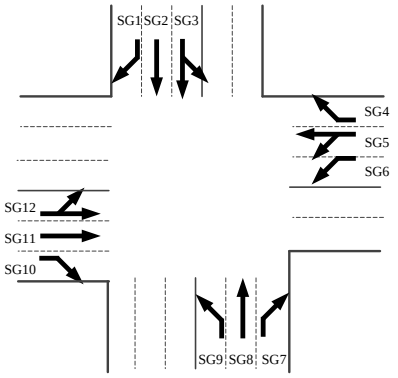

(b) Intersection 2

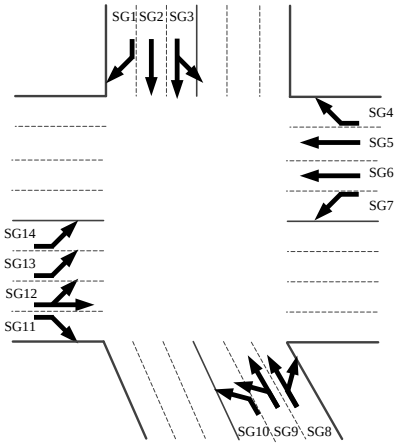

(c) Intersection 3

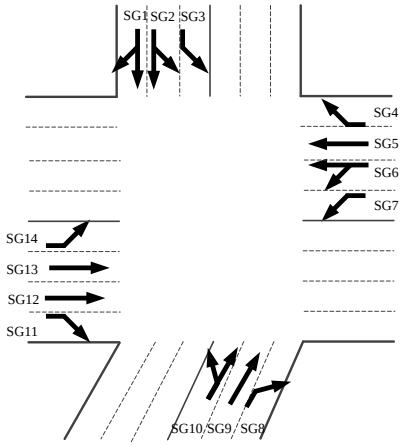

(d) Intersection 4

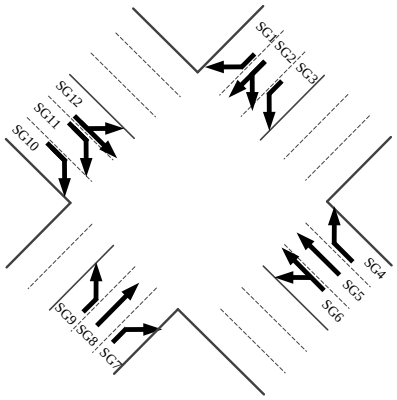

(e) Intersection 5

Figure A.1.: Lane markings without left turn prohibition in the lane-based method.

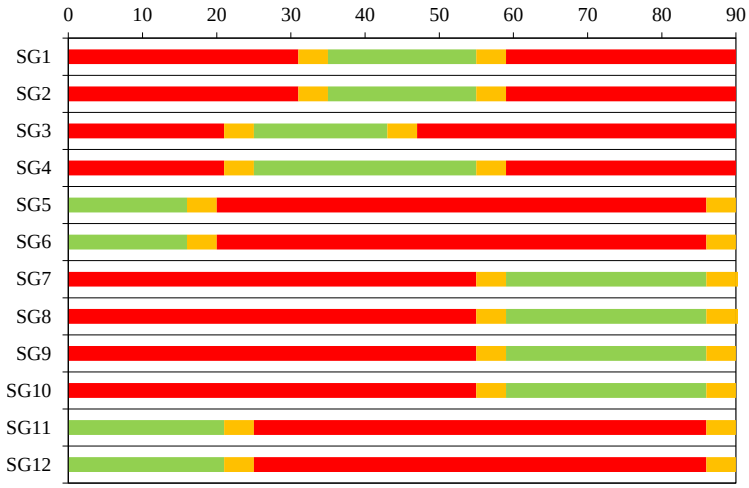

(a) Intersection 1

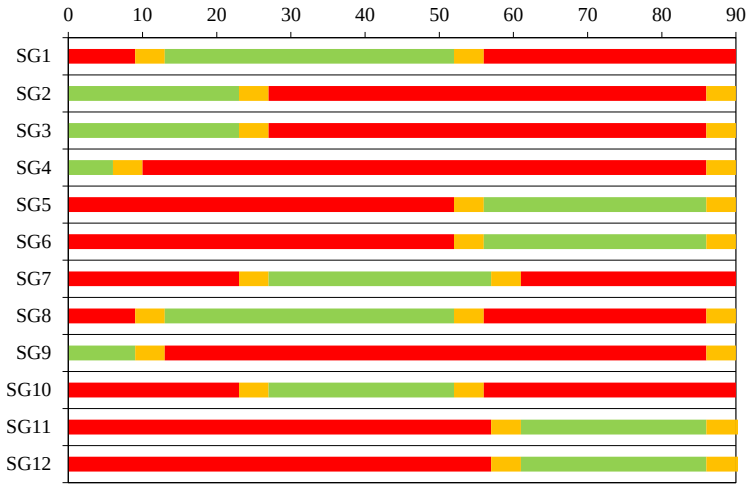

(b) Intersection 2

Figure A.2.: Signal timing plan without left turn prohibition in the lane-based method.

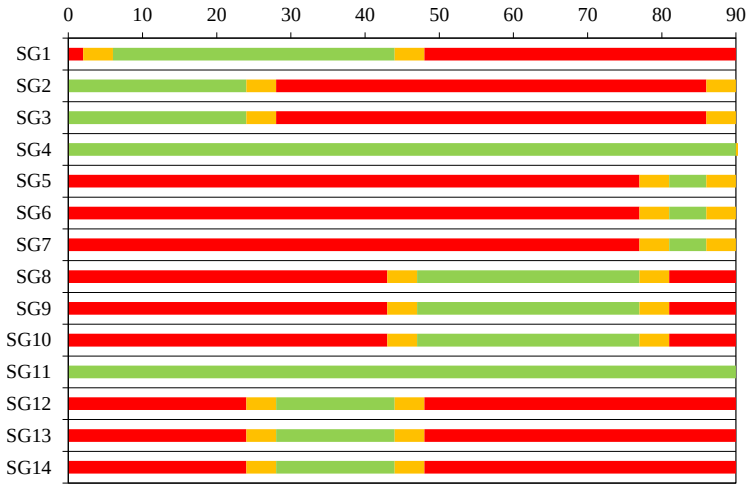

(a) Intersection 3

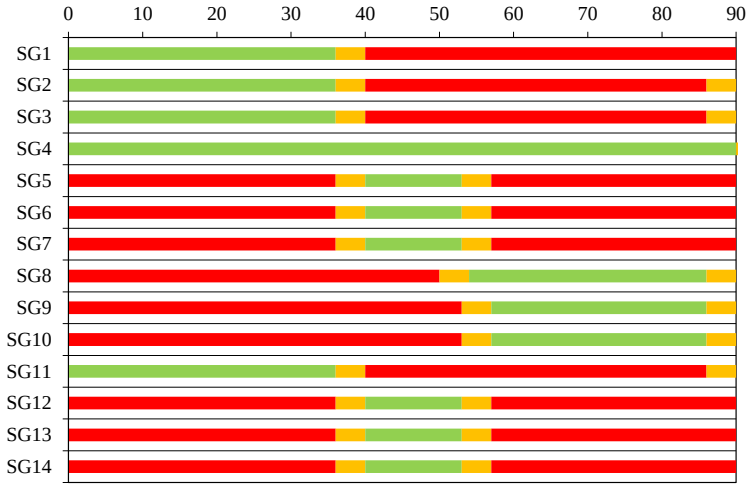

(b) Intersection 4

Figure A.3.: Signal timing plan without left turn prohibition in the lane-based method (continued).

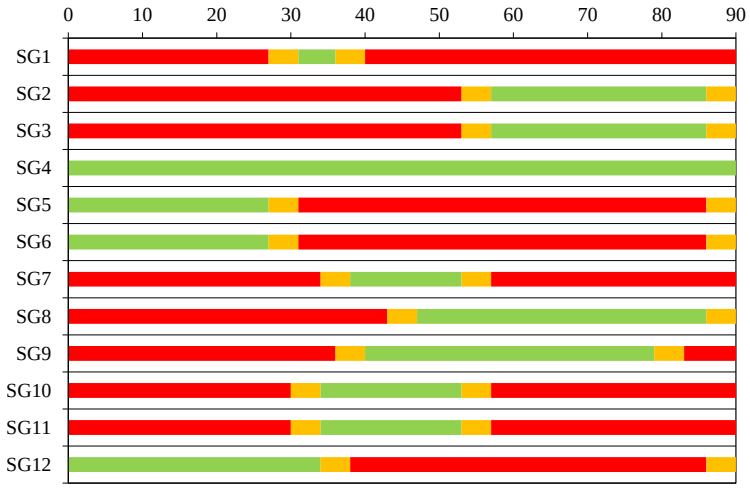

(a) Intersection 5

Figure A.4.: Signal timing plan without left turn prohibition in the lane-based method (continued).

A.1.2. With left turn prohibition

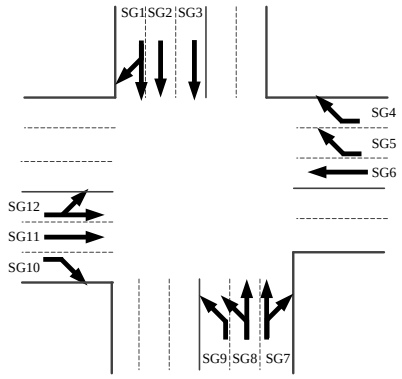

(a) Intersection 1

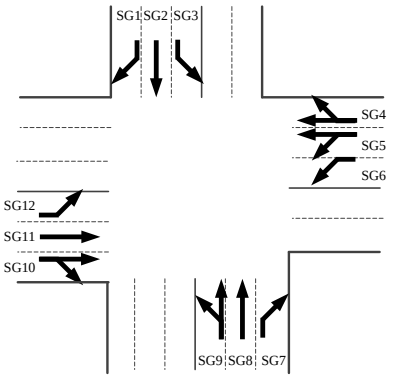

(b) Intersection 2

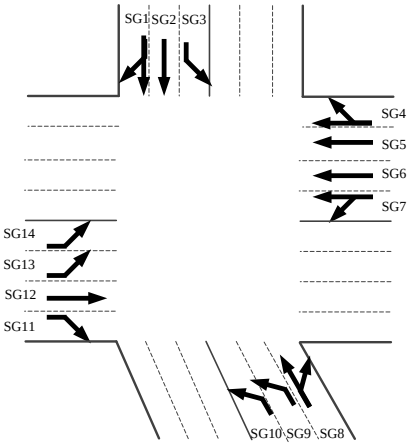

(c) Intersection 3

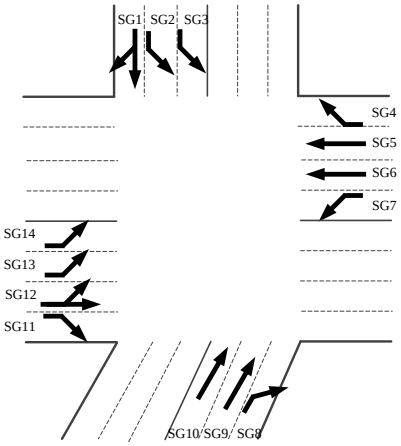

(d) Intersection 4

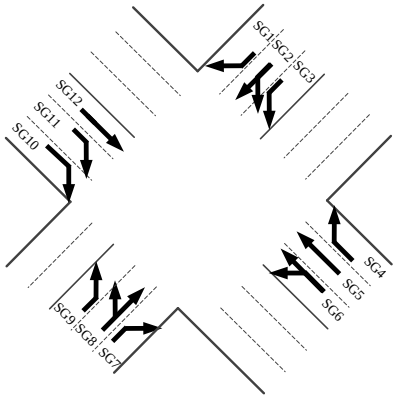

(e) Intersection 5

Figure A.5.: Lane markings with left turn prohibition in the lane-based method.

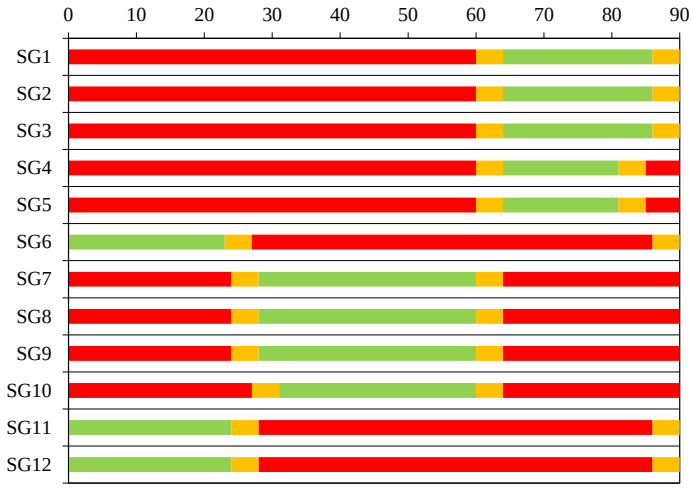

(a) Intersection 1

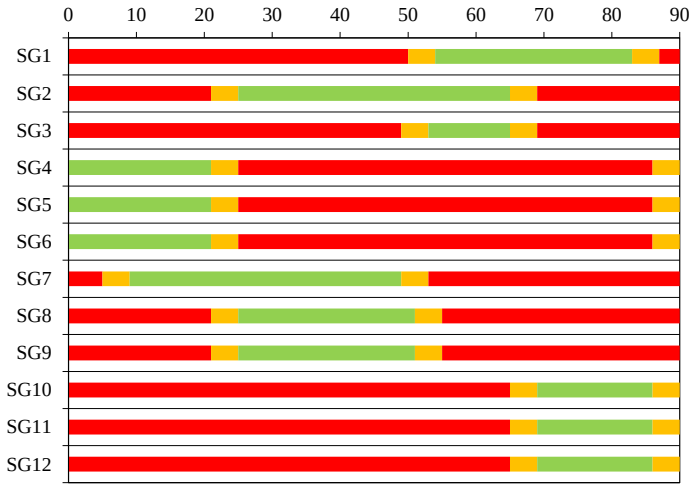

(b) Intersection 2

Figure A.6.: Signal timing plan with left turn prohibition in the lane-based method.

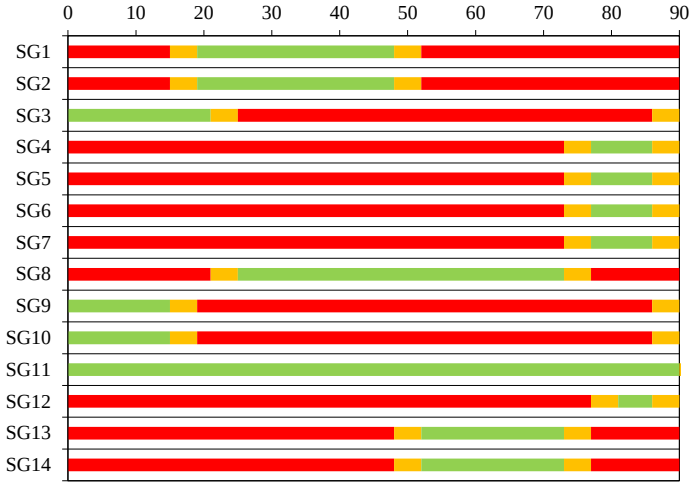

(a) Intersection 3

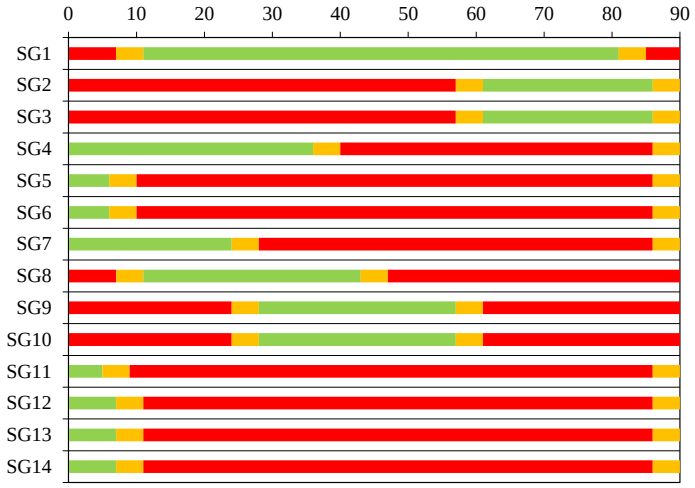

(b) Intersection 4

Figure A.7.: Signal timing plan with left turn prohibition in the lane-based method (continued).

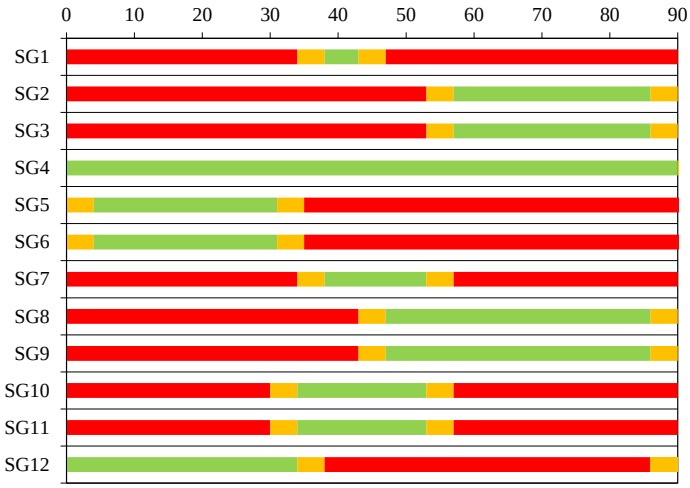

(a) Intersection 5

Figure A.8.: Signal timing plan with left turn prohibition in the lane-based method (continued).

A.2. Stage-based method

A.2.1. Without left turn prohibition

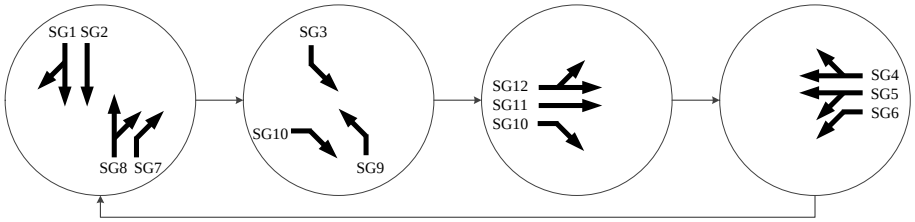

(a) Intersection 1

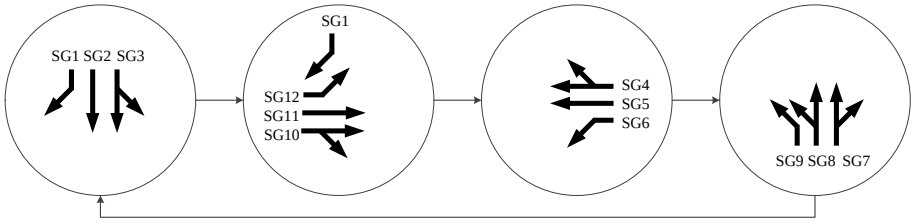

(b) Intersection 2

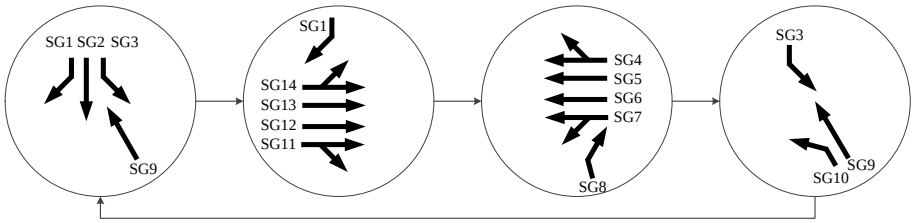

(c) Intersection 3

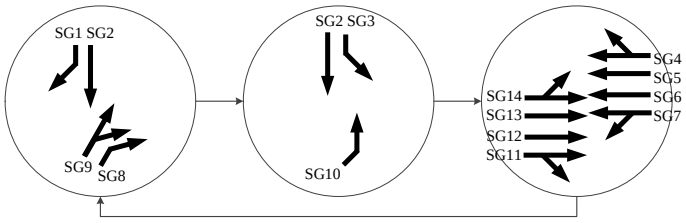

(d) Intersection 4

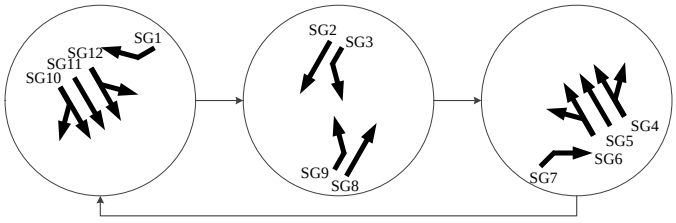

(e) Intersection 5

Figure A.9.: Stages without left turn prohibition in the stage-based method.

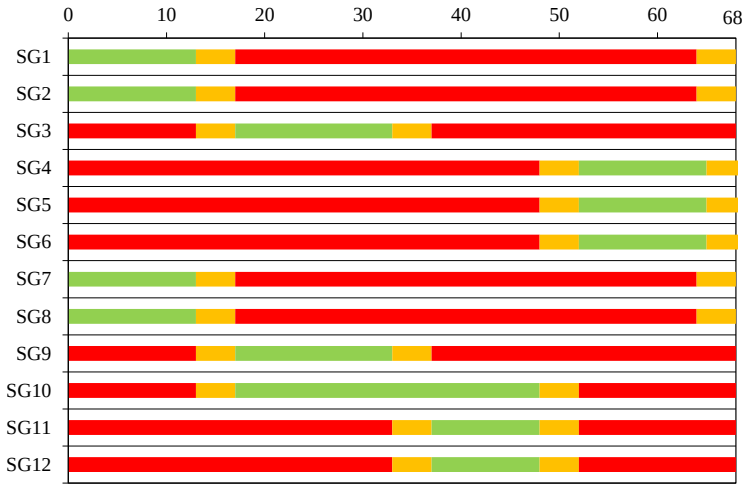

(a) Intersection 1

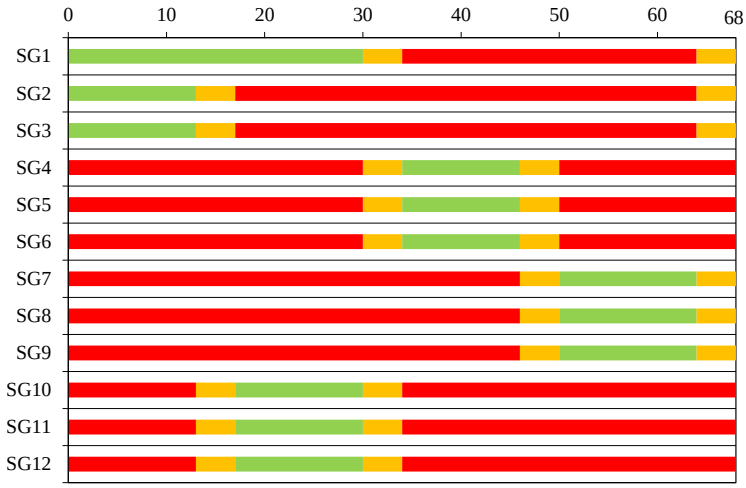

(b) Intersection 2

Figure A.10.: Signal timing plan without left turn prohibition in the stage-based method.

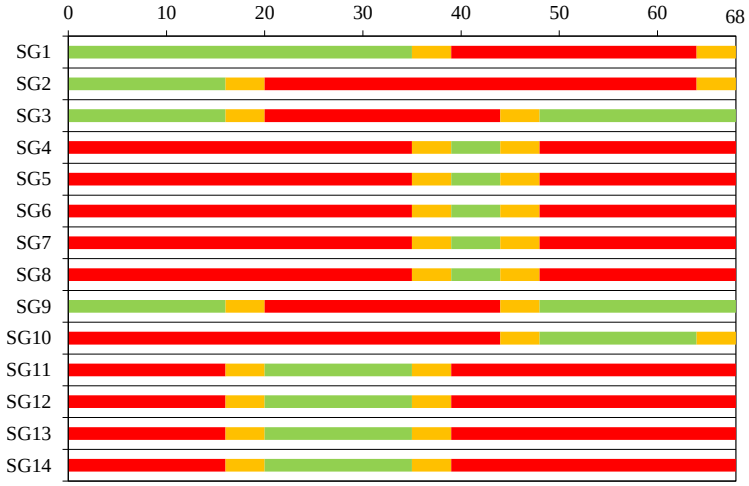

(a) Intersection 3

(b) Intersection 4

Figure A.11.: Signal timing plan without left turn prohibition in the stage-based method (continued).

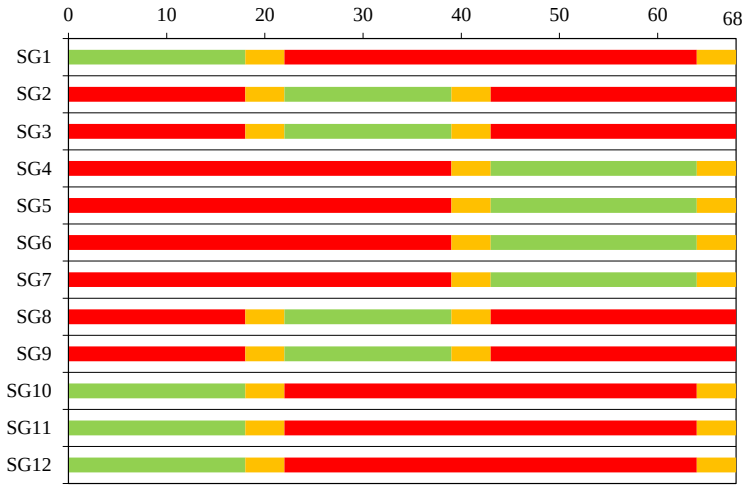

(a) Intersection 5

Figure A.12.: Signal timing plan without left turn prohibition in the stage-based method (continued).

A.2.2. With left turn prohibition

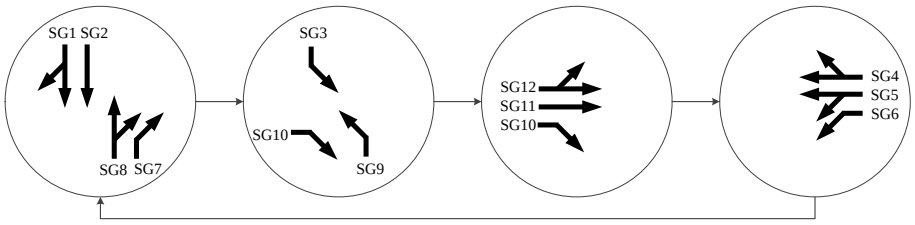

(a) Intersection 1

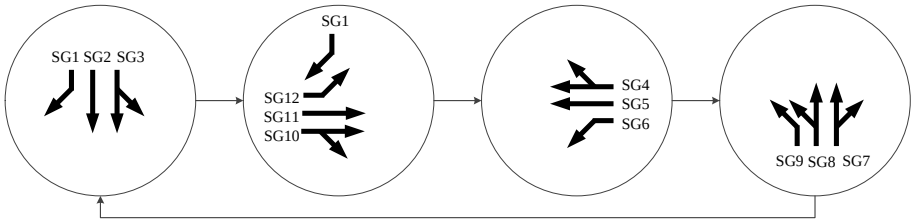

(b) Intersection 2

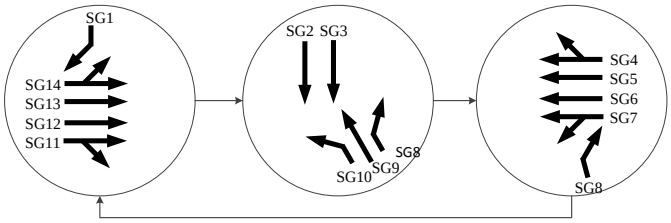

(c) Intersection 3

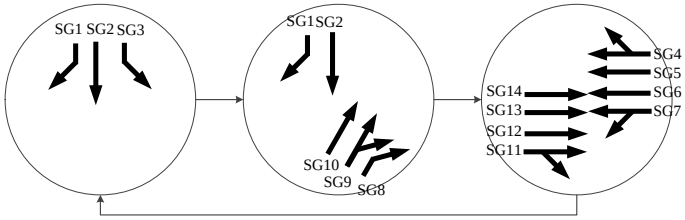

(d) Intersection 4

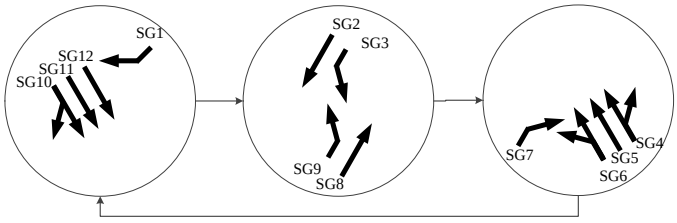

(e) Intersection 5

Figure A.13.: Stages with left turn prohibition in the stage-based method.

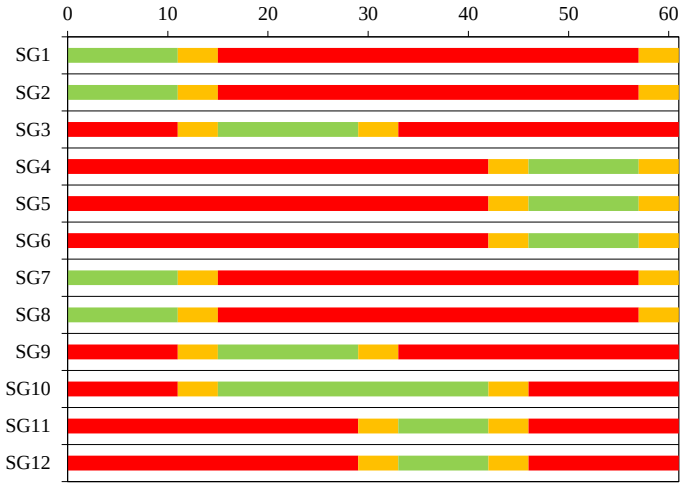

(a) Intersection 1

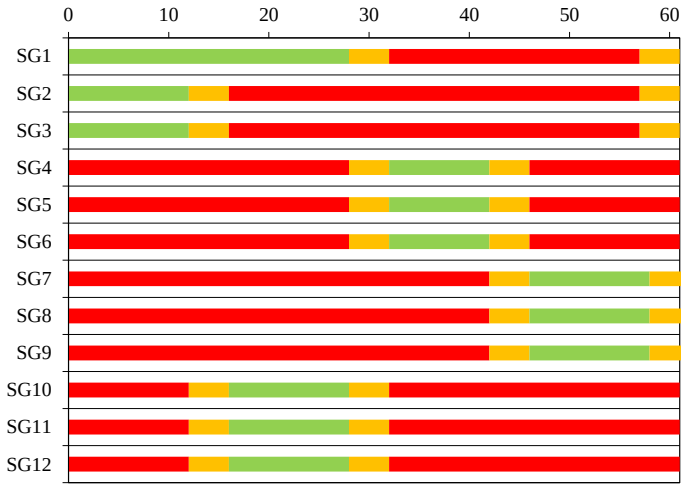

(b) Intersection 2

Figure A.14.: Signal timing plan with left turn prohibition in the stage-based method.

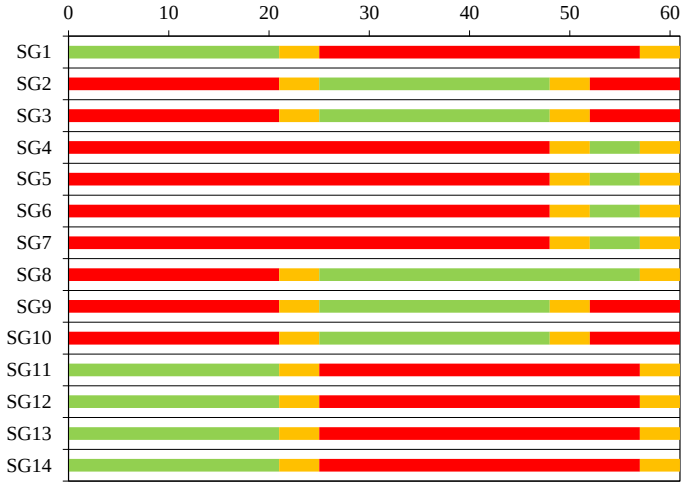

(a) Intersection 3

(b) Intersection 4

Figure A.15.: Signal timing plan with left turn prohibition in the stage-based method (continued).

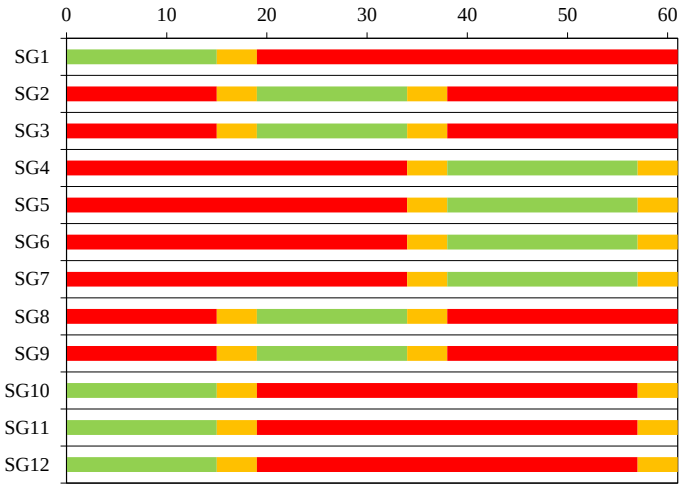

(a) Intersection 5

Figure A.16.: Signal timing plan with left turn prohibition in the lane-based method (continued).

B. Simulation study

B.1. Link flows and turning rate from the proposed model

Table B.1.: Turning rate in equilibrium state from the proposed model with the lane-based method without left turn prohibition

Intersection 1			
Arm	Direction	Link flow (veh/h)	Turning rate
1	RT	100	0.24
	TH	205	0.49
	LT	115	0.27
2	RT	175	0.44
	TH	143	0.36
	LT	78	0.20
3	RT	42	0.07
	TH	245	0.43
	LT	278	0.49
4	RT	209	0.44
	TH	201	0.41
	LT	70	0.15
Intersection 2			
1	RT	195	0.38
	TH	245	0.47
	LT	80	0.15
2	RT	40	0.10
	TH	160	0.39
	LT	210	0.51
3	RT	196	0.38
	TH	282	0.54
	LT	40	0.07
4	RT	76	0.21
	TH	144	0.40
	LT	138	0.39

Table B.2.: Turning rate in equilibrium state from the proposed model with the lane-based method without left turn prohibition (continued)

Intersection 3			
Arm	Direction	Link flow (veh/h)	Turning rate
1	RT	158	0.32
	TH	267	0.54
	LT	67	0.14
2	RT	60	0.33
	TH	109	0.60
	LT	13	0.07
3	RT	9	0.02
	TH	293	0.58
	LT	203	0.40
4	RT	135	0.35
	TH	42	0.11
	LT	212	0.54
Intersection 4			
1	RT	71	0.13
	TH	223	0.42
	LT	237	0.45
2	RT	147	0.39
	TH	103	0.27
	LT	131	0.34
3	RT	156	0.32
	TH	319	0.66
	LT	9	0.02
4	RT	0	0.00
	TH	67	0.56
	LT	52	0.43
Intersection 5			
1	RT	18	0.05
	TH	176	0.50
	LT	159	0.45
2	RT	252	0.45
	TH	258	0.46
	LT	50	0.09
3	RT	80	0.15
	TH	221	0.42
	LT	229	0.43
4	RT	194	0.47
	TH	211	0.51
	LT	11	0.03

B.2. Calibration of link flows

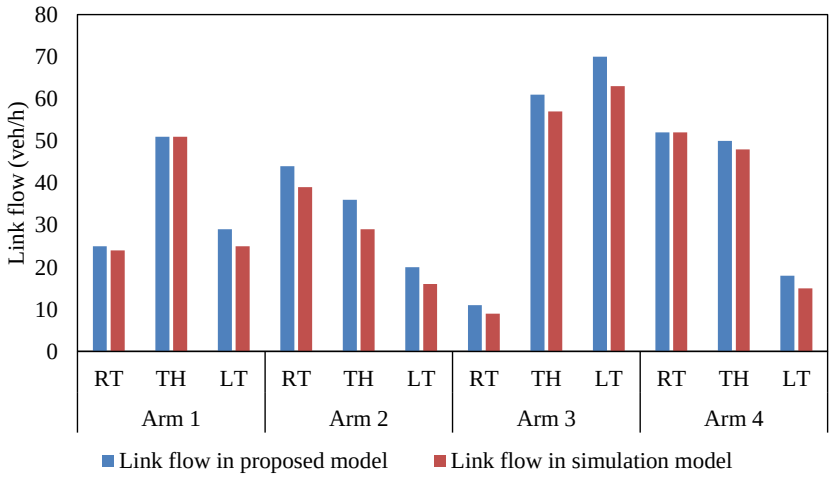

(a) Intersection 1

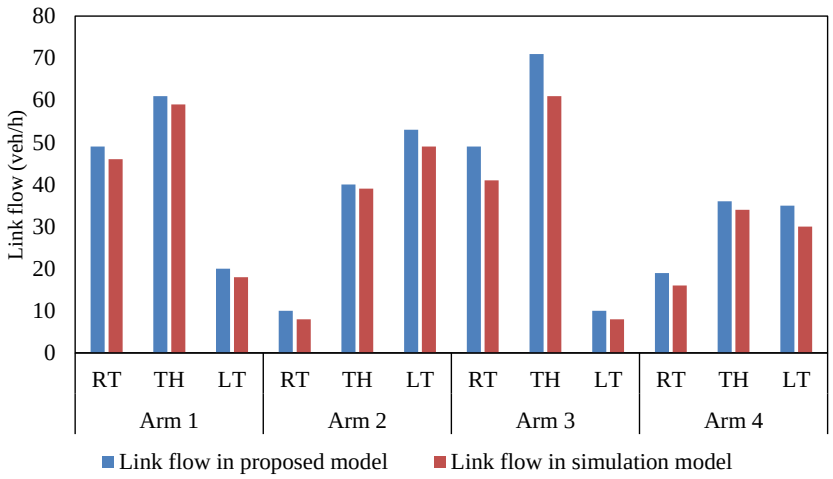

(b) Intersection 2

Figure B.1.: Calibration of link flows.

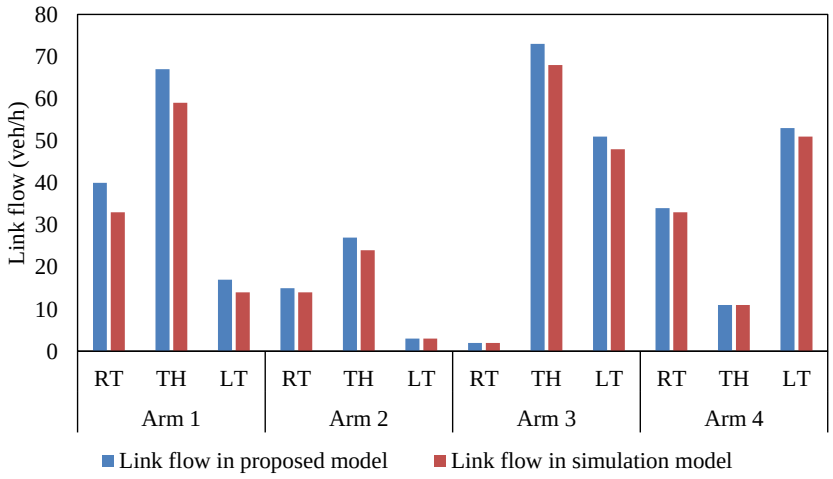

(a) Intersection 3

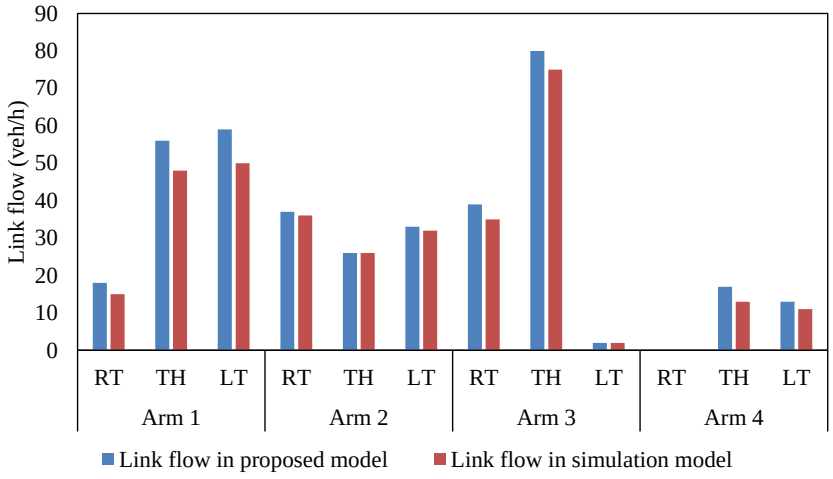

(b) Intersection 4

Figure B.2.: Calibration of link flows (continued).

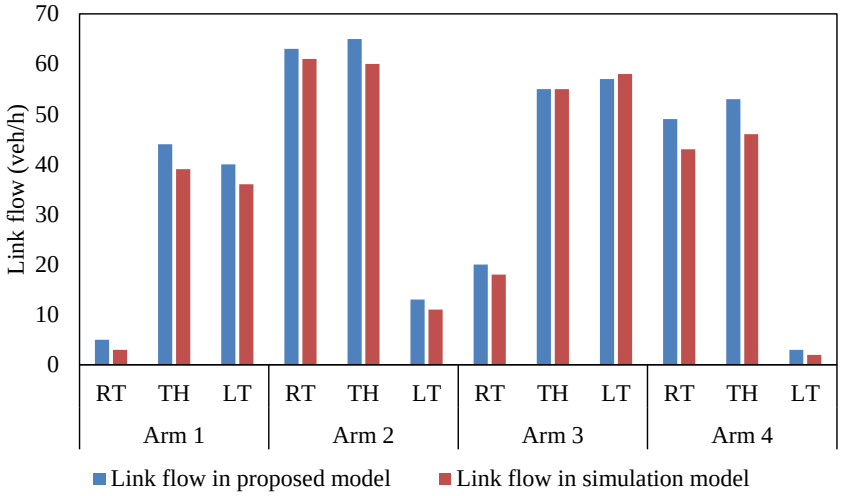

(a) Intersection 5

Figure B.3.: Calibration of link delays.

B.3. Comparison against link delays

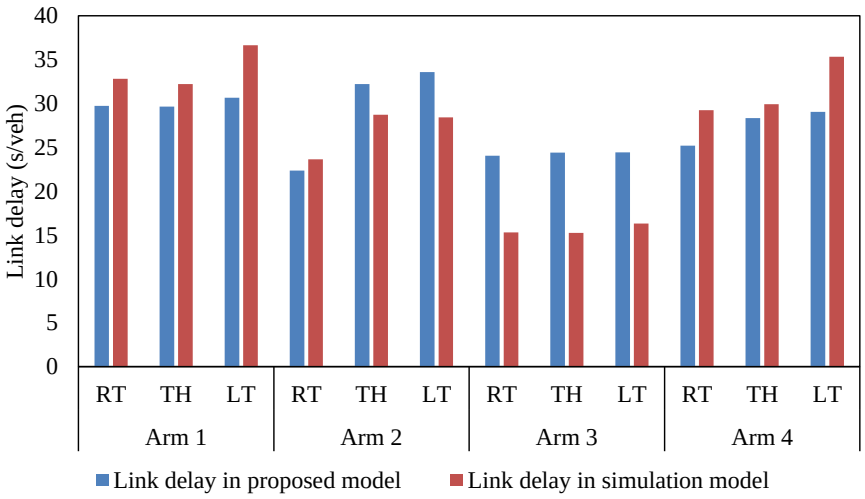

(a) Intersection 1

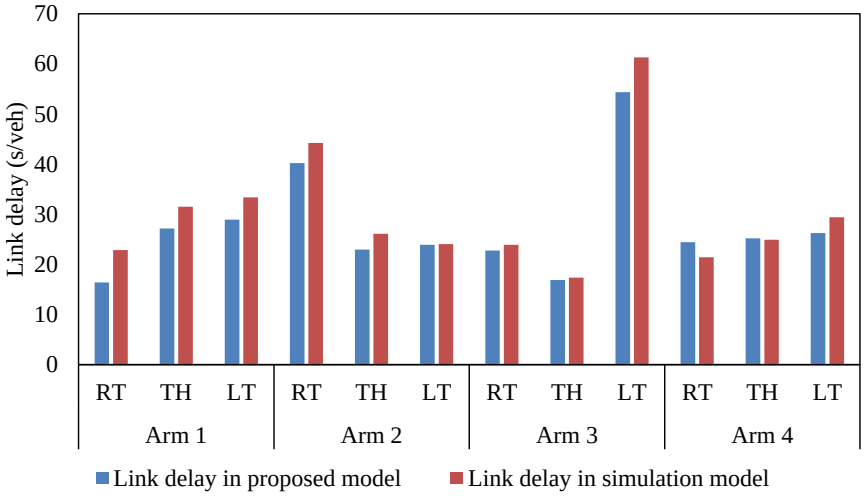

(b) Intersection 2

Figure B.4.: Calibration of link delays.

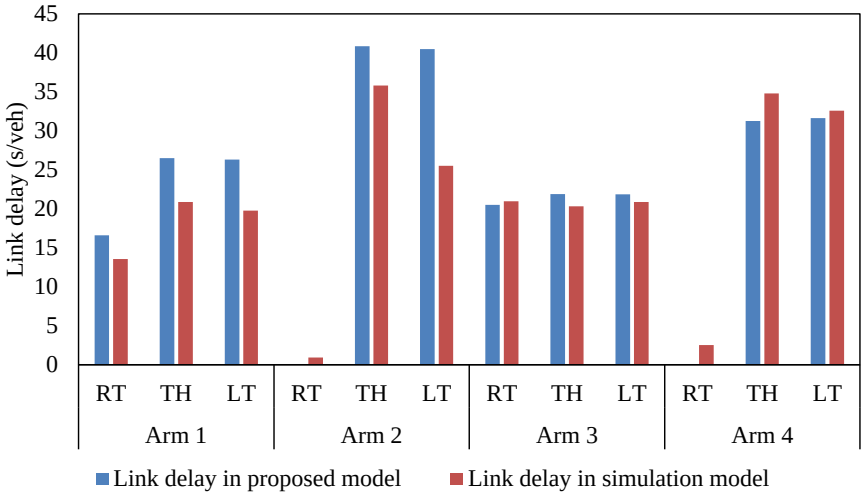

(a) Intersection 3

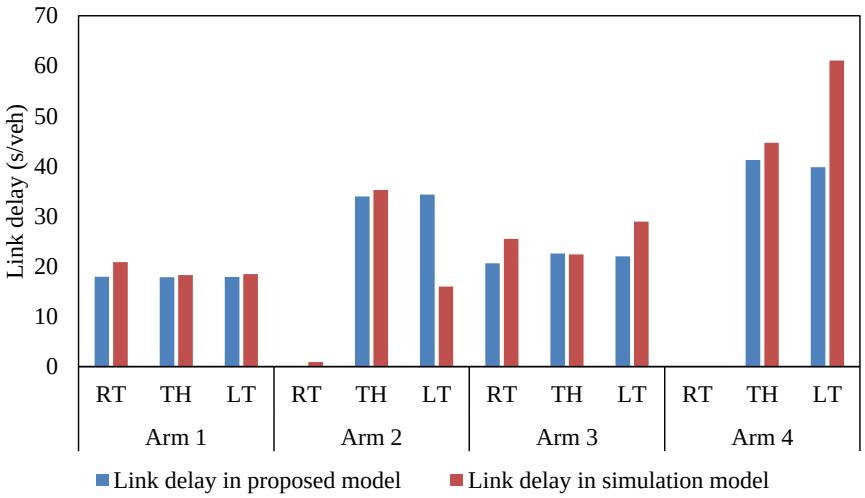

(b) Intersection 4

Figure B.5.: Calibration of link delays (continued).

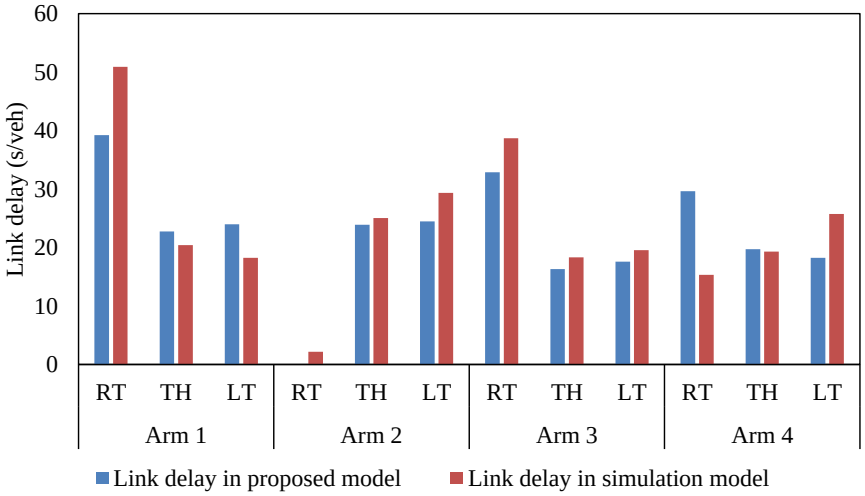

(a) Intersection 5

Figure B.6.: Calibration of link delays (continued).

C. Test Origin-Destination matrices

C.1. Demand variance

Table C.1.: OD demands generated by randomly adding variances in interval $[-5, 5]$ (veh/h)

Origin \ Destination	A	B	C	D	E	F	G	H	Origin total
A	0	72	86	57	103	60	48	55	481
B	97	0	33	59	43	68	91	30	421
C	82	89	0	83	90	56	73	51	524
D	42	72	40	0	85	17	59	98	413
E	59	27	73	42	0	92	39	54	386
F	95	81	90	81	75	0	47	102	571
G	61	66	99	46	79	80	0	95	526
H	89	85	37	49	2	71	60	0	393
Destination total	525	492	458	417	477	444	417	485	3715

Table C.2.: OD demands generated by randomly adding variances in interval $[-10, 10]$ (veh/h)

Origin \ Destination	A	B	C	D	E	F	G	H	Origin total
A	0	77	89	65	106	69	56	43	505
B	108	0	25	60	40	74	99	30	436
C	89	91	0	86	93	57	67	55	538
D	32	69	41	0	77	18	65	108	410
E	53	26	67	35	0	96	48	45	370
F	95	75	83	90	76	0	46	110	575
G	67	79	99	52	77	79	0	82	535
H	96	72	48	49	4	61	54	0	384
Destination total	540	489	452	437	473	454	435	473	3753

C.2. Factors influencing left turn prohibition

Table C.3.: OD demands generated by randomly adding variances in interval $[-15, 15]$ (veh/h)

Origin \ Destination	A	B	C	D	E	F	G	H	Origin total
A	0	61	87	53	97	67	61	43	469
B	97	0	17	69	35	59	100	29	406
C	72	91	0	78	86	47	65	49	488
D	32	85	30	0	78	19	64	105	413
E	67	42	73	28	0	91	43	62	397
F	83	81	91	73	78	0	48	103	557
G	60	62	91	46	80	77	0	79	495
H	93	80	53	63	0	85	48	0	422
Destination total	504	502	442	410	454	445	420	470	3647

Table C.4.: OD demands generated by randomly adding variances in interval $[-20, 20]$ (veh/h)

Origin \ Destination	A	B	C	D	E	F	G	H	Origin total
A	0	65	85	58	99	67	56	31	461
B	97	0	26	43	53	64	93	49	425
C	69	80	0	76	72	60	55	65	477
D	53	58	22	0	76	30	52	90	381
E	44	13	58	43	0	95	26	66	345
F	108	62	110	67	79	0	56	117	599
G	79	86	120	33	97	95	0	92	602
H	95	80	21	62	2	52	77	0	389
Destination total	545	444	442	382	478	463	415	510	3679

Table C.5.: OD demands generated by randomly adding variances in interval $[-25, 25]$ (veh/h)

Origin \ Destination	A	B	C	D	E	F	G	H	Origin total
A	0	72	103	47	90	51	52	61	476
B	107	0	11	64	51	69	81	6	389
C	57	105	0	84	78	71	70	61	526
D	25	49	22	0	56	44	70	104	370
E	42	6	85	32	0	102	21	65	353
F	72	85	69	90	77	0	72	124	589
G	70	67	104	52	96	0	81	572	
H	100	71	49	74	24	50	77	0	445
Destination total	473	455	443	443	472	489	443	502	3720

Table C.6.: OD demands generated by randomly adding variances in interval $[-30, 30]$ (veh/h)

Origin \ Destination	A	B	C	D	E	F	G	H	Origin total
A	0	58	70	55	93	39	53	50	418
B	82	0	48	35	31	42	103	13	354
C	90	115	0	62	97	79	100	22	565
D	34	85	38	0	55	3	56	116	387
E	54	35	87	46	0	103	20	31	376
F	61	90	80	76	42	0	77	89	515
G	48	43	88	42	68	63	0	99	451
H	85	73	48	40	27	79	33	0	385
Destination total	454	499	459	356	413	408	442	420	3451

Table C.7.: OD demands generated by randomly adding variances in interval $[-35, 35]$ (veh/h)

Origin \ Destination	A	B	C	D	E	F	G	H	Origin total
A	0	41	113	88	74	26	46	20	408
B	117	0	4	27	13	44	78	11	294
C	88	65	0	80	92	44	95	84	548
D	45	78	74	0	54	40	89	83	463
E	45	0	80	74	0	109	28	39	375
F	112	114	97	99	90	0	77	106	695
G	71	91	120	81	105	99	0	118	685
H	104	88	73	58	0	92	58	0	473
Destination total	582	477	561	507	428	454	471	461	3941

Table C.8.: OD demands generated by randomly adding variances in interval $[-40, 40]$ (veh/h)

Origin \ Destination	A	B	C	D	E	F	G	H	Origin total
A	0	89	73	50	64	41	88	40	445
B	113	0	44	21	64	107	90	11	450
C	72	90	0	57	70	53	83	31	456
D	26	44	40	0	57	0	60	140	367
E	87	23	92	31	0	86	9	54	382
F	112	64	130	70	34	0	30	85	525
G	78	81	81	63	112	94	0	113	622
H	72	65	3	37	38	34	89	0	338
Destination total	560	456	463	329	439	415	449	474	3585

Table C.9.: OD demands generated by randomly adding variance in interval $[-10, 0]$ (veh/h)

Origin \ Destination	A	B	C	D	E	F	G	H	Origin total
A	0	64	84	56	93	57	46	49	449
B	98	0	24	54	31	70	87	27	391
C	80	88	0	73	83	56	62	41	483
D	37	69	34	0	76	15	57	97	385
E	52	27	65	40	0	90	40	44	358
F	87	79	82	80	69	0	46	99	542
G	54	70	95	45	75	74	0	82	495
H	83	79	31	42	0	62	60	0	357
Destination total	491	476	415	390	427	424	398	439	3460

Table C.10.: OD demands generated by randomly adding variances in interval $[0, 10]$ (veh/h)

Origin \ Destination	A	B	C	D	E	F	G	H	Origin total
A	0	77	95	67	102	65	51	50	507
B	100	0	36	69	42	76	99	38	460
C	83	90	0	85	91	68	79	51	547
D	41	80	49	0	85	25	68	107	455
E	66	35	74	45	0	95	48	51	414
F	100	84	94	80	80	0	57	101	596
G	61	73	102	53	88	88	0	90	555
H	98	86	50	57	6	79	70	0	446
Destination total	549	525	500	456	494	496	472	488	3980

Table C.11.: OD demands generated by randomly adding variances in interval $[10, 20]$ (veh/h)

Origin \ Destination	A	B	C	D	E	F	G	H	Origin total
A	0	87	108	80	113	73	64	62	587
B	112	0	46	76	50	82	105	47	518
C	94	109	0	91	103	71	86	66	620
D	60	80	57	0	97	39	80	113	526
E	73	47	80	58	0	108	52	65	483
F	108	90	105	91	90	0	61	117	662
G	73	85	119	69	100	91	0	103	640
H	100	93	54	65	10	82	77	0	481
Destination total	620	591	569	530	563	546	525	573	4517

Table C.12.: OD demands generated by randomly adding variances in interval $[20, 30]$ (veh/h)

Origin \ Destination	A	B	C	D	E	F	G	H	Origin total
A	0	93	111	85	126	90	72	76	653
B	124	0	57	88	69	91	114	51	594
C	101	111	0	110	118	88	92	76	696
D	65	99	69	0	102	48	83	130	596
E	90	54	97	66	0	118	65	80	570
F	116	100	112	106	98	0	77	123	732
G	83	90	124	75	101	102	0	111	686
H	119	108	62	77	26	91	85	0	568
Destination total	698	655	632	607	640	628	588	647	5095

Table C.13.: OD demands generated by randomly adding variances in interval $[30, 40]$ (veh/h)

Origin \ Destination	A	B	C	D	E	F	G	H	Origin total
A	0	110	128	96	139	90	87	90	740
B	140	0	63	98	73	108	129	61	672
C	115	122	0	119	122	97	108	90	773
D	80	106	79	0	119	55	100	132	671
E	100	69	103	77	0	125	76	81	631
F	120	110	120	116	101	0	80	135	782
G	93	110	139	86	115	116	0	127	786
H	120	118	77	88	37	107	99	0	646
Destination total	768	745	709	680	706	698	679	716	5701

Table C.14.: OD demands generated by randomly adding variances in interval $[40, 50]$ (veh/h)

Origin \ Destination	A	B	C	D	E	F	G	H	Origin total
A	0	118	134	105	143	108	94	92	794
B	140	0	74	100	87	118	138	77	734
C	124	134	0	120	136	108	113	98	833
D	87	120	80	0	121	60	110	143	721
E	100	76	114	84	0	135	80	92	681
F	140	121	140	129	115	0	99	141	885
G	102	115	140	95	126	130	0	131	839
H	137	121	85	100	46	116	107	0	712
Destination total	830	805	767	733	774	775	741	774	6199

Table C.15.: OD demands generated by randomly adding variances in interval $[50, 60]$ (veh/h)

Origin \ Destination	A	B	C	D	E	F	G	H	Origin total
A	0	130	145	112	160	112	101	103	863
B	151	0	88	114	96	130	150	86	815
C	135	140	0	137	148	113	126	109	908
D	93	123	95	0	135	76	117	158	797
E	110	84	128	93	0	147	97	100	759
F	145	139	140	136	124	0	101	157	942
G	117	120	153	109	133	132	0	141	905
H	141	133	91	107	55	130	110	0	767
Destination total	892	869	840	808	851	840	802	854	6756

Table C.16.: OD demands generated by randomly adding variances in interval $[60, 70]$ (veh/h)

Origin \ Destination	A	B	C	D	E	F	G	H	Origin total
A	0	131	153	121	164	128	120	113	930
B	161	0	90	127	101	132	150	98	859
C	150	156	0	148	156	130	140	119	999
D	108	133	103	0	150	83	122	167	866
E	122	94	130	101	0	158	101	112	818
F	150	145	153	149	137	0	113	170	1017
G	123	135	164	114	148	141	0	150	975
H	160	147	103	114	60	140	121	0	845
Destination total	974	941	896	874	916	912	867	929	7309

Braunschweig 2019
https://doi.org/10.24355/dbbs.084-201902211149-0